A HEAT TRANSFER MODEL APPLICABLE TO THE REFUELLING PROCESS FOR NATURAL GAS VEHICLES

A THESIS SUBMITTED IN FULFILMENT OF
THE REQUIREMENT FOR THE DEGREE OF
MASTER OF ENGINEERING IN MECHANICAL ENGINEERING

BY

HAI LI

DEPARTMENT OF MECHANICAL ENGINEERING
VICTORIA UNIVERSITY OF TECHNOLOGY (FOOTSCRAY)
VICTORIA, AUSTRALIA

JANUARY 1993

ABSTRACT

This research presents a study of transient heat transfer phenomena taking place between a storage cylinder and the incoming gas during the cylinder charging process. A theoretical model of convective heat transfer between the gas and the cylinder is described. Experiments with the high pressure gas (Δp=14.5-16.5MPa) charging process to a vehicle supply tank were carried out. For reasons of safety and comparison with other work, air was used instead of Natural Gas. The whole charging process can be divided into three phases: forced convection, free convection and conduction. The experimental results were used to develop empirical equations for convection between the gas and the tank for both the forced and free convection phases. In addition, a simulation method was developed to predict the heat transfer parameters appropriate to the charging process and the predictions correspond well with the experimental results.

ACKNOWLEDGMENTS

I wish to express my deep appreciation to Mr. E.E.Milkins, the senior technical adviser of NGV Australia, for his excellent supervision and enthusiastic support for this project, and for his counsel in the preparation of this thesis. I also thank my supervisor Mr. Kevin Hunt and my acting supervisor Dr. Michael Sek, for their advice and encouragement throughout the period of the research.

Acknowledgment is made to Professor Geoff Lleonart, the Head of Mechanical Engineering Department, for his guidance and assistance on my study.

Special thanks to Mr. Raymond McIntosh, for his help with making the apparatus, and Mr. Vincent Rouiliard for his great help in data taking. Also, to fellow graduate Mr. Ming Yu, for his assistance on my preparation of this thesis.

The experiments were carried out at the NGV Australia Division of Gas and Fuel Corporation of Victoria. Thanks to all in the corporation, especially Mr. Peter Chase and Mr. Andrew Robbins. They provided much of the equipment and facilities, along with a willingness to help with any problems or requests.

This research was supported by NGV Australia.

DEDICATION

To my loving wife Hui and our beloved daughter Yi, who have sacrificed so much in order that I may accomplish this work.

To my parents, Wenda Li and Ying Wang, and to my brother and sister-in-law, Dr.Jinhe Li and Junli Ma, for their moral and financial support in times of difficulty.

CONTENTS

LIST OF FIGURES

LIST OF TABLES

NOMENCLATURE

A - Heat Transfer Area, m^2

c - specific heat kJ/kgK

c_p- specific heat at constant pressure, kJ/kgK

c_v- specific heat at constant volume, kJ/kgK

d - diameter of inlet flow nozzle throat, m

D - tank diameter, m

e - specific stored energy, kJ/kg

E - stored energy, kJ

g - acceleration of gravity, 9.8 m/s^2

Gr- Grashof number, $g\beta(T-T_w)D^3/\nu^2$

h_{en} - enthalpy, kJ/kg

h - convective heat transfer coefficient, W/m^2K

k - thermal conductivity, W/m°C

L - tank length, m

$\dot{m}$ - mass flow rate, kg/min

m - mass, kg

Nu- Nusselt number, hD/k

p - gas pressure, Pa

Δp- pressure rise during charging, Pa

$\dot{p}$ - p-time derivative, MPa/s

p_c- gas critical pressure, Pa

p_n- charging nozzle throat pressure, Pa

p_o- stagnation pressure upstream of inlet flow nozzle, Pa

Pr- Prandtl number, $c_p\mu/k$

Q - heat transfer, kJ

q - heat transfer rate, kJ/s

R - gas constant, kJ/kg K

Ra- Rayleigh number, $GrPr$

Re- Reynolds number, $\rho Vd/\mu$

t - time, s

T - average gas temperature, K

$\dot{T}$ - T-time derivative, K/s

T_c- gas critical temperature , K

T_i- inlet gas temperature, K

$\dot{T}_i$- T_i-time derivative, K/s

T_w- tank wall temperature, K

u - specific internal energy of gas, kJ/kg

u_w- specific internal energy of cylinder wall, kJ/kg

U - total internal energy of gas, kJ

U_w - total internal energy of tank wall, kJ

$\dot{U}_w$- U_w-time derivative, kJ/s

v - specific volume of gas, m^3/kg

V - gas velocity, m/s

V_c - tank volume, m^3

W - total Work, kJ

Z - gas compressibility factor

γ - ratio of specific heat, c_p/c_v

α - thermal diffusivity, $k/\rho c$, m^2/s

β - temperature coefficient of volumetric expansion, 1/K

ε - emissivity

ρ - density, kg/m^3

σ - Stefan-Boltzmann constant

Subscripts

i - conditions of inlet

in- conditions inside the cylinder

∞ - conditions outside the cylinder

o - initial condition

CHAPTER 1

INTRODUCTION

1.1 THE APPLICATION OF NATURAL GAS FOR VEHICLES

Natural gas is an excellent engine fuel. Its major constituent, methane, has physical and thermodynamic properties that make it well suited to spark ignition engines. As a diesel supplement and replacement it has been widely researched and is well established in practice.

Economic relativities between fuels, and the substitution of an indigenous fuel for oil, provide the underlying reasons for national support for natural gas vehicles. Apart from better operating economics, environmental benefits, such as lower emissions and noise levels can be achieved. A vehicle burning natural gas emits less carbon dioxide, less photo chemically reactive hydrocarbons, less air toxins, including benzene, toluene and 1,3-butadiene. It also emits fewer solid particles, which cause urban grime and possibly respiratory allergies, than vehicles running on petrol and diesel.

The use of natural gas can enhance the utilisation efficiency of natural resources and improve the longer term security of transport fuels. Natural gas , while still in its infancy as a road transport fuel in Australia, has the potential to take up a significant proportion of the supply deficiency, so extending our fuel self-sufficiency.

Australia has 2129 billion cubic meters of known economically

recoverable reserves of natural gas [15]. This could be increased markedly by further exploration and new production techniques .

At present in Australia there are only about 500 road vehicles running on natural gas while there are 270,000 in Italy and 70,000 in Argentina. New Zealand has over 45,000 vehicles running on natural gas [15].

Within the next few years, it is quite likely that a significant number of cars, buses and the trucks on Australian roads will be running on natural gas instead of on petrol or diesel fuel.

1.2 NATURAL GAS FUELLING SYSTEM LOGIC

NGV is an acronym for Natural Gas for Vehicles and includes either compressed natural gas (CNG) or liquefied natural gas (LNG). CNG is stored as a gas at high pressure, up to around 20 MPa, in a cylinder. LNG is stored as a liquid at atmospheric pressure in special containers at temperatures below -160 degree C. NGV in relation to this project is compressed natural gas.

Natural Gas for Vehicles (NGV) Refuelling systems range from small home-based compressors providing $2m^3$/hour, to very large facilities dispensing up to 1000-2000 m^3/hour. There are two main filling procedures - fast fill from a large storage and slow fill with the vehicles connected directly to one or more compressors. For quick filling, the station storage is usually divided into three different storage pressure levels. The dispenser sequences through the required pressure levels and the compressors are automatically controlled to give priority to charging the highest storage bank as pressures fall.

A typical compression/fuelling system contains three main components:

- Compressors
- The gas storage, cascade
- Dispenser

The gas is drawn from the local supply line and passed through the compressor, the compressed gas is then fed into a bank of cylinders (cascade) via a priority fill panel.

The function of the panel is to direct the compressed gas in order of priority to the highest need storage bank, or direct to the dispenser.

The cascade usually consists of three banks, a low pressure, medium pressure, and high pressure bank, each consisting of a number of cylinders manifolded together in order to supply a large volume gas reservoir.

The stored pressurised gas is then accessed via a dispensing unit. This unit uses either electronic or mechanical control to select between the cascade banks. For instance when a vehicle commences refuelling, the gas is supplied from the low pressure storage bank until equal pressure is obtained, at this point the sequencing in the dispenser signals the medium bank to open and the above functions are repeated. This process is continued until the dome load regulator closes the system at a preset maximum fill pressure.

Fig. 1.1 shows a complete refuelling system operating on a pressure differential system using three banks of compressed gas storage.

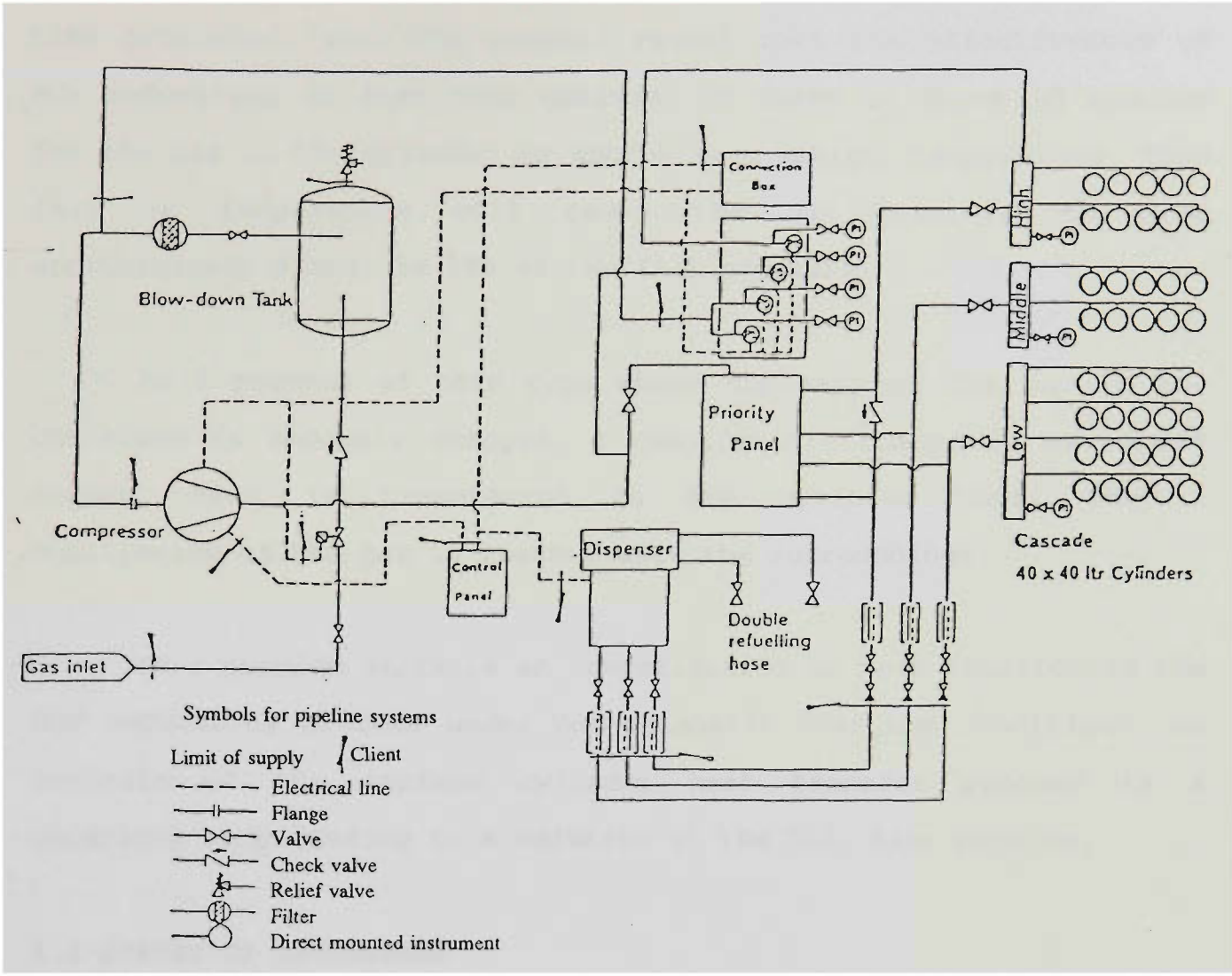

Fig.1.1 Typical refuelling system

1.3 A PROBLEM ASSOCIATED WITH THE REFUELLING PROCESS

There are number of technical areas related to the application of NGV which warrant further development. One of these concerns the need to effectively reduce the time required to charge NGV when refuelling. During refuelling of NGV it is observed that the

temperature of the gas in the vehicle storage cylinder increases until it is some 20-30 degree C higher than ambient. The high gas temperature causes the mass flow rate to diminish. The total mass delivered into the cylinder is therefore reduced and the filling time prolonged, with the overall result that the effectiveness of NGV refuelling is less than optimum. It takes at least 30 minutes for the gas in the cylinder to approximate ambient temperature. This fall in temperature will cause the gas pressure to drop approximately 2 MPa, ie 10% of the fill pressure.

In a process of this type where the mass of the gas in the container is suddenly changed, a considerable change in gas state occurs. Heat is transferred to the cylinder until thermal equilibrium of the gas is reached with the surroundings.

This problem warrants an investigation of heat transfer in the NGV refuelling process under non-adiabatic charging conditions. An analysis of the storage cylinder heat transfer process is a necessary step leading to a solution of the fill time problem.

1.4 SURVEY OF LITERATURE

A review of the limited literature reveals that a considerable research effect has been devoted to heat transfer in a tank storing compressed gas.

In 1958, Reynolds and Kays [23] obtained general solutions for both charging and blowdown systems, as well as simple solutions for limiting cases. They noted that the heat transfer coefficient rose rapidly from zero in the first few seconds and then did not vary markedly thereafter. They suggested McAdams' [18] correlation for

vertical flat plates as a reasonable analysis of the heat transfer during injection, which was given by

$$Nu = 0.13\ Ra^{\frac{1}{3}} \qquad (1\text{-}1)$$

Also, in 1964, Ring [24] suggested the same equation as above for convective heat transfer in a closed container.

The transient state between the end of the injection period and start of free convection was studied by Ulrich, Wirtz and Nunn [25] in 1969, wherein they outlined a procedure for determining the closed container heat transfer coefficient after mass injection. They showed that immediately after injection the instantaneous spatial-average heat transfer coefficient was approximately twice that predicted by free convection. This high value decayed rather rapidly during the first few seconds.

Research was only carried out on one of the several phases of heat transfer in the charging (blowdown) process, until Means and Ulrich [19], in 1975, presented experimental data correlations for the spatially averaged convective heat transfer coefficient for thin walled closed containers during and after injection. In Means' and Ulrich's experiments (ΔP=0.125-1.133 MPa), the injection processes were terminated when the desired pressure was reached. For the injection period (for sonic injection velocities), they proved that heat transfer was not a function of the geometric variables tested. They also showed that the very high heat transfer rates in some cases immediately after injection, were of special significance.

Other relevant experimental work was carried out more recently. A high pressure (ΔP=20-21MPa) quick fill test was conducted by Wyman [29] in 1983, and detailed temperature and

pressure changes during the refuelling process were described. In Australia, Armstrong and McEwen [2] obtained high pressure(ΔP=17-18 MPa) experimental data for temperature, pressure and mass flow rate changes in a vehicle tank in 1990.

The principal results drawn from this literature survey are as follows:

1. During the fast filling process, the gas temperature increased until it was 20 to 30 degree C higher than ambient.

2. Free convection describes at 1least a portion of the heat transfer cycle in a closed container after injection. Most agree that it may be described by an equation of the form

$$Nu = C\,Ra^{m}$$

Where C was found to vary from 0.0201 to 0.53 and m from 1/3 to 2/5.

3. There appears to be a portion of the heat transfer cycle immediately after injection that may not be predicted with certainty.

4. The heat transfer coefficients during injection were found to be very high.

In this thesis it will be shown that the transient heat transfer process which takes place during refuelling of NGV involves three modes of heat transfer and is rather more complex than previously realized.

1.5 AIMS AND SIGNIFICANCE OF PRESENT STUDY

In order to better understand the basic refuelling process, there is a need to carry out a theoretical and experimental study of the heat transfer process between the natural gas and supply cylinder walls.

Models for predicting the gas charging process are generally based on an adiabatic thermodynamic process. However, neglecting the effects of heat transfer leads to substantial errors in the prediction of system behaviour during the refuelling of NGV.

The principle aim of this project is to conduct a comprehensive series of experimental measurements related to gas cylinder re-charging and to use the results in a theoretical model developed to predict heat transfer coefficients appropriate to the process.

The detailed objectives of this project are as follows:

1. Set up a simple theoretical heat transfer model for calculating heat transfer coefficients during the charging process.

2. Establish a refuelling system for the NGV vehicle storage cylinder, and carry out experimental measurements at high pressure fast charging conditions.

3. Derive the transient convective heat transfer data correlation equations.

4. Develop a method for predicting the heat transfer

parameters, by incorporating the model into a computer program which simulates the charging process.

The work outlined above will be carried out with air as the working fluid. This is for experimental safety reasons, and for comparing results with those of similar studies, which have, with one exception, used air as the working fluid.

The outcome of this research should lead to better design of natural gas fuel systems characterised by: optimum filling times, improved safety and increased use of NGV. Further improvement in NGV systems would lead to important economic benefits and increased market opportunities for NGV equipment manufactures as well as favourable ecological outcomes arising from reduced emissions.

A paper [16] including the principal work of this research (Chapter 4 and Chapter 5) has been accepted for presentation and publication at The 6th International Symposium on Transport Phenomena in Thermal Engineering, Seoul, Korea, May 9-13, 1993.

CHAPTER 2

THEORETICAL MODEL OF HEAT TRANSFER

In this chapter, a simple heat transfer model for the storage cylinder charging process is presented. The model may be applied in calculating the heat transfer coefficients, both for deriving the heat transfer data correlations (Chapter 5) and in the simulation used to predict the heat transfer parameters (Chapter 6).

2.1 SIMPLE MODEL

The model of the cylinder charging system employed in the present analysis is shown schematically in Fig 2-1 .

The total heat transfer zone will be divided into three parts: inside cylinder, outside cylinder and cylinder wall. They are modelled as one-dimensional regions.

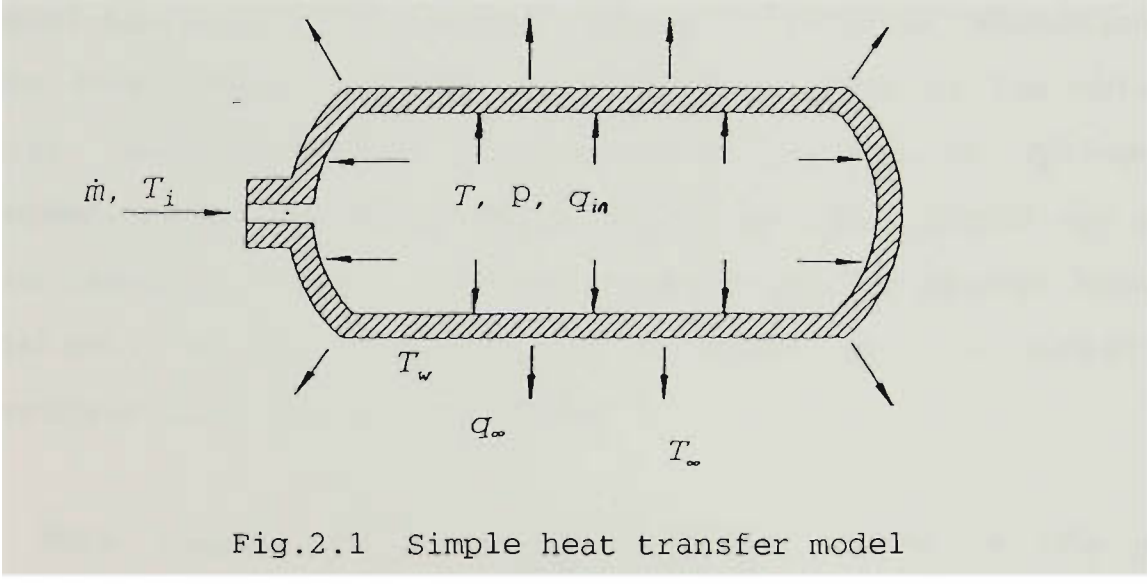

Fig.2.1 Simple heat transfer model

To set up the model, the following assumptions are made:

(1) The cylinder volume, and the mass and specific heat of its walls are constant.

(2) The gas in the cylinder is mixed and at the same state

everywhere in the cylinder. This means that the gas temperature in the cylinder may be regarded as uniform throughout, although in fact it varies locally (this is studied in chapter 4).

(3) The temperature of the cylinder wall is uniform.

These assumptions made it possible to use average temperatures as well as average heat transfer coefficients as variables, and the cylinder is treated using the lumped capacitance method.

2.2 LUMPED CAPACITANCE METHOD

It has been observed that the temperatures increase significantly during the charging process. As the temperature inside the cylinder is changed, the temperature at each point in the system is also changed. Consider that the cylinder is at ambient temperature initially and then is heated by an influx of hot gas suddenly. Energy is transferred by convection from gas to the internal surface of the cylinder. Energy transfer by conduction then occurs from internal surface to external surface of the cylinder. Finally, energy transfer from external surface of cylinder to atmosphere is by convection again. As the boundary conditions of the system change with time, the heat transfer process becomes transient in nature. Changes will continue to occur until a steady-state temperature distribution is reached.

With respect to a control volume, a form of the energy conservation equation that is useful for heat transfer analysis may be stated as follows: " The rate at which thermal and mechanical energy enters a control volume minus the rate at which this energy leaves the control volume must equal the rate at which this energy is stored in the control volume."

Consider applying energy conservation to the system shown in Fig. 2.2 . The energy conservation equation is expressed as

$$Q_i - Q_o = E_{st} \qquad (2-1)$$

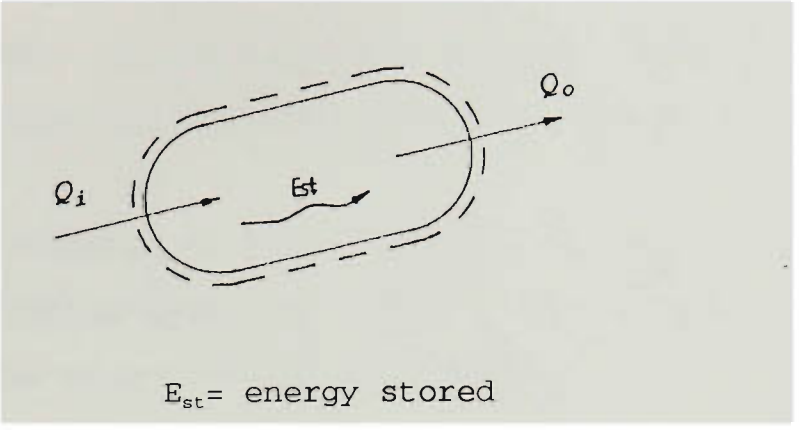

Fig.2-2, Control volume of cylinder wall

The key feature of the lumped capacitance method is the assumption that the temperature of the solid is spatially uniform at any instant during the transient process. This assumption means that temperature gradients within the solid are negligible. From Fourier's law, heat conduction in the absence of a temperature gradient implies the existence of infinite thermal conductivity, such a condition is clearly impossible. However, although the condition is never satisfied exactly, it is closely approximately if the resistance to conduction within the solid is small compared with the resistance to heat transfer between the solid and its surroundings.

The lumped capacitance method is simple and convenient. It is important to determine whether it may be used with acceptable accuracy in this research. In relation to cylinder charging, Reynolds and Kays [23] used the lumped parameters method in their research and derived very accurate theoretical results. In this research, the applicability of the lumped heat capacitance method is

proven in chapter 4.

2.3 THERMODYNAMIC ANALYSIS OF SYSTEM

The cylinder charging process in this research is a transient fluid flow, which can best be studied as a unsteady-flow problem.

For our purpose of this research, a control volume has been selected, as indicated by the dashed line in Fig.2.3, which includes essentially the volume inside the cylinder.

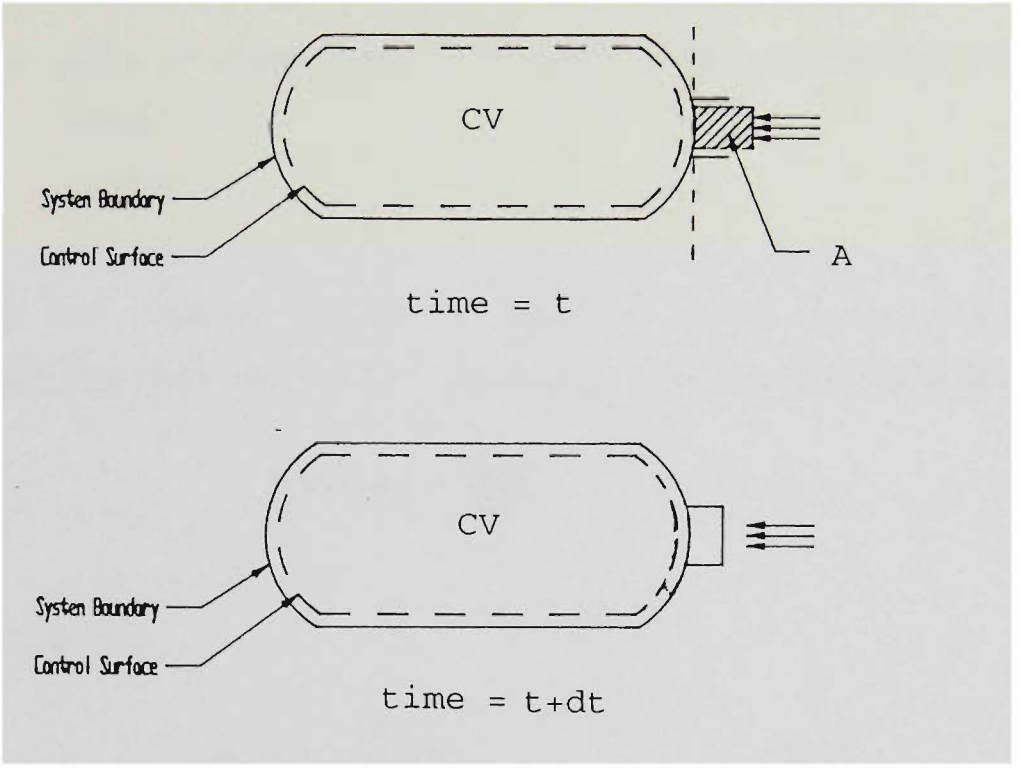

Fig.2.3

Energy conservation for a control-volume analysis

Fig.2.3 illustrates the general procedure. A control mass consisting initially of mass within region A and the control volume (CV) is followed over a time dt as mass within region A enters the control volume.

In standard texts of thermodynamics, a general conservation of

energy statement for a control volume in unsteady flow is developed by extending the energy equation developed for a control mass. In Wark's book [28], the standard unsteady flow energy equation (UFEE) is expressed as

$$\dot{Q}+\dot{W} = \frac{dE_{cv}}{dt}+\sum_{o} e\dot{m}-\sum_{i} e\dot{m}$$

where $\dot{Q}$ - rate of heat transfer to or from the control volume;

$\dot{W}$ - rate of any forms of work associated with the control volume;

dE_{cv}/dt - rate of energy of control volume;

e - energy of fluid crossing the control volume;

$\dot{m}$ - rate of mass flowing in or out the control volume.

i - inlet

o - outlet

Consider our control volume in Fig.2.3, since there are no outlet terms $\sum_{o} e\dot{m}$ and only one inlet term $e_i\dot{m}_i$, the general equation becomes

$$\dot{Q}+\dot{W}+e_i\dot{m}_i = \frac{dE_{cv}}{dt} \qquad (2\text{-}2)$$

By introducing

$$e_i = u_i+\frac{V_i^2}{2}+gz_i \qquad (2\text{-}3)$$

and since the work term in equation (2-2) only includes flow work on the basis of the cylinder charging process, that is

$$\dot{W} = p_i v_i \dot{m} \qquad (2\text{-}4)$$

equation (2-2) becomes

$$\dot{Q} + \left(u_i + \frac{V_i^2}{2} + gz_i + p_i v_i\right)\dot{m} = \frac{dE_{cv}}{dt} \qquad (2\text{-}5)$$

as the enthalpy h_{en}= u+pv,

We obtain

$$\dot{Q} + \left(h_{en_i} + \frac{V_i^2}{2} + gz_i\right)\dot{m} = \frac{dE_{cv}}{dt} \qquad (2\text{-}6)$$

According to Wark's work[28], if the velocity of the flow stream in the high pressure line is relatively low (e.g. less than 60 m/s) and the entrance pipe relatively short in the vertical direction, then the kinetic and potential energies of any unit mass on the line may be neglected. It will be shown in this research (Chapter 4) that the maximum velocity of the gas in the cylinder charging process was less than 60 m/s. Whence equation (2-6) can be simplified to

$$\dot{Q} + h_{en}\,\dot{m} = \frac{dU_{cv}}{dt} \qquad (2\text{-}7)$$

where dU_{cv}/dt is the rate of change of internal energy in the control volume.

During the cylinder charging process the ranges of gas temperature and pressure changes are T= 15 - 60 (C) and p= 0.101 - 20 (MPa), the compressibility Z of air is from 0.99 to 1.04. Under these conditions, air can be treated as ideal gas. We then have

$$h_{en_i} = c_p T_i \qquad (2\text{-}8)$$

$$U_{cv} = mu = mc_v T \qquad (2\text{-}9)$$

Note that c_v and c_p are treated as constants, since as shown in reference [9] and [12], as well as in section 5.1, that over the temperature and pressure ranges encountered in the cylinder charging

process c_p and c_v of air change by only a small amount.

Thus, substituting equation (2-8) and (2-9) into equation (2-7), we obtain

$$\frac{d(mc_vT)}{dt} = \dot{m}c_pT_i + \dot{Q} \qquad (2\text{-}10)$$

then, re-writing in terms of heat transfer parameters,

$$\frac{d(mc_vT)}{dt} = \dot{m}c_pT_i - h_{in}A_{in}(T - T_w) \qquad (2\text{-}11)$$

Equation (2-11) is the same as the equation derived in the study of Means and Ulrich [19].

By re-arranging, we finally obtain

$$h_{in} = \frac{\dot{m}c_pT_i - c_v(T\dot{m} + \dot{T}m)}{A_{in}(T - T_w)} \qquad (2\text{-}12)$$

Equation (2-12) is sufficient to determine the heat transfer coefficient from experimental measurements of the parameters involved, provided that reliable experimental data can be obtained. The measured values include gas temperature T, cylinder wall temperature T_w, cylinder inlet temperature T_i, gas pressure p and mass flow rate $\dot{m}$. The variable time derivatives of the gas temperature T and the cylinder inlet temperature T_i could be also obtained by curve fitting the measured data and the first derivative of these two variables with respect to time t. The calculation procedures of c_p and c_v are described in chapter 5.

CHAPTER 3

EXPERIMENTAL APPARATUS AND TECHNIQUES

In this research program the principal measurements performed during the gas storage cylinder refuelling process relate to determining the conditions within the cylinder as well as at the inlet and external to it.

Measurement of the internal conditions was a demanding task, especially the temperature changes inside the cylinder. In the refuelling process, due to high velocities, and mixing and turbulence of the gas flow, there are significant changes in temperature throughout the cylinder. Moreover, the final pressure in the cylinder was extremely high (about 17-20 MPa), so stringent safety measures were required for the experiments. Accurate calibration of the measurement system, along with rapidly responding thermocouples and effective sealing of the cylinder were also required.

The details of equipment and calibration are given in this chapter.

3.1 Experimental Apparatus

The test apparatus consisted of a cascade storage unit, gas cylinder, thermocouple array assembly, pressure transducer, mass flow meter, and a data acquisition system. The schematic layout of the apparatus and associated equipment is shown in Fig.3.1.

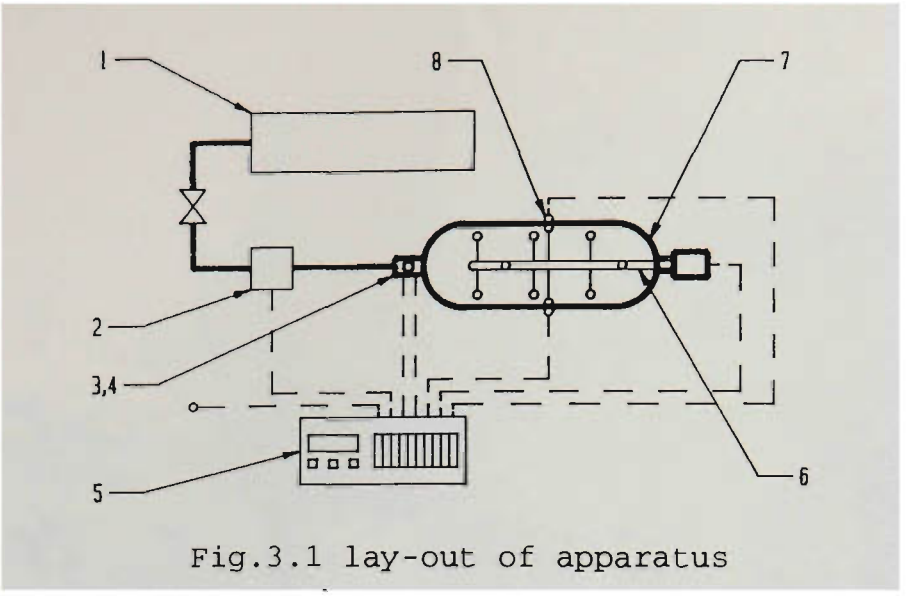

Fig.3.1 lay-out of apparatus

The gas storage cylinder (7), with a filling connection at both ends, was installed on a frame. One end of the cylinder was sealed off with a thermocouple array (6) on which there were ten thermocouples, while the opposite end was connected by tubing to the cascade storage. A pressure transducer (4) and type J thermocouple (3) were placed just downstream of the fill valve. Another two thermocouples (8) were cemented onto outside surface of the cylinder with epoxy resin. The paint on the cylinder where the thermocouples were attached was removed. A mass flow meter (2) was positioned close to the neck of the cylinder. The output cables of the thermocouples, pressure transducer and the mass flow meter were connected to a data acquisition system (5) which recorded the temperature, pressure and mass flow rate along with the filling time. The gas storage cascade (1) supplied gas to the cylinder. Both a thermocouple and a glass thermometer were used to obtain ambient temperatures.

A photograph of the apparatus set-up may be seen in Fig.3.2.

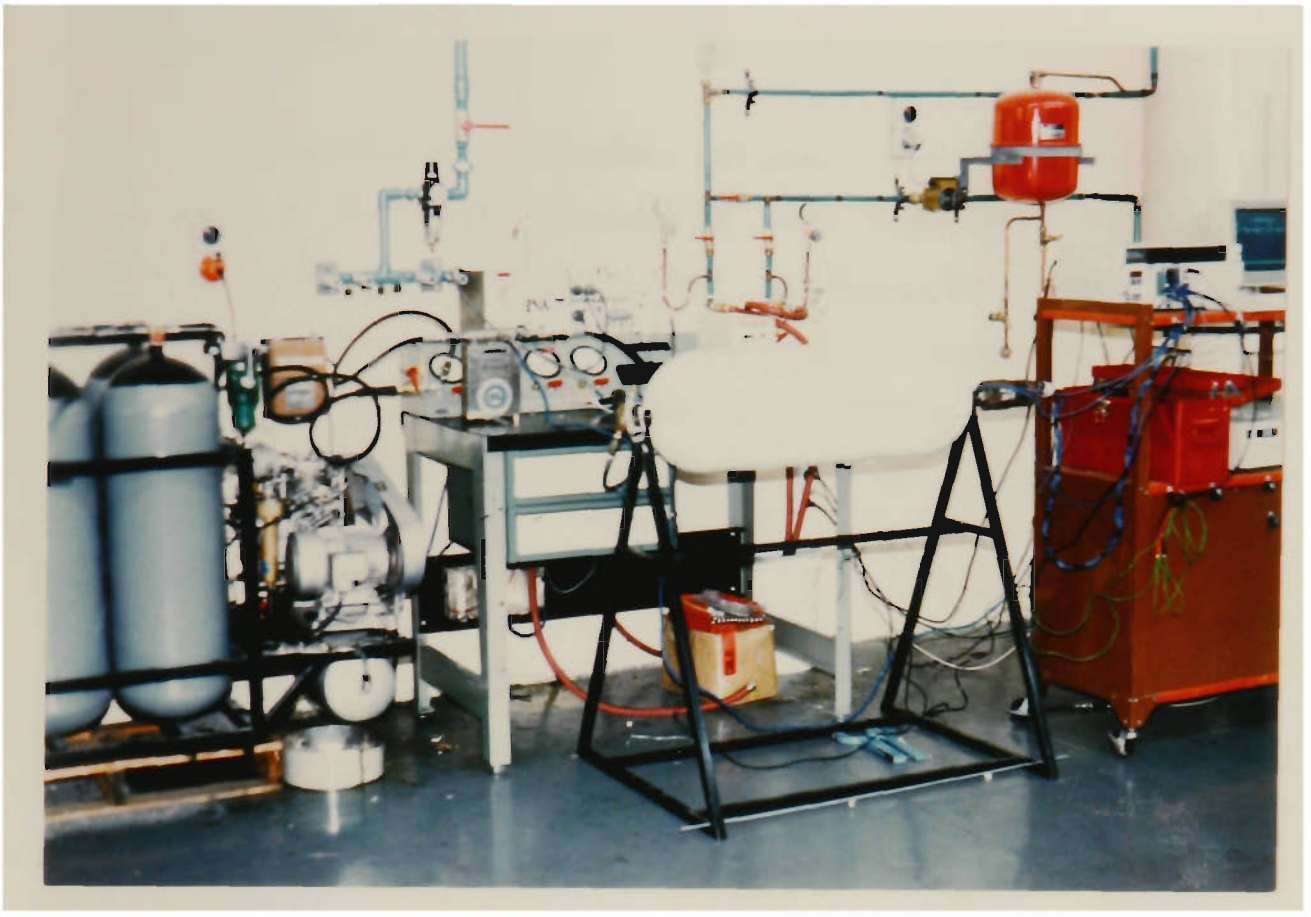

Fig.(3.2) Photograghs of apparatus set-up

3.1.1 Cylinder

The instrumented cylinder designed for NGV storage in vehicles, with a 3/4" NTP fitting in both ends was used in the experiment as the gas cylinder. This allowed the normal filling apparatus to be fixed in one end while a temperature measuring device (thermocouple array) could be fixed in the other end. The cylinder was 56 litres in volume and made of Cr-Mo steel. More details are shown in Fig.3.3.

3.1.2 Thermocouple Array

A Thermocouple array was designed and made for measuring the gas temperature and its distribution during the charging process. It accommodated ten thermocouples, as shown in Fig.3.3. It consisted of an arm and an end piece to form a cantilever beam. The type T thermocouples were set in stainless steel tubing supports. The ends of the arm had long holes through it. The stainless steel tubes were forced into closed coil tension springs that were screwed into holes tapped into the cantilever. The details are shown in Fig.3.4. This was a convenient way of folding all the equipment so it could fit through the threaded opening in the cylinder but allow the tubes to spread out into fixed positions once inside the cylinder. The tubes were also flexible enough to be removed when required. There were a total of ten thermocouples distributed evenly throughout the cylinder. They were all fixed in the one plane allowing different planes to be studied by rotating the cylinder. Photographs of the thermocouples array assembly can be seen in Fig.3.5.

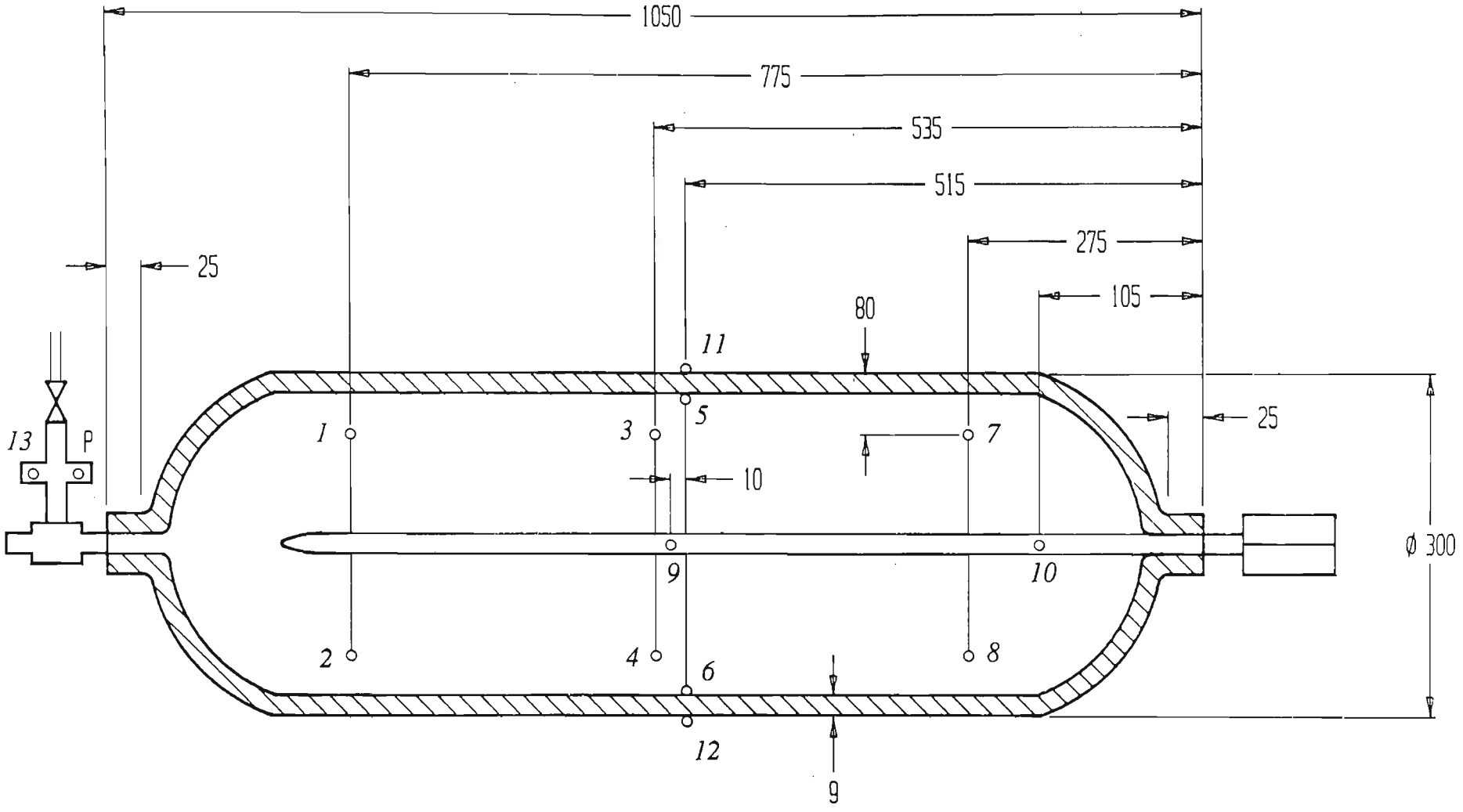

Fig.3.3 Cylinder and thermocouples array assembly

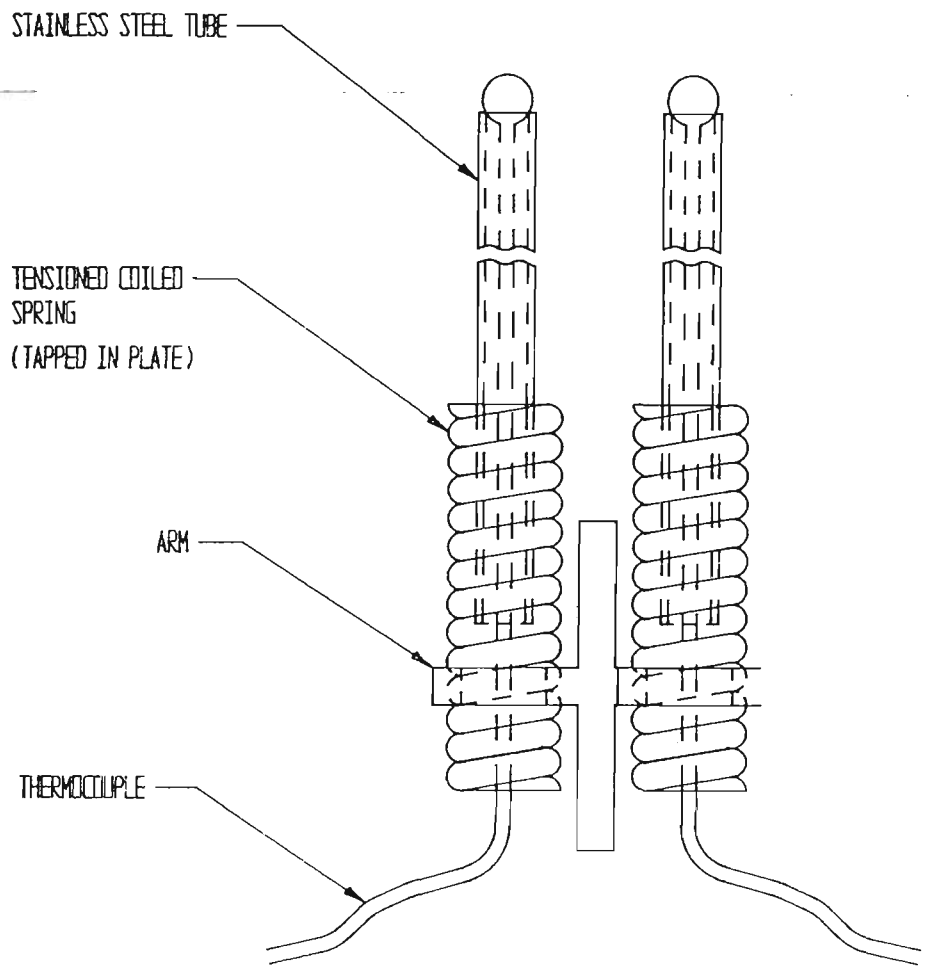

Fig. 3.4 Details of thermocouples array assembly

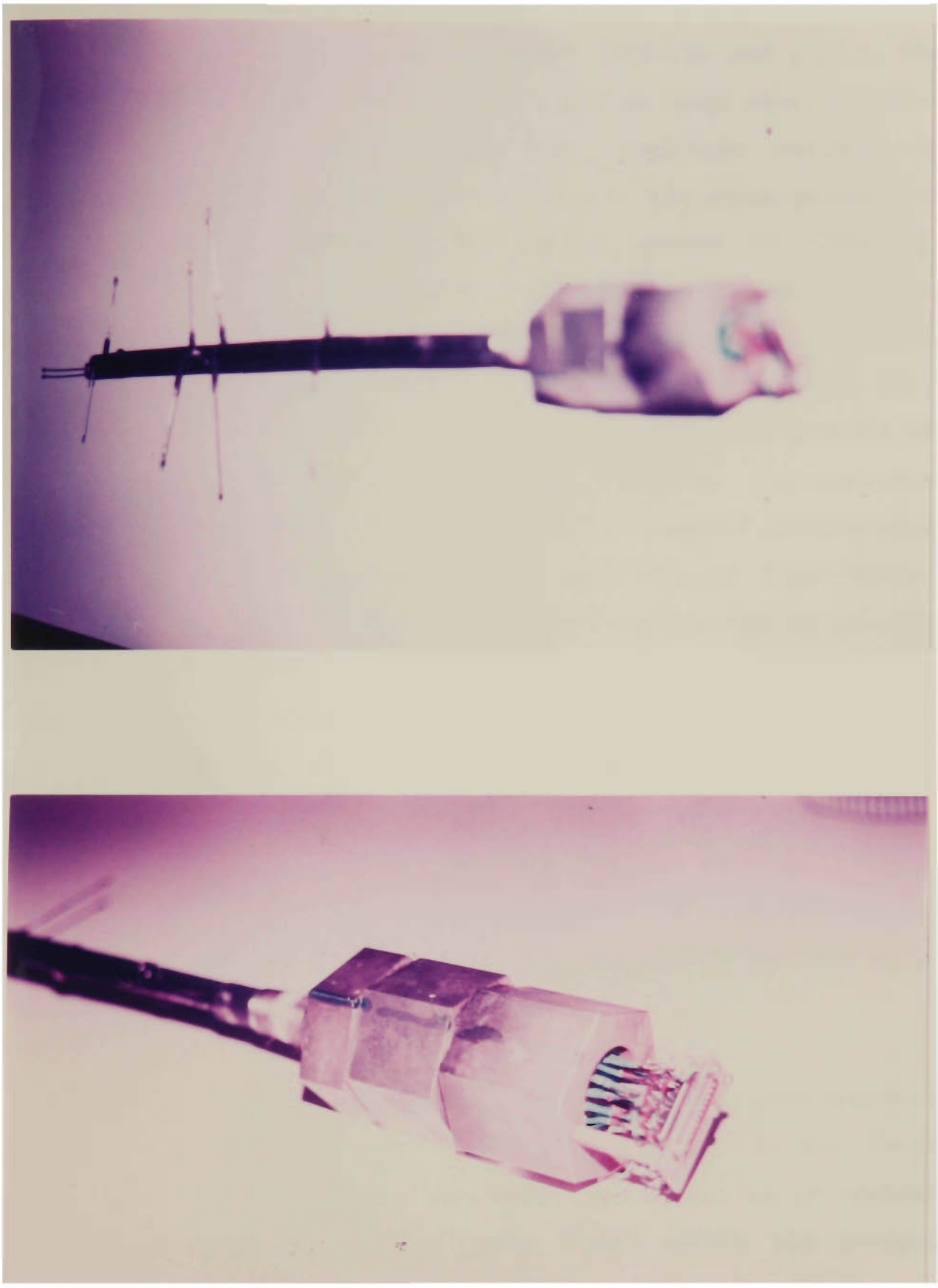

Fig.(3.5) Photographs of thermocouples array assembly

The thermocouple wires were fed back into the end piece. The pressure of gas used in this experiment was so high that adequate sealing in the end piece became most important during the manufacture. The end piece is shown in Fig.3.6. The wires passed out though the holes drilled through (1) and (2). Rubber "o" rings (6) were used to seal the gaps between each element. Element (5) was made of bakelite with enough hardness to withstand the extruding effect of the high pressure. Twenty holes were drilled through (5), and then twenty bolts (4) were inserted through the holes and all of these were secured by nuts. Small holes (diameter= 1.0 mm) were drilled through each bolt, each single metal sheathed thermocouple wire was bared and then passed through each hole in these bolts. Silver solder was used to fill these holes through the bolts. The length of silver solder in holes was long enough to ensure good sealing. The preparations above were for sealing were not only between wires and the end piece, but also to prevent leakage the leaking between wires and the insulation of the thermocouples.

Finally, the wires were insulated again after leaving the end piece and then connected to a plug (8), which may be seen in a photograph in Fig.3.5 on previous page.

The ability of the experimental system to withstand pressure was carefully examined to ensure effective sealing. It was found that the system satisfied the requirement quite well as no leaking of gas was detected around the whole system within the maximum pressure value (20 MPa).

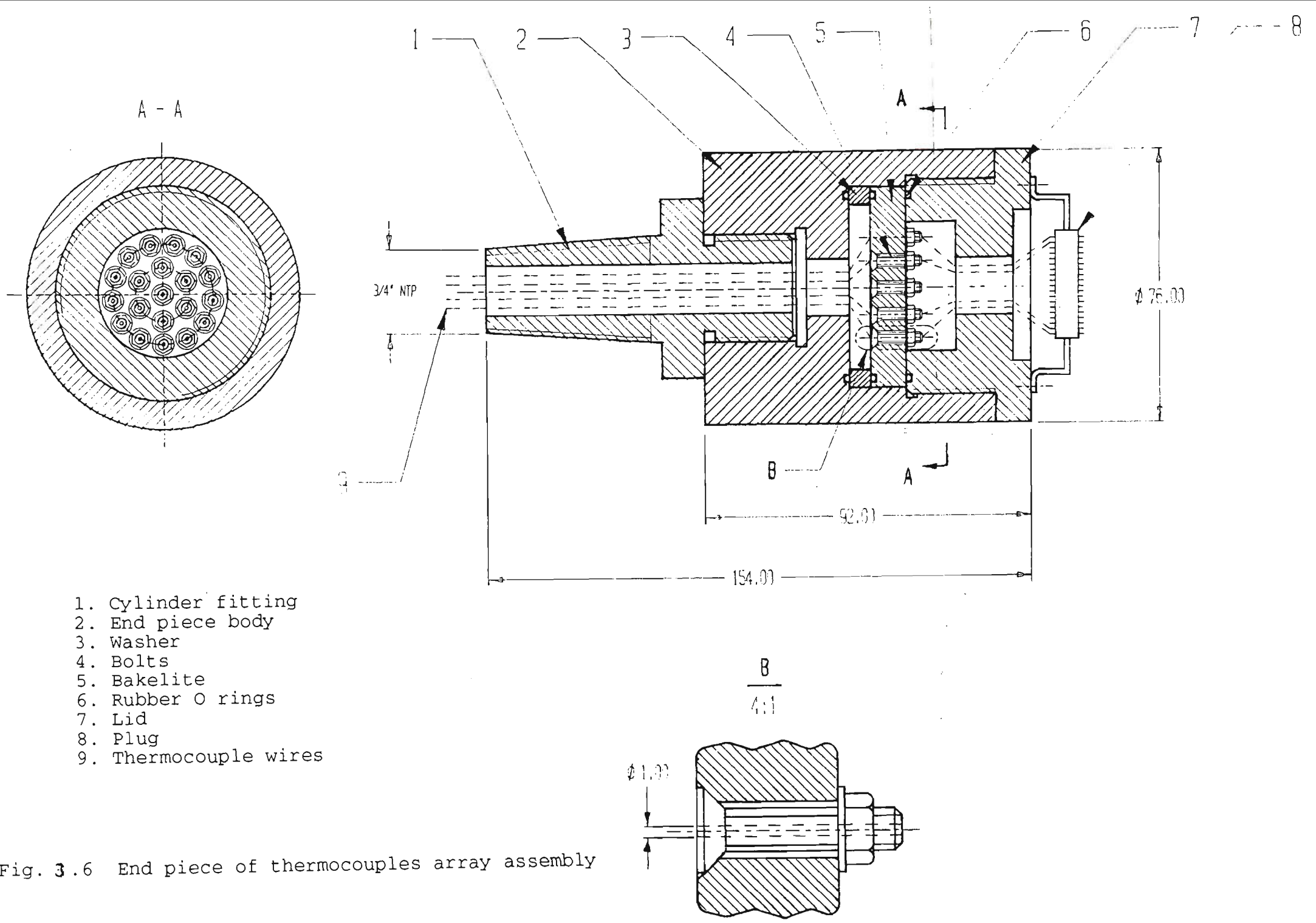

1. Cylinder fitting
2. End piece body
3. Washer
4. Bolts
5. Bakelite
6. Rubber O rings
7. Lid
8. Plug
9. Thermocouple wires

Fig. 3.6 End piece of thermocouples array assembly

3.1.3 Instrumentation and Data Acquisition System

MDAS Modular Data Acquisition System 7002 (KAYE) was used for the experiments. Its functional block diagram is shown in Fig.3.7. MDAS provided high speed data collection, storage and manipulation for measurement applications and dynamic testing. During the test, MDAS streamed data directly to its hard disk for long term storage. The MDAS software controlled the system. It sent commands (digital words) to the measurement and control hardware and measured data. The data was in integer format. The programming software required the user to write programs. In this research, a program was made in which the I/O cards, signals, sampling period and the amount of data were determined. The sampling period was set at 1 second, that is, all the channels were scanned once per second, over a total data collection period of 10 minutes. Two thermocouple I/O cards were plugged into MDAS. Each card had seven channels "A" through "G" of voltage input. The thermocouple wires from the plug of the cylinder were connected to these cards. Finally, a PC computer was used in communicating between user and MDAS, for delogging and subsequent data processing.

Pressure Transducer A capacitive type pressure transducer model 280E Setra was chosen. It provided a 0-5 VDC output. A capacitor was formed between the sensor body and an insulated electrode plate. An increase in pressure caused a deflection of the diaphragm which decreases the capacitance. The output cables were connected to MDAS voltage I/O card.

Mass flow Meter The mass flow meter used in this experiment was Model D25H-SS Micro Motion portable mass flow meter. It consisted of a sensor unit operating on the 'Coriolis' principle and a remote

signal processing unit. Signal connection was made via the interconnect cables between the sensor unit and terminals of the remote electronics unit. The output cables were connected to MDAS voltage I/O card.

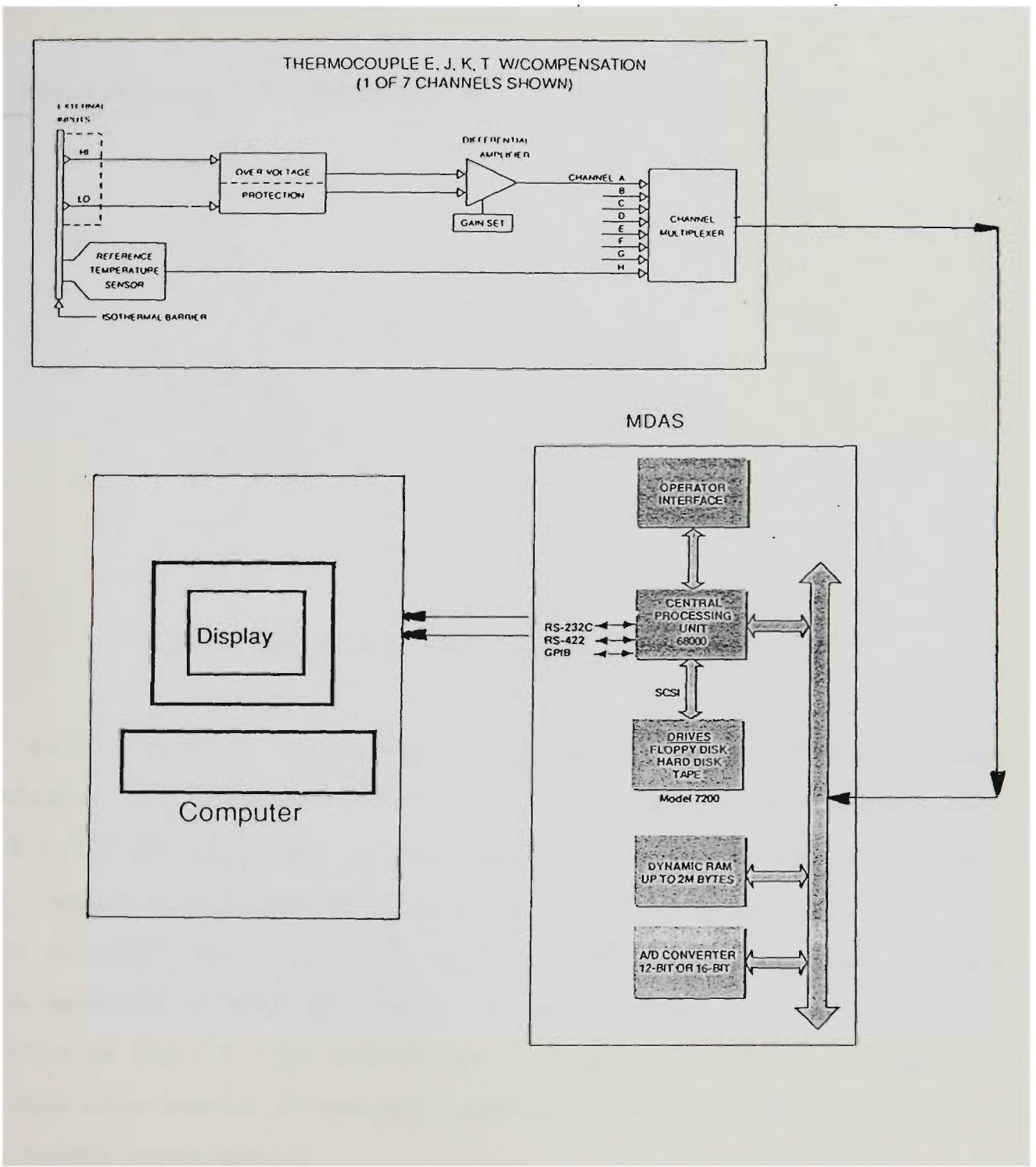

Fig.3.7 MDAS functional block diagram

3.2 CALIBRATIONS FOR TEMPERATURE MEASUREMENT

To ensure more precise temperature measurement, many repeat calibrations were done before and after the experiments.

3.2.1 Calibration method

Fig.3.8 shows the components of the calibration system.

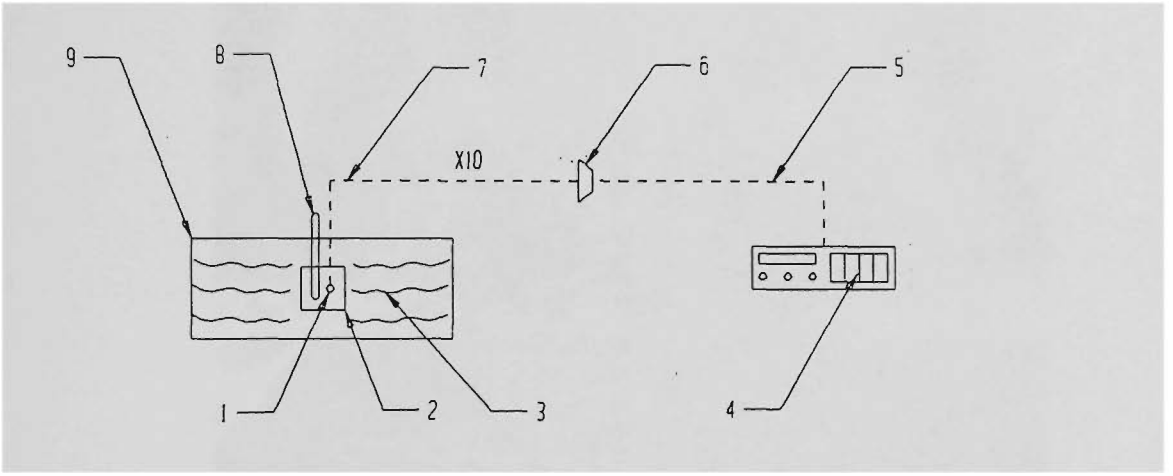

Fig.3.8 Components of calibration system

As it is shown, thermocouples (1) were inserted in holes of the container (2) together with the reference glass thermometers (8) with 0.1 °C accuracy. All of them were put in the stirred liquid bath (9) which was filled with water (3). The thermocouple wires (7) were connected to the extension wires (5) through the plug (6) and were inserted in MDAS I/O cards (4). A photograph of the set up may be seen in Fig.3.9. The significance of the installation is that the devices were tested as one unit and the conditions were the same as the formal experiments.

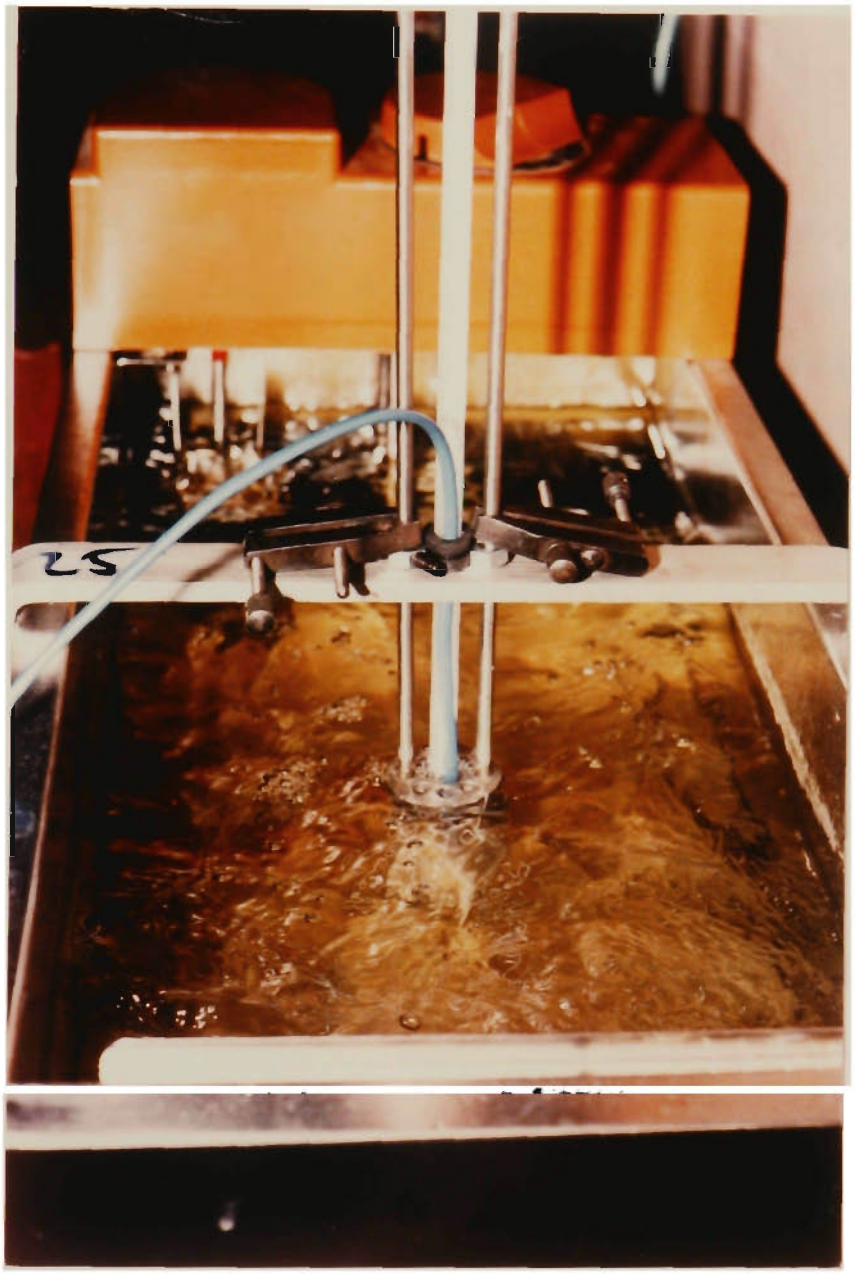

Fig.(3.9) Photographs of temperature measurement calibration devices

At temperature range from ambient to 100 °C, the stirred liquid bath provided an isothermal medium for bringing thermocouples and reference thermometer to the same temperature.

The calibration consisted of the measurements determined for a finite number of known temperatures taken over three runs.

3.2.2 Calibration Result

The data obtained from the MDAS are digital numbers. Interpolation between the calibration points was possible since the emf changed only slowly and smoothly with temperature. The calibration data was presented directly in terms of temperature and digital numbers, on a scale so chosen that the information appeared well represented by a single curve in Fig.3.10 and a simple equation was derived as:

$$T=0.00146N+29.17 \qquad (3-1)$$

(*N-integer number*)

It is noted that the data between the eleven channels are similar enough that single curve and equation were taken as the result of calibration.

The accuracy was obtained at each calibration point by comparison with standard reference thermometer with 0.1 C accuracy. The data is shown in table 3.1. As a result, the most probable error of the system is ±0.24 °C.

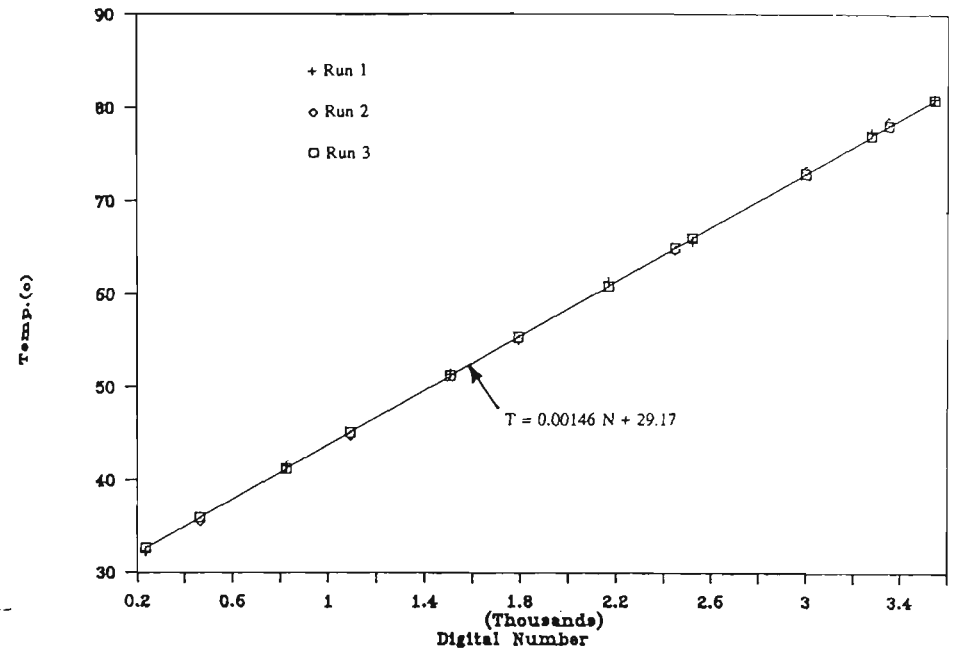

Fig.3.10 Calibration results of temperature measurement system

Table 3.1 Calibration data of temperature measurement

Run no.	Tr (C)	Ta (C)	Error (C)
1	32.30	32.65	0.35
2	35.50	35.97	0.47
1	41.50	41.26	-0.24
2	44.80	45.16	0.36
1	51.40	51.23	-0.17
2	55.10	55.38	0.28
1	61.30	60.86	-0.44
2	64.70	64.94	0.24
1	65.70	66.02	0.32
2	73.40	73.00	-0.40
1	77.40	77.06	-0.34

Tr - Temperature of reference thermometer

Ta - Temperature of acquisition by system

3.2.3 Radiation Effect

In the experiments, radiation shields were initially used for each thermocouple junction. However, as it is shown later in Fig.3.12, the response time of thermocouples was prolonged. In order to decrease the response time, the thermocouples shields were finally removed. In this case, the radiation effect must be taken into account in calculations to avoid error.

When the temperature was being measured by the thermocouples inside the cylinder, the temperature indicated was determined by the overall energy balance of the thermocouples. The energy would be transferred by convection to the thermocouples and dissipated by radiation to the surroundings. Thus the energy balance becomes:

$$hA(T_g - T_t) = \sigma \epsilon A(T_t^4 - T_s^4) \qquad (3\text{-}2)$$

T_g - Gas temperature;

T_t - Thermocouple temperature;

T_s - Surrounding temperature.

ε - emissivity of thermocouple junction

Therefore, the temperature indicated by the thermocouples could not be the true temperature. In this research, the average heat transfer coefficient h could be derived depending on experimental data. By equation 3-2, the correction of T_g could be done relative to a particular time.

3.3 TIME CONSTANT OF THERMOCOUPLES

3.3.1 Measurement

During the filling process, especially in the first stage, the temperature change inside the cylinder is expected to be rapid. The real process can not be determined precisely if the response time of the thermocouples is not rapid enough.

To get the quickest response time of thermocouples, thermocouple junctions with low mass (diameter=1.5mm) have been selected. To determine the thermocouple response a dynamic calibration was undertaken. The lay-out of the measurement devices is shown in Fig.3.11. It was carried out with a cross flow heat exchanger. A thermocouple was heated by placing it in a cylindrical electric heater (3). The heater was supplied with current at a low voltage from a rectifier and raised temperature of the thermocouple to a maximum of about 80 C. A fan was driven by motor (2) and air entered the apparatus by way of a bell mouth (4). Air velocity could be controlled by adjusting a throttle valve (1).

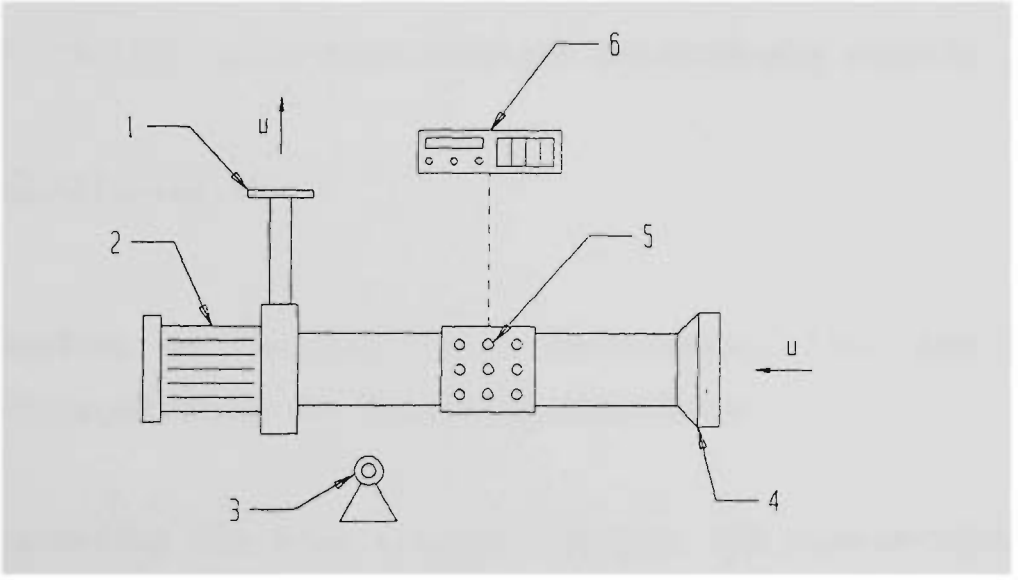

Fig.3.11 Thermocouple time constant measurement devices

When the test began, a stable air velocity was set up, then, the thermocouple, used in the formal experiments, was withdrawn from the heater and dropped into the working section (5) through a hole on the top of the section as rapidly as possible. The data of temperature change was taken by MDAS (6) during the whole process.

Relative to several different velocity values, the temperature changes with time of the thermocouple were recorded. Fig. 3.12 shows the test result.

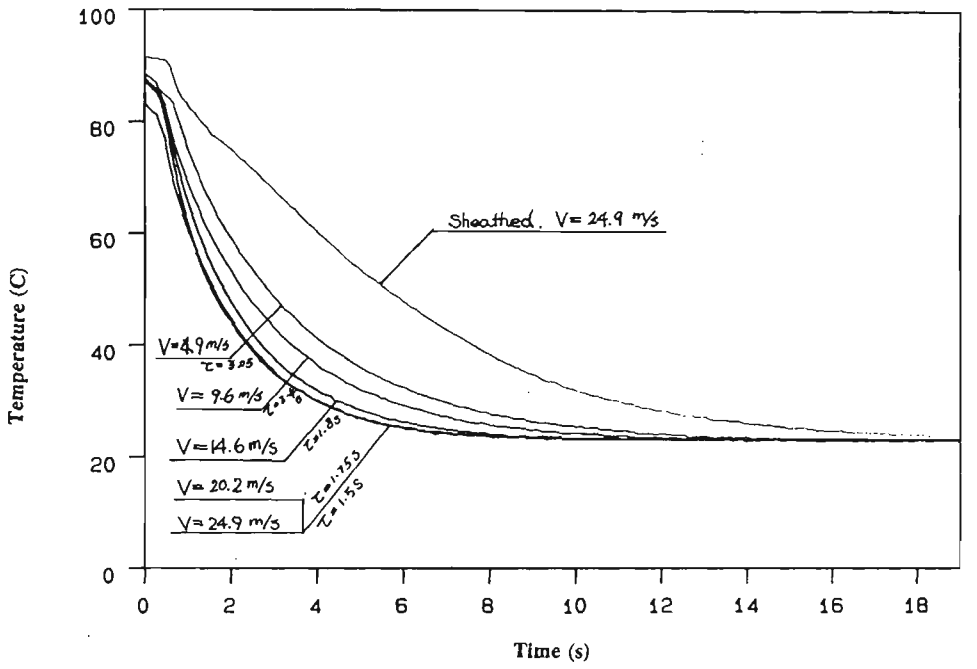

Fig. 3.12 Thermocouples time constant measurements results

3.3.2 Calculation

Depending on the particular measurement, the time constants were calculated using the following procedure:

Considering the heat transfer between the thermocouple and the gas flow, we have:

$$q = hA(T_t - T) \qquad (3-3)$$

$$-qdt = mCdT_t \qquad (3-4)$$

m - mass of thermocouple junction

C - specific heat of thermocouple junction

t - time

T_t - Thermocouple temperature

By the combination of equation (3-3) and (3-4), and integrating,

$$\ln(T_t - T) - \ln(T_o - T) = -(\frac{hA}{mC})t \qquad (3-5)$$

T_o is the initial temperature of thermocouple.

Since the definition of time constant is:

$$\tau = \frac{mC}{hA} \qquad (3-6)$$

equation (3-5) could be written as:

$$\ln(T_t - T_g) - \ln(T_o - T_g) = -\frac{t}{\tau} \qquad (3-7)$$

For convenience in plotting,

$$lg(T - T_g) = -2.3\frac{t}{\tau} + 2.3lg(T_o - T_g) \qquad (3-8)$$

Plotting $lg(T-T_g)$ against t, the slope S of this curve should be

$$S = \frac{1}{\tau} \qquad (3-9)$$

And then , the time constant could be calculated by

$$\tau = \frac{1}{S} \qquad (3-10)$$

Table 3.2 shows result of the calculation.

Table 3.2 Thermocouple time constant measurement result

	Run1	Run2	Run3	Run4	Run5
Throttle Opening (%)	100	80	60	40	20
V (m/s)	24.9	20.2	14.6	9.6	4.9
Temp. range	80.9-23	77.1-23	82.4-23	84.1-23	85.3-23
Time constant(s)	1.5	1.75	1.8	2.4	3.1
Re	2372.9	1925.0	1391.4	914.9	467.0
h(W/m^2C)	1266.15	1085.32	1055.24	791.43	622.84
Nu	73.44	62.95	61.20	45.95	36.12

The heat transfer coefficient h was calculated by

$$h=-2.3\left(\frac{mC}{A}\right)S=0.77\frac{r\rho C}{\tau} \qquad (3\text{-}11)$$

where

C= 0.3695 kJ/kg.C

r= 0.0007 m

ρ= 8,9926 kg/m^3

3.3.3 Analysis

(1) During the cylinder charging process, the thermocouple response time varies as a function of time, since the gas velocity changes with fill time. Also, it is difficult to estimate the velocity profile inside the cylinder. Therefore, the temperature data could not be corrected with a fixed time constant value or any other fixed time lag factors, because of the variation of the thermocouple time response.

(2) To obtain satisfactory experimental results, a batter approach is to carefully select the thermocouple so that its time constant error is negligible. In this research, the thermocouples with lowest mass have been achieved. The measured results of the thermocouple time constants in this Chapter (Fig.3.12) are very significant to be used for estimating the upper limit and lower limit errors of the experimental results, depending on the velocity changes. The experimental results would be reliable if the errors are "accepted".

3.4 CALIBRATION OF PRESSURE AND MASS FLOW RATE MEASUREMENT

Like the calibration of the temperature measurement system, the calibration of pressure and mass flow rate were carried out by treating the system as one unit, ie overall system calibrations rather than component calibrations.

For pressure measurement the transducer and cables comprise the system. A pressure gauge with 0.05 MPa accuracy connected in the pipe between the storage cascade and the cylinder was given a reference value. While several steady states of pressure were set up, MDAS was run and the output voltages were recorded. The result is shown in Fig.3.14 and table 3.3.

Table 3.3 Calibration of pressure measurement

p(MPa)	2.3	5.2	7.3	9.6	12	13.4
Voltage(v)	0.5	1.2	1.7	2.3	2.9	3.2

As a result, the following equation was obtained

$$p = 4.07V+0.3 \qquad (3-12)$$

The most probable error of the equation 3-12 is within ±0.02 Mpa.

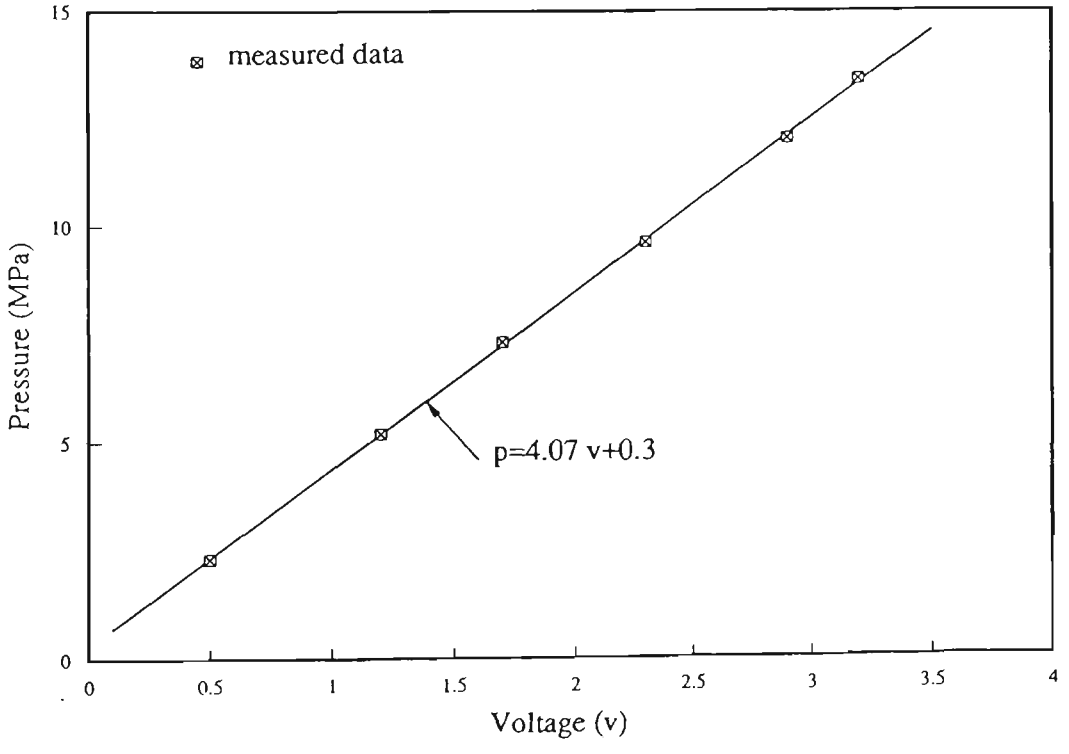

Fig.3.14 Calibration of pressure measurement

For mass flow rate measurement, the mass flow meter, cables and MDAS form a unit to be calibrated. Another reference mass flow meter with mass flow rate value displayed is used as calibration reference. The reference flow meter has the accuracy of ±2% of rate, which is traceable to a NBS certificate. During the calibration, when mass flow rate was kept on certain figure shown by the display, MDAS run and the mass flow rate value was recorded. Fig.3.15 and table 3.4 shows the results.

Table 3.4 Calibration of $\dot{m}$ measurement

$\dot{m}$(kg/min)	0	0.5	0.98	1.7	3.34
Voltage(v)	1	1.42	1.76	2.3	3.52

By curve fitting, the following equation was found

$$\dot{m}=1.33V-1.37 \qquad (3\text{-}13)$$

The most probable error of equation (3-13) is within ±0.018 kg/min.

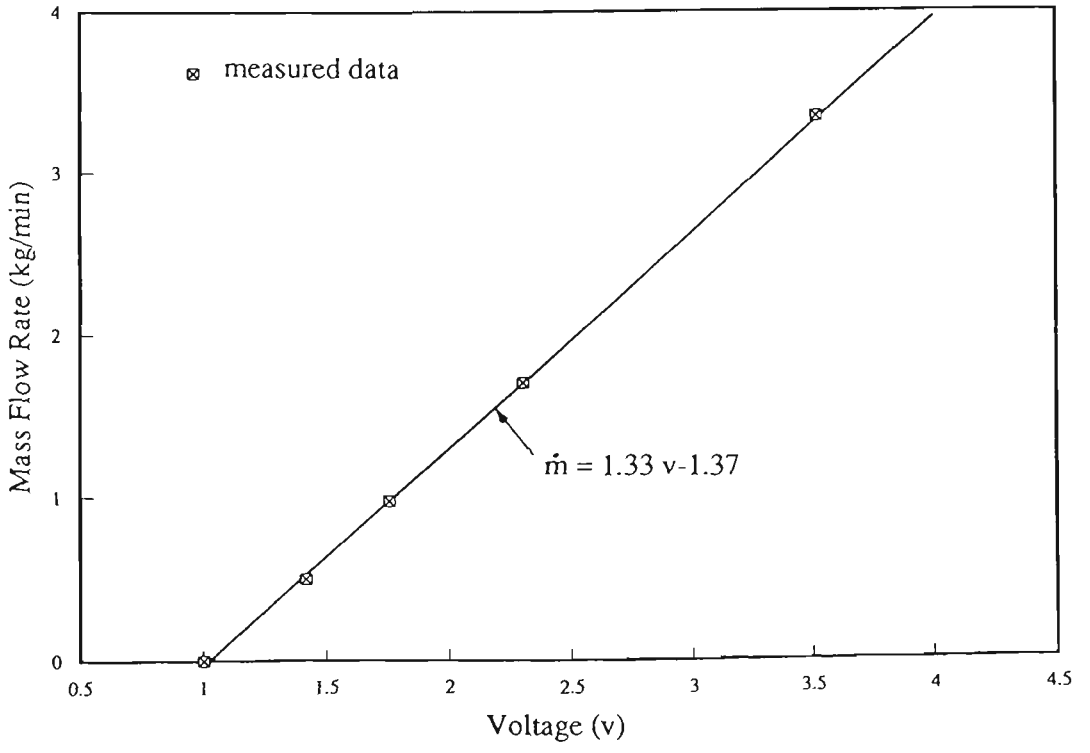

Fig.3.15 Calibration of mass flow rate measurement

CHAPTER 4

EXPERIMENTAL RESULTS AND ANALYSIS

The parameters of fundamental importance in the experiments are the temperature, pressure and mass flow rate changes with time. The experimental results not only can be used in investigating the heat transfer mechanism of the charging process, and the data correlations made, but also the comparison with simulation results can be carried out (Chapter 6).

In this chapter, nine experimental runs are described. Detailed results of three typical tests are displayed in tables and graphs. The results are analysed and discussed and interesting points raised in the experiment results are analysed. Finally, the charging process are divided into three phases.

4.1 WORKING FLUID

Although the final purpose of this project was the development of a heat transfer model that could be used in a CNG (Compressed Natural Gas) refuelling model, the working fluid chosen for these experiments was air, not CNG.

The primary reason for this choice of air instead of natural gas is for reasons of safety. Inevitably in the development of unique apparatus for high pressure experiments there will be leakage and the laboratory environment associated for these experiments, both at Victoria University of Technology and at NGV-Australia, could not be used safely with natural gas.

Since the project task is to develop and verify a general heat transfer model, with applicability beyond the working fluid, the choice of air instead of natural gas for this basic study was deemed acceptable.

Before these experiments with air, and the subsequent model, can be used in a CNG model it will be desirable to conduct tests with CNG, for which a safe experimental environment will be needed. This is one of the recommendations for further work following this project.

4.2 EXPERIMENTAL PROCEDURE

Nine experimental runs were carried out. The thermocouple array plane was changed from horizontal to vertical for some of the runs in order to measure the temperature gradients in both horizontal and vertical planes within the cylinder. Also, in order to investigate differences between horizontal and vertical filling, the cylinder was set up vertically and filled from the bottom in the last two runs and thermocouples 14 and 15 added as shown in Fig.4.2(b), while thermocouple 7 was disconnected from MDAS. The storage pressure and ambient temperature were slightly different between runs. The specification of the runs are listed in table 4.1. The different cylinder positions and thermocouple array planes are indicated schematically in Fig.4.1 and 4.2.

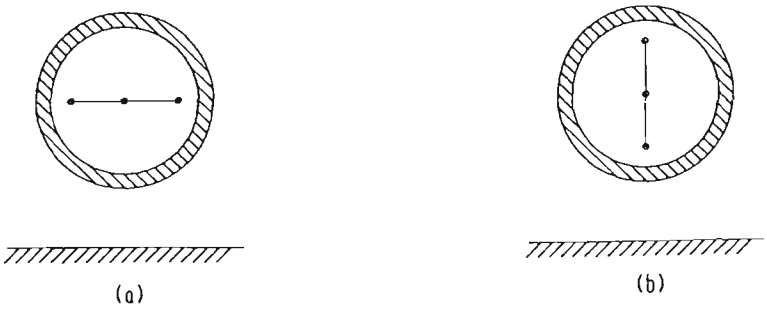

(a) Horizontal plane (B) Vertical plane

Fig.4.1 Thermocouple array planes in tests

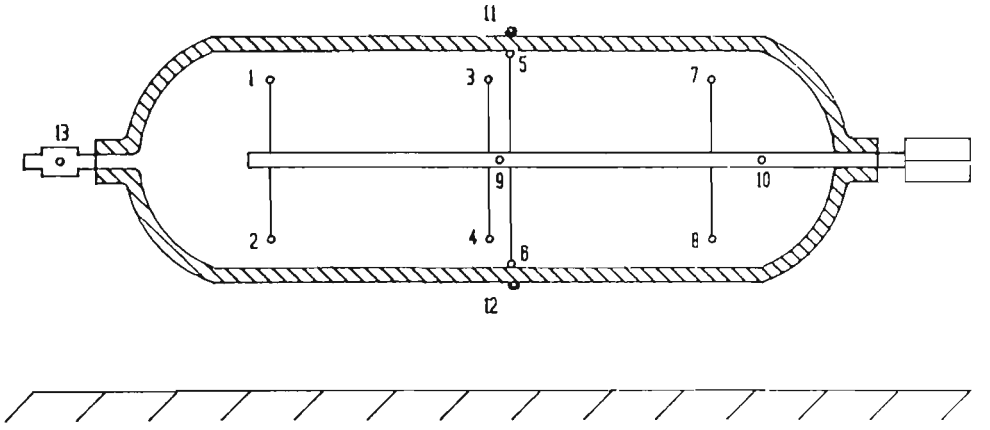

(a) Horizontal

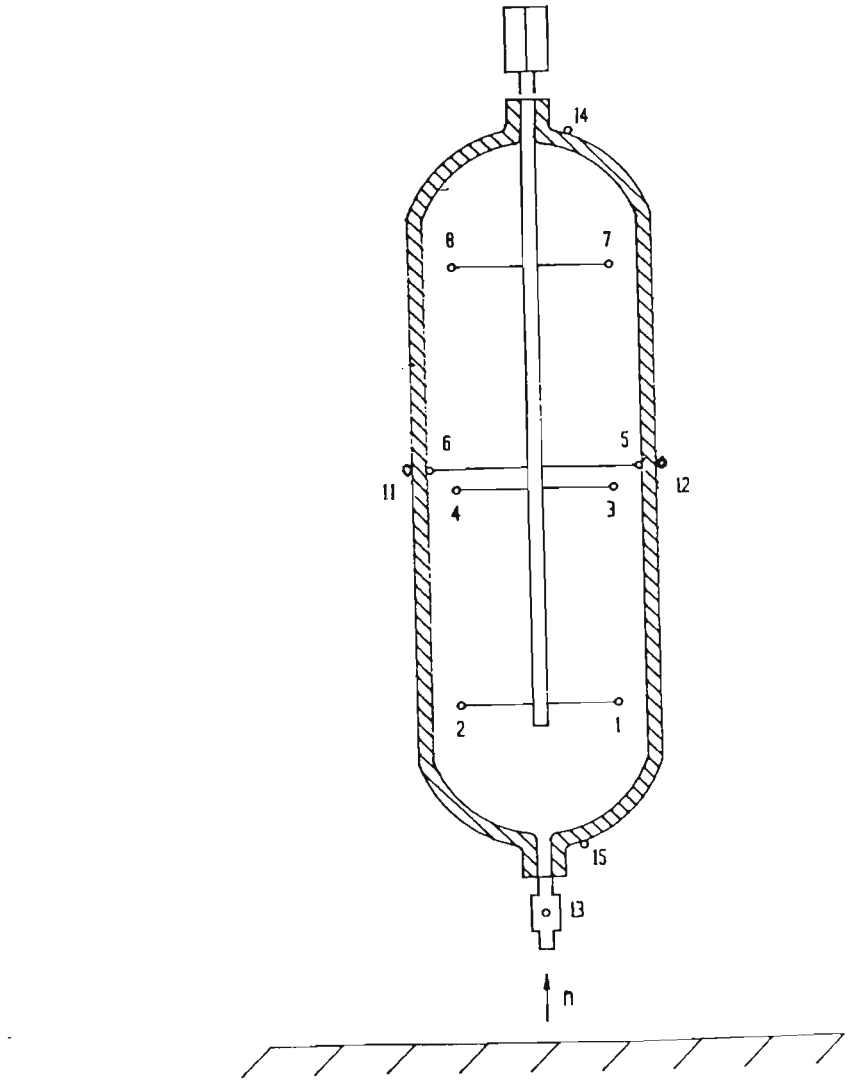

(b) Vertical

Fig. 4.2 Cylinder axis positions in tests

4.3 EXPERIMENTAL RESULTS

Three typical tests, run 1, run 6 and run 8 are shown in Fig 4.3-4.5. These include horizontal cylinder with horizontal thermocouples plane, horizontal cylinder with vertical thermocouples plane and vertical cylinder. Data for these three tests are provided in Appendix A.

The experimental results presented in Fig 4.3-4.5 show that both the gas temperature and pressure in the cylinder increase rapidly during the first few seconds and then more slowly up to a maximum value in about 80 seconds. The mass flow rate reaches the maximum and then drops gradually to a very small flow. Beyond this point, the gas temperature decreases gradually but the pressure remaining approximately constant. During the whole process, the cylinder wall temperature increases rapidly at first, and then asymptotes to the gas temperature, while the inlet temperature first decreases and rises smoothly later on. This temperature drop is a consequence of the Joule-Thomson effect.

For the temperature curve, the sampling period was 1 second, and this sampling period is sufficiently frequent for the temperature readings to be corrected for thermocouple response.

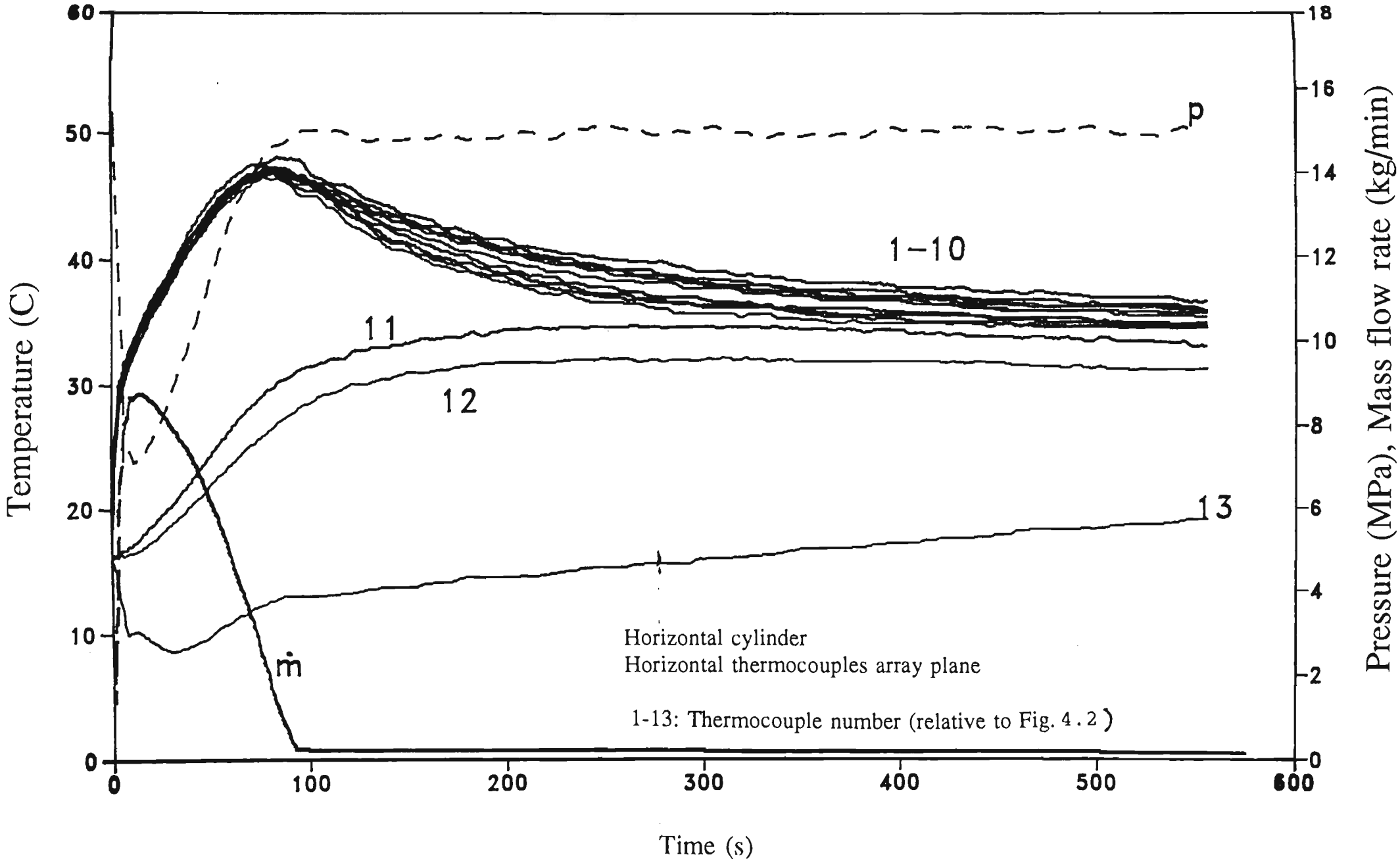

Fig.4.3 Experimental result for test 1

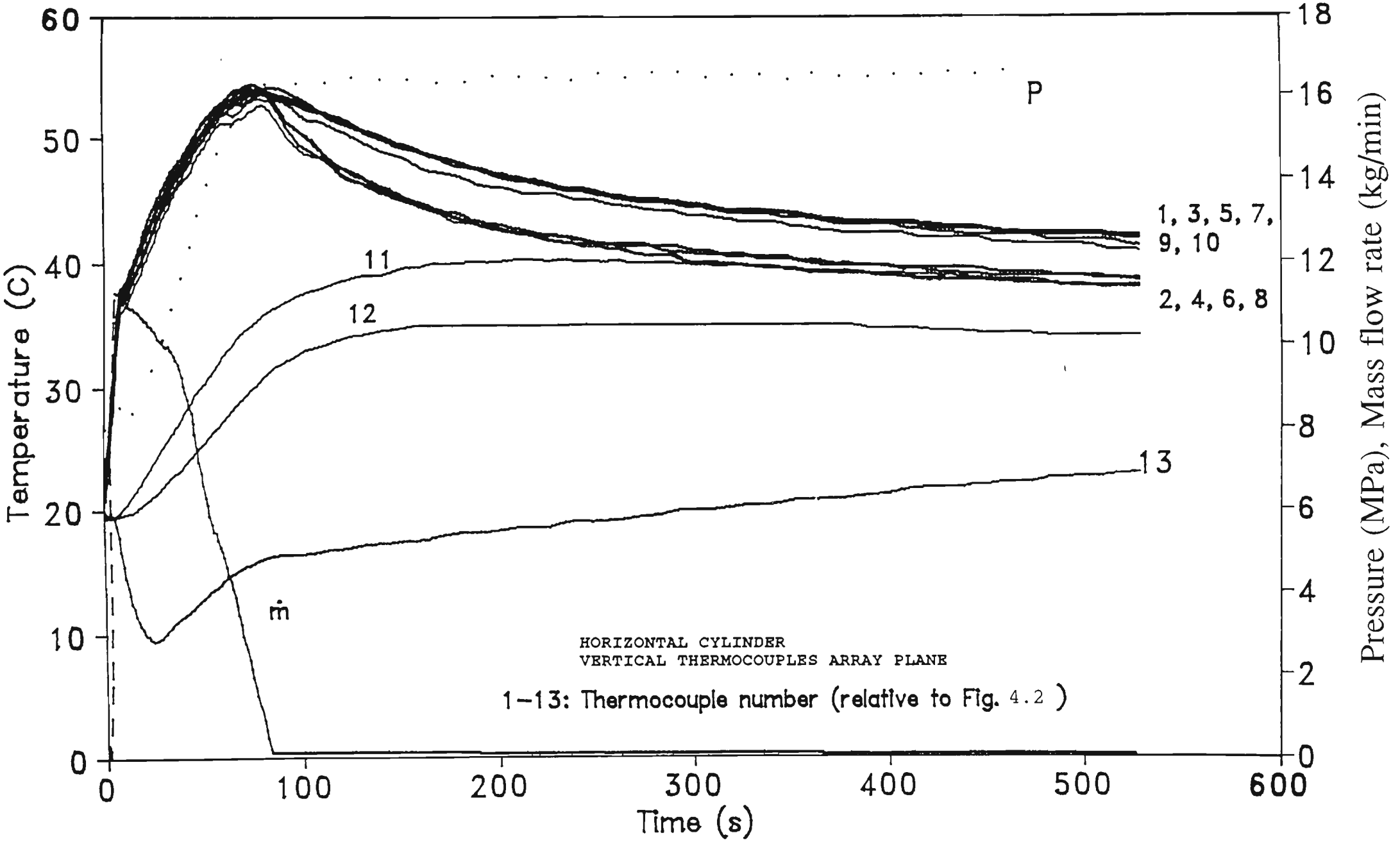

Fig.4.4 Experimental result for test 6

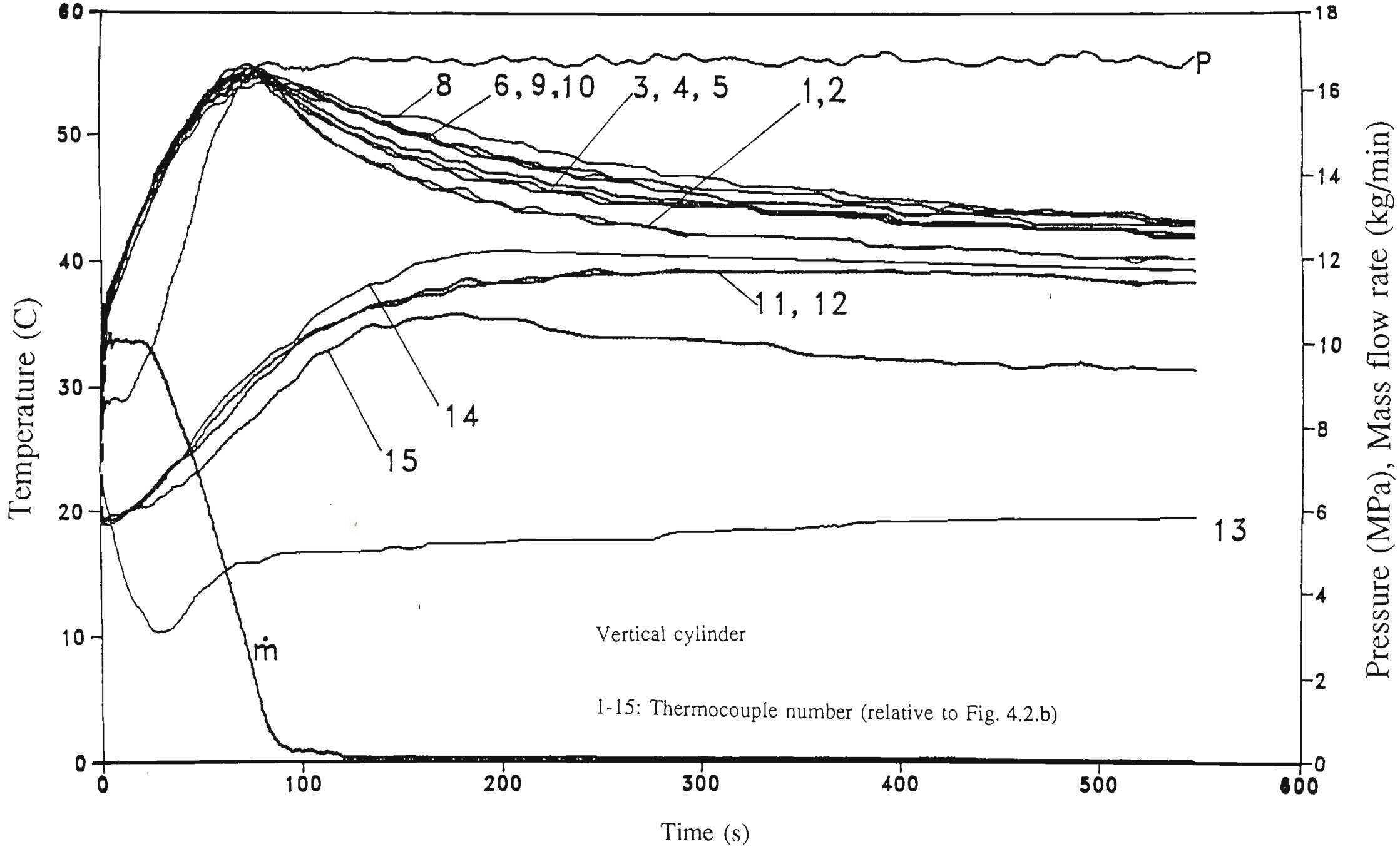

Fig.4.5 Experimental result for test 8

4.4 TEMPERATURE MEASUREMENT ERROR

4.4.1. Error of the thermocouple time response

During the first 80 seconds of the charging process, the gas temperature increases rapidly. As described in section 3.3.3, the thermocouple response time varies as a function of time, since the gas velocity changes with fill time. It is difficult to correct the temperature data obtained depending on a particular fixed time constant value of thermocouples.

However, the time response errors of the thermocouples can be estimated. The time constant measurement of thermocouples has been presented in chapter 3.3. During the first 60 seconds of the cylinder charging process, the gas velocity changes at the cylinder inlet are shown in fig.4.6.

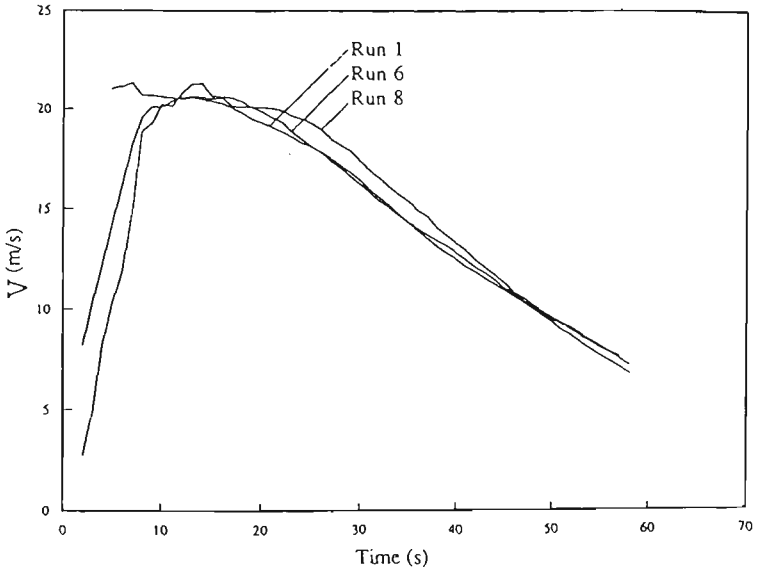

Fig.4.6 Gas velocities change with time

On the average the velocity V is about 14 m/s over the first 60 seconds. On the basis of the results of Fig.3.12, the time constant would be 1.8 seconds relative to this average velocity value over this period. Meanwhile, the average gas temperature changes are shown in Table 4.2.

Table 4.2 The average gas temperature

Time (S)	Run 1	Run 6	Run 8	Time (S)	Run 1	Run 6	Run 8
0	16.18	19.52	19.65	47	43.31	49.12	50.85
1	19.51	20.82	30.57	48	43.54	49.41	51.22
2	23.46	22.18	35.83	49	43.72	49.68	51.54
3	26.79	23.44	35.16	50	43.91	49.95	51.88
4	29.18	24.97	36.53	51	44.08	50.20	52.06
5	29.91	28.10	36.78	52	44.26	50.43	52.31
6	30.74	30.24	37.16	53	44.45	50.64	52.47
7	31.47	32.41	37.53	54	44.62	50.85	52.65
8	31.89	34.68	38.05	55	44.80	51.05	52.74
9	32.51	36.69	38.46	56	44.97	51.22	52.90
10	32.82	37.19	39.03	57	45.12	51.41	52.88
11	33.22	37.42	39.44	58	45.24	51.59	53.04
12	33.57	37.65	39.83	59	45.45	51.77	53.20
13	33.95	37.99	40.19	60	45.60	51.94	53.34
14	34.28	38.37	40.67	61	45.76	52.11	53.43
15	34.63	38.76	41.01	62	45.89	52.27	53.52
16	35.01	39.16	41.47	63	46.05	52.39	53.57
17	35.36	39.57	41.90	64	46.12	52.45	53.64
18	35.65	39.94	42.33	65	46.24	52.53	53.84
19	35.99	40.35	42.65	66	46.39	52.60	53.93
20	36.32	40.74	43.00	67	46.53	52.67	54.14
21	36.59	41.15	43.34	68	46.64	52.73	54.32
22	36.88	41.51	43.64	69	46.78	52.86	54.43
23	37.19	41.90	43.87	70	46.84	52.94	54.45
24	37.44	42.27	44.25	71	46.88	53.04	54.68
25	37.65	42.66	44.64	72	46.91	53.10	54.70
26	37.92	43.03	45.03	73	46.91	53.20	54.75
27	38.13	43.42	45.48	74	46.91	53.31	54.77
28	38.36	43.78	46.05	75	46.95	53.41	54.84
29	38.63	44.10	46.37	76	47.01	53.47	54.86
30	38.96	44.43	46.73	77	47.11	53.53	54.93
31	39.23	44.76	47.03	78	47.20	53.57	54.91
32	39.54	45.07	47.29	79	47.22	53.61	54.97
33	39.85	45.39	47.49	80	47.26	53.63	54.74
34	40.12	45.72	47.79	81	47.30	53.61	54.64
35	40.42	46.02	48.09	82	47.34	53.59	54.55
36	40.69	46.34	48.43	83	47.38	53.53	54.40
37	40.96	46.59	48.70	84	47.45	53.47	54.26
38	41.21	46.84	48.97	85	47.40	53.40	54.10
39	41.52	47.08	49.22	86	47.28	53.31	53.93
40	41.75	47.33	49.50	87	47.17	53.21	53.82
41	42.00	47.52	49.71	88	47.12	53.10	53.67
42	42.23	47.76	49.95	89	47.00	52.99	53.62
43	42.43	48.02	50.09	90	46.97	52.89	53.55
44	42.62	48.29	50.21	91	46.94	52.76	53.36
45	42.83	48.53	50.35	92	46.91	52.64	53.22
46	43.08	48.83	50.55	93	46.81	52.50	53.09

By omitting the first 4 seconds of the charging process, the upper limit error at time t = 5 seconds can be calculated as follows:

For run 1, at t= 5 seconds, T_m = 29.91 °C.

From fig.3.12, the time constant τ= 1.8 seconds when V=14 m/s, then we may find out from table 4.2 that

$$T-T_m = 1.5\ ^{\circ}C$$

Where

T - average gas temperature

T_m- measured average temperature

whence

$$\text{the upper limit error} = (T-T_m)/T$$
$$= 1.5/(29.91+1.5)$$
$$= 5.0\%$$

For the lower limit, although the time constant of the thermocouples increases more and more with the decreasing velocity of the gas, the temperature change also occurs progressively and over a smaller range so that time constant will not be significant influencing factor on the readings of temperature, when the gas temperature change is slow. The detailed calculation may be:

When $V=0$, $T_m=47.26\ ^{\circ}C$, from fig 3.12 we have time constant $\tau=4$ seconds. According to table 4.2, we obtain

$$T-T_m=0.15\ ^{\circ}C$$

therefore

$$\text{the lower limit error} = (T-T_m)/T$$
$$= 0.15/(47.26+0.15)$$
$$= 0.3\%$$

The results imply that the thermocouple time response errors in our experiments are between 0.3% to 5.0%, subject to the most probable error of $\pm 0.5\ ^{\circ}C$ of the temperature measurement system calibration.

The thermocouple time response error of 5.0% are thought to be acceptable. Especially, the absolute temperature values would be

used in following calculations and correlations in this research and the error should therefore be smaller than 5%. Although this was obviously a simplified estimation for the thermocouple response error, a more refined temperature correction was not deemed justified.

4.4.2. Correction of radiation effect

For correcting the radiation effect, Equation (3-2) in section 3.2.3 can be written as:

$$T_g = T_t + \frac{\sigma\epsilon(T_t^4 - T_s^4)}{h} \qquad (4-1)$$

T_g - gas temperature

T_t - thermocouple temperature

T_s - surrounding temperature

In section 3.3.2 of this thesis, the average heat transfer coefficient h between the gas and the thermocouples has been derived depending on measured data of thermocouple time constant. Also, we have

$$T_w = T_s$$

$$\sigma = 5.669 \times 10^{-8} \quad W/m^2K^4$$

$$\epsilon = 0.65$$

Then the values of T_g were calculated using equation (4-1), relative to different h values. The calculation result based on the data of T_w and T_t in test 1 is listed in table (4.3). The result shows that the difference between the gas temperature T_g and thermocouple temperature T_t is so small that the effect of radiation can be ignored in this study.

Table 4.3 Correction of radiation effect

V (m/s)	h ($W/m^2 C$)	T_w (C)	T_t (C)	T_g (C)
24.9	11266.15	16.7	33.82	33.92004
20.2	1085.32	17.0	34.28	34.38504
14.6	1055.24	20.1	40.5	40.58009
9.6	791.43	22.2	43.0	43.11015
4.9	622.84	25.5	45.6	45.70023
0	30.00	32.5	39.31	39.43896

4.5 GAS TEMPERATURE GRADIENT AND ANALYSIS

One of the important features presented in these experiments was the gas temperature stratification that existed in the cylinder after it reached the its maximum value, especially in direction of gravity. As observed, the temperature gradient along the gravity direction happened not only in horizontal cylinder charging, but also in vertical cylinder charging.

The experimental results with the thermocouple array in both the vertical plane and horizontal plane show that there was about 4 to 7 degree C temperature difference between top and bottom of the cylinder, while gradient difference between the horizontal charging and vertical charging was slight. Also, the temperature difference between entry and opposite end was very small for horizontal cylinder charging. In summary, for the horizontal cylinder, the temperature difference between thermocouples (1) and (2), (3) and (4), (5) and (6), (7) and (8) was about 4 to 7 degree C, while

between (1),(3),(4),(7) and (2),(4),(6),(8) the temperature difference was small. (see Fig.4.2)

The reason for the temperature gradient is thought to be a consequence of free convection both outside and inside cylinder. As soon as the metal cylinder becomes warmer then ambient, external natural convection commences and this causes the lower part of the cylinder to become cooler than the upper part, because the air temperature gradient near the bottom surface is greater than near the top surface. Inside the cylinder, the heat related density differences could be the reason for the higher temperature at the top of the cylinder. The density of gases and liquids depends on temperature differences, generally decreasing (due to fluid expansion) with increasing temperature. That is, the hotter regions of gas are less dense than the colder region, as is shown in Fig.4.10 a.

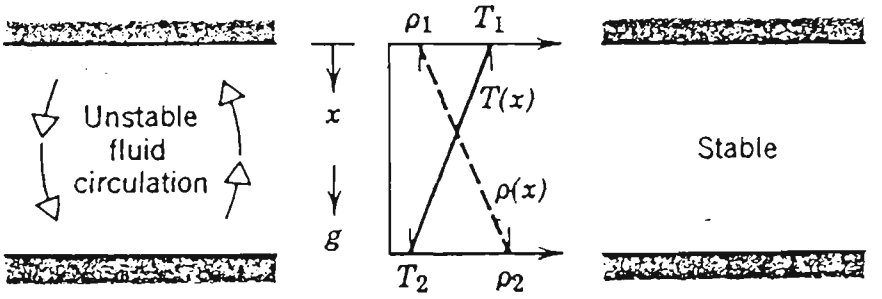

Fig.4.10 Temperature gradient conditions

The hotter regions, with higher enthalpy means increased molecular excitation thus forcing particles further apart, which causes the hotter regions to be less dense. The heavier gas will descend, while the lighter gas will rise.

After the mass flow rate approaches zero in the charging

process, the temperature difference between top and bottom tends towards stability and the presence of a gas density gradient in a gravitation field will mitigate against tha presence of free convection. The conditions are stable, because the density no longer decreases in the direction of the gravitational force, and there is no bulk gas motion (because the mass flow rate is close to zero), see Fig.4.10 b. As a result, we can conclude that heat transfer across the space inside cylinder occurs by conduction. Since the overall gradient persisted throughout the experiment, it is apparent that conductive heat transfer was dominant inside the cylinder after the mass flow rate diminished to a low rate. It is likely that conduction of heat through the metal of the cylinder, from top to bottom, occurs at a rate which will support a slow convective flow inside the cylinder.

The inlet temperature T_i (thermocouple 13) dropped first during the process. This temperature drop is a consequence of Joule-Thomson effect. The charging process was known as throttling. The gas pressure was reduced as it flowed through the throttle valve. There was no change in enthalpy (total heat). Over a specific pressure drop from given starting conditions, the Joule-Thomson coefficient is

$$\mu = \frac{\Delta T_i}{\Delta p}$$

The coefficient is positive when pressure difference is between 1 to 200 MPa and temperature difference is from -150 to 300 degree C. Since $\mu>0$, when $\Delta p<0$, we obtain

$$\Delta T_i<0$$

As a result, the temperature falls as pressure is reduced by throttling at constant enthalpy.

4.6 PRESSURE RESPONSE AND CONVERSION

Corrections to pressure response data should also be carried out.

During the first phase of the charging process, the gas conditions vary considerably with time, so the externally measured pressure will not be the same as that in the cylinder.

To charge the cylinder, all the tests were performed by opening the valve of the storage cascade, except for run 1 which was done by opening the cylinder valve while the storage valve remained open.(see Fig.4.11)

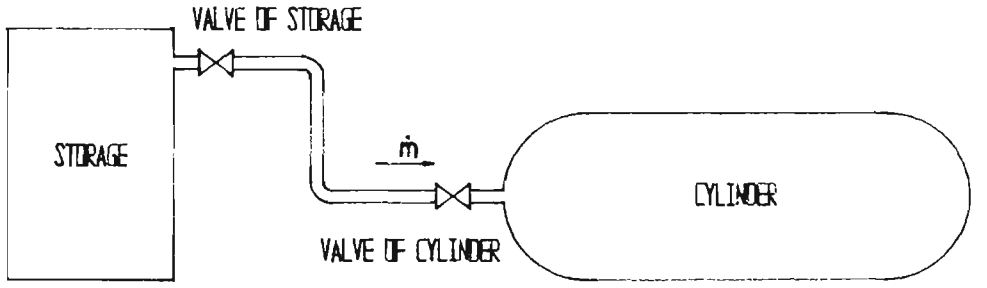

Fig.4.11 Valve control in the experiments

The pressure data which was taken by the transducer increased to approximately 50% of final pressure in just two seconds after opening the valve. This result is thought to be the limitation due to the position of the pressure transducer. This position does not measure the gas pressure in the cylinder at high flow rates. In a previous study [29], a calibration test was made to account for the error for pressure difference between the inlet and inside of the cylinder. In the experiment, one pressure transducer was placed into

the neck of cylinder, while another transducer was inserted into the centre of cylinder. Under the conditions of 24.1 MPa of storage pressure and -12.2 C ambient temperature, the results show that the pressure drop between these two points was almost 4 MPa during first 10 seconds. Fig.4.12 shows the result of the experiment.

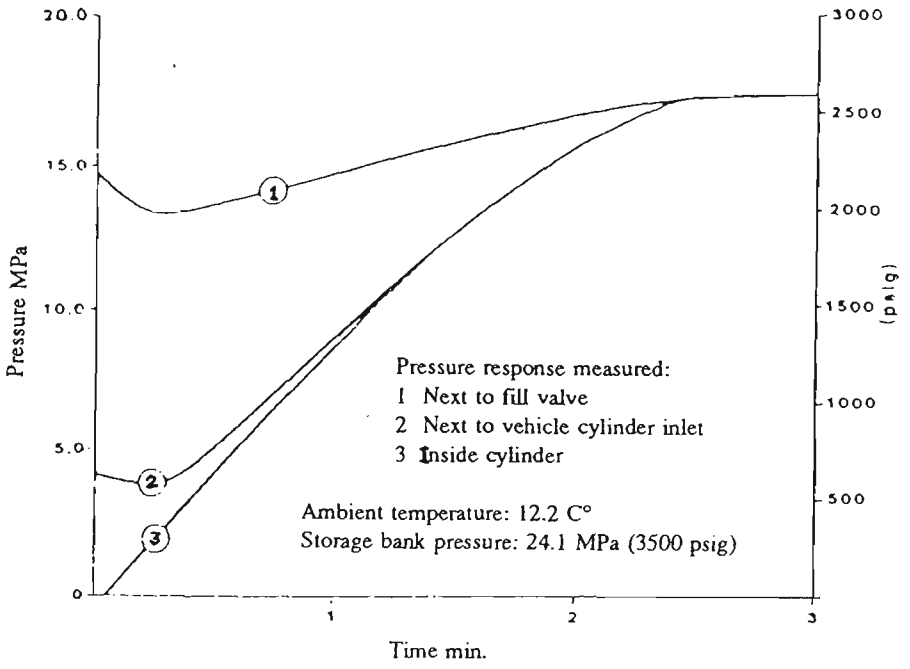

Fig.4.12 Comparison of measured pressure during cylinder filling in ref.[29].

It was also shown that the pressure of both the inlet and inside were equal after 1 minute.

The problem of pressure lag in the experiments influenced the accuracy of the data obtained. However, as we have discussed, the real gas pressure can be derived by using the equation,

$$pV_m/T=mRZ$$

The determination of the Z factor is important since neglecting the variation in Z with pressure and temperature can lead to substantial error in the calculation.

For this purpose, functional relations between Z and p,T are needed. The Z functions required in this section is the relationship between Z and pressure values, relative to different temperature ranges. That is

$$Z=f(p) \qquad (4-2)$$

To obtain Z functions, curve fitting is employed, based on the compressibility chart in reference [17]. As noted in reference [17], the functional relation between pressure p and Z factor is very close to second order equation,

$$Z=a_i p^2+b_i p+c_i \qquad (4-3)$$

i- the number of temperature group

Also, we can obtain the data from the Chart. According to each group of the data, relative to particular temperature ranges, we can derive each curve fitted equation using the least squares method, with a computer program (Appendix B). As a result, four equations were derived, relative to four temperature ranges. Table 4.3 list the values of a_i, b_i, and c_i , relative to different temperature ranges.

Table 4.4 a,b and c values of Z functions

	Equation 1 T=15.6-26.7(C)	Equation 2 T=26.8-37.8(C)	Equation 3 T=37.9-51.9(C)	Equation 4 T=52.o-66.0(C)
a_i	0.0002484	0.0002083	0.0001893	0.0001733
b_i	-0.0034396	-0.0021339	-0.0015435	-0.0004246
c_i	0.9996198	0.9994516	0.9995712	0.9997614

So far we can get four Z functions with the form of equation (4-3). By the pVT equation, we have

$$p=\frac{TmRZ}{V}=TmR(a_ip^2+b_ip+c_i) \qquad (4-4)$$

or,

$$a_ip^2+(b_i-\frac{V}{TmR})p+c_i=0 \qquad (4-5)$$

Therefore, the corrected pressure values would be each solution of this equation, that is,

$$p=\frac{(1-b_i\frac{TmR}{V})-[(b_i\frac{TmR}{V})^2-4(\frac{TmR}{V})^2a_ic_i]^{\frac{1}{2}}}{2a_i\frac{TmR}{V}} \qquad (4-6)$$

The calculation results are compared with the measured pressure data. Fig.4.12-4.14 show the comparisons of pressure for experiment runs 1, 6 and 8 . It is also shown in table 4.5.

The comparisons show a similar pressure lag situation to the one shown in Fig.4.12, which was from reference [29]. The pressure drop between measured inlet data and inside values is very significant in the first period, while they were fairly close in second period.

Table 4.5 Pressure conversion of test 1,6 and 8

p_m= TmRZ/V
p_g= measured inlet pressure

Run 1 Time S	Mass kg	T C	Pm MPa	Pg MPa	Z (aP^2+bP+c)
6	0.46	30.74	9.44	0.74	0.997984
11	1.16	33.22	7.21	1.88	0.996174
16	1.89	35.01	7.34	3.08	0.994856
21	2.61	36.59	7.63	4.27	0.994137
26	3.31	37.92	8.14	5.45	0.996784
31	3.98	39.23	8.81	6.59	0.997622
36	4.63	40.69	9.46	7.71	0.998928
41	5.25	42.00	10.16	8.80	1.000644
46	5.82	43.08	10.87	9.81	1.002639
51	6.35	44.08	11.59	10.76	1.004872
56	6.83	44.97	12.26	11.63	1.007224
61	7.25	45.76	12.93	12.40	1.009552
66	7.60	46.39	13.42	13.06	1.011688
71	7.90	46.88	13.84	13.62	1.013661
76	8.12	47.01	14.27	14.02	1.015158
81	8.28	47.30	14.62	14.33	1.016327
86	8.37	47.28	14.68	14.49	1.016969
91	8.42	46.94	14.79	14.57	1.017267

Run 6 Time S	Mass kg	T C	Pm MPa	Pg MPa	Z (aP^2+bP+c)
0			0.10		
6	0.35	30.24	8.46	0.56	0.998316
11	1.28	37.42	8.45	2.10	0.995884
16	2.16	39.16	8.39	3.57	0.996473
21	2.95	41.15	8.89	4.91	0.996556
26	3.71	43.03	9.42	6.22	0.997292
31	4.52	44.76	10.05	7.63	0.998811
36	5.35	46.34	10.86	9.09	1.001190
41	6.14	47.52	11.71	10.51	1.004253
46	6.87	48.83	12.51	11.85	1.007855
51	7.50	50.20	13.34	13.04	1.011624
56	8.01	51.22	14.19	14.02	1.015126
61	8.45	52.11	15.19	15.08	1.032791
66	8.82	52.60	15.94	15.82	1.036440

Run 8 Time S	Mass kg	T C	Pm MPa	Pg MPa	Z (aP^2+bP+c)
0			0.10		
6	0.75	36.78	8.55	1.23	0.997139
11	1.58	39.03	8.64	2.61	0.996831
16	2.42	41.01	8.74	4.03	0.996425
21	3.26	43.00	9.28	5.46	0.996787
26	4.09	44.64	9.75	6.89	0.997926
31	4.89	46.73	10.45	8.31	0.999819
36	5.65	48.09	11.31	9.67	1.002342
41	6.35	49.50	11.97	10.95	1.005358
46	7.00	50.35	12.76	12.14	1.008729
51	7.59	51.88	13.64	13.27	1.012434
56	8.10	52.74	14.53	14.45	1.029793
61	8.55	53.34	15.14	15.34	1.034025
66	8.91	53.84	15.98	16.07	1.037672
71	9.20	54.45	16.65	16.67	1.040846

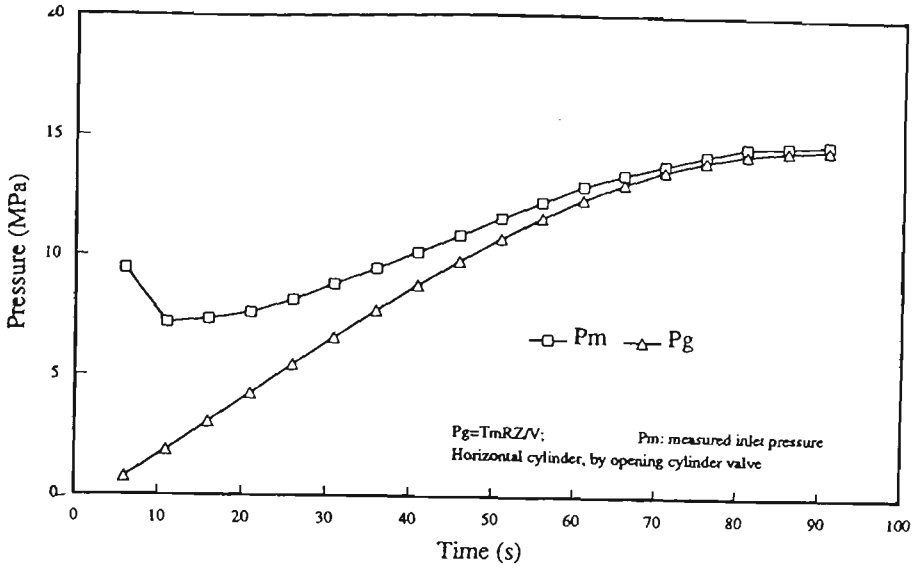

Fig.(4.12) Pressure conversion of test 1

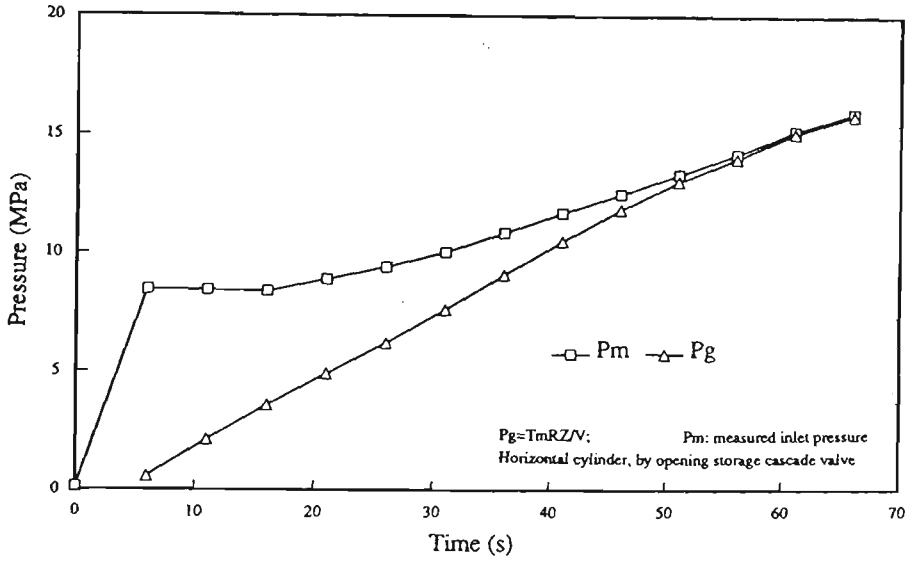

Fig.(4.13) Pressure conversion of test 6

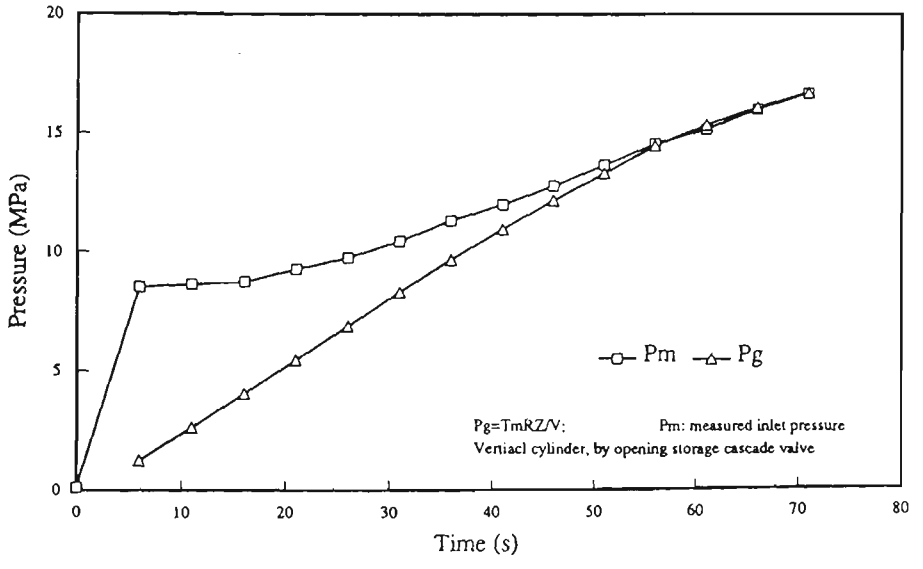

Fig.(4.14) Pressure conversion of test 8

4.7 HEAT TRANSFER PHASE DIFFERENTIATION AND ANALYSIS

Based on the heat transfer mechanism in the cylinder, the whole charging process may be divided into three different periods.

The first period is dominated by forced convection during the time when the changes of both the gas pressure and the gas temperature are large and mass flow rate is high. During this period, the mass flow rate increases rapidly, and the temperature difference between the gas and the cylinder wall is high, with a consequential large heat transfer coefficient.

In the charging process, when the mass flow rate $\dot{m} < 0.5$ kg/min, the Reynolds number is fairly small. By the criteria produced in Holman' text [13], we have

$$\frac{Gr}{Re^2} > 10 \qquad (4\text{-}7)$$

that is, free convection is predominant. During this phase, the wall temperature increased so that the temperature difference between the gas and the wall was getting smaller and the heat transfer coefficients dropped smoothly.

Finally, since a significant temperature difference always occurred along the gravitational direction in the cylinder, as shown in Fig.4.3-4.5, with the gas temperature at the top higher than at the bottom, this period is termed the conduction phase. The Nusselt number was close to unity during this time.

As discussed above, free convection is predominant after $\dot{m} <$ 0.5 kg/min, this corresponding time, t=80 seconds, and relevant parameters will be taken as the starting point of free convection

period. It has been shown in reference [13] that, when conductive heat transfer occurs in horizontally enclosed spaces, Nu=1.0. This implies the heat transfer coefficient h_{in} is small. Because the heat transfer coefficient in the cylinder h_{in} is close to zero when the filling time reaches about 210 seconds, and the experimental results show that the temperature difference between the top and bottom of the cylinder approaches a stable state, this point therefore must be the start of the conduction made across the space in the cylinder.

Fig.4.15 shows the Nusselt numbers change during the whole process and the differentiation of the three phases.

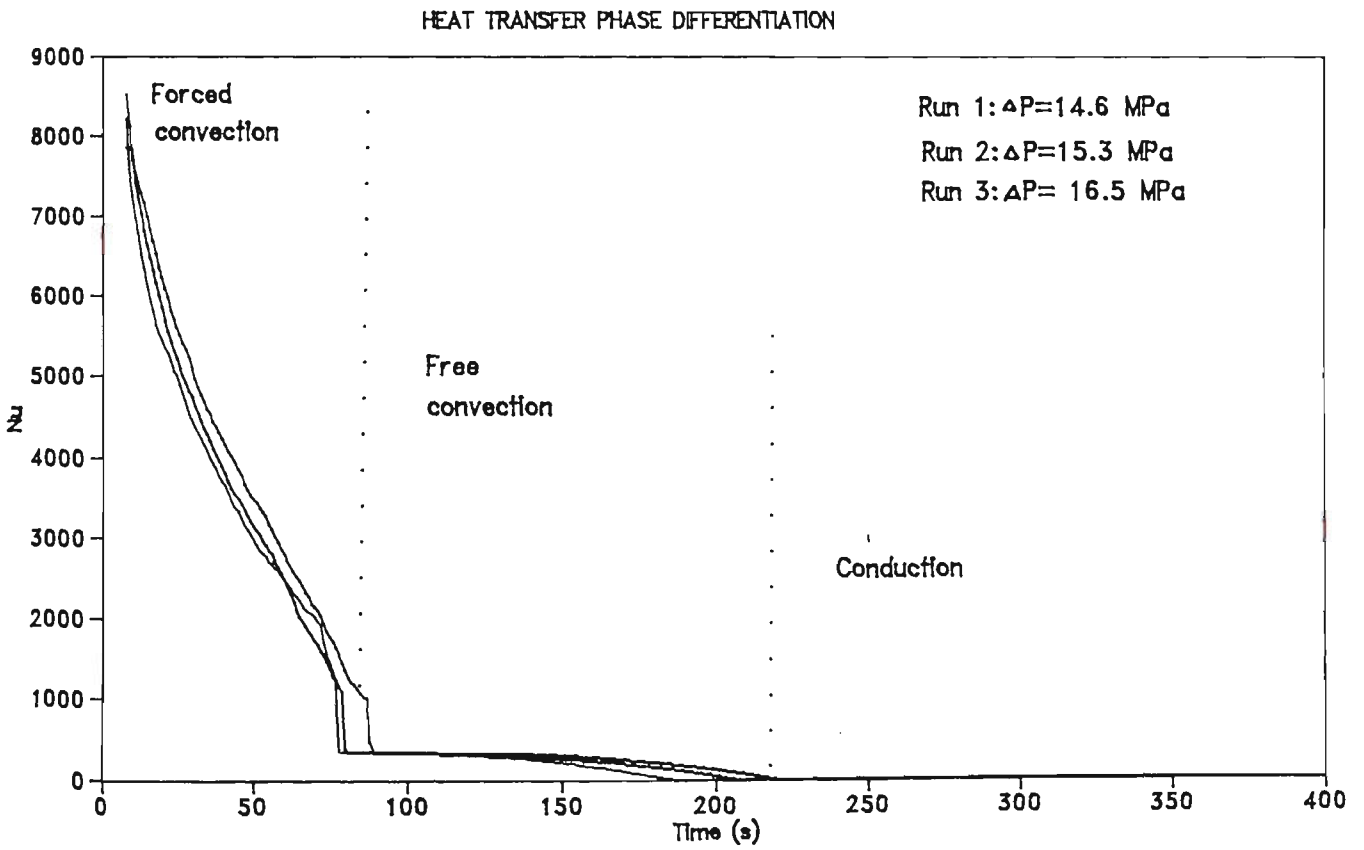

Fig.4.15 Heat transfer phase differentiation

For the heat transfer situation outside the cylinder, since the cylinder is exposed to ambient room air without an external source of motion, a movement of the air is experienced as a result of the density gradients near the cylinder. Thus free convection takes place. The main variable is the cylinder wall temperature, which increased when the wall was heated during the charging process, resulting in an increase in the outside heat transfer coefficient. Finally the value of h_∞ reached a constant when the temperature was stable.

4.8 THE APPLICABILITY OF LUMPED CAPACITANCE METHOD

Consider steady-state conduction through a plane wall of area A, Fig.4.16.

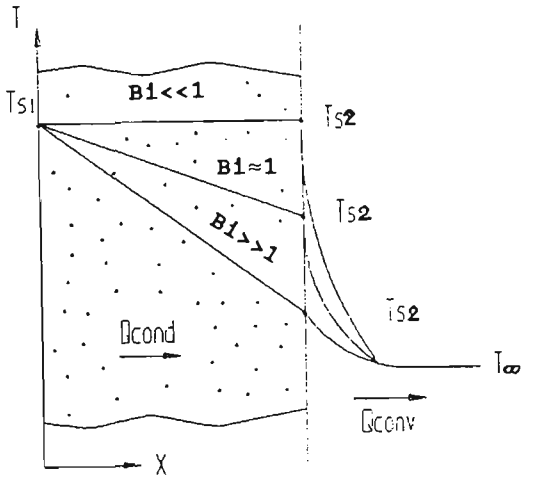

Fig.4.16 Effect of Biot number

Although steady-state conditions are assumed, this criterion can be extended to transient process. Note that $T_\infty<T_{s2}<T_{s1}$, and under steady-state conditions

$$Q_{cond}=Q_{conv}$$

or

$$\frac{kA}{L}(T_{s1}-T_{s2})=hA(T_{s2}-T_{\infty})$$

Re-arranging, we obtain

$$\frac{T_{s1}-T_{s2}}{T_{s2}-T_{\infty}}=\frac{hL}{k}=Bi \qquad (4-8)$$

The dimensionless quantity Biot number Bi plays a fundamental role in problems that involve surface convective effects. According to equation (4-8), the Biot number is a measure of the temperature drop in the solid relative to the temperature difference between the surface and gas. If the following condition is satisfied

$$Bi=\frac{hL_c}{k}\leq 0.1 \qquad (4-9)$$

the error in using the lumped capacitance method is small. The characteristic length $L_c = V_m/A_s$.

For heat transfer between the atmosphere and external surface of the cylinder, the average maximum value of hi which was calculated from experimental results is 4 W/m^2K, and L_c=0.01 m, k=17 W/mK, we have

$$Bi=\frac{hL_c}{k}=0.002<0.1 \qquad (4-10)$$

Therefore the use of the lumped capacitance method in this study appears well justified.

CHAPTER 5

EXPERIMENTAL DATA CORRELATIONS

In this chapter, correlations are presented for the forced and free convective phases. The rate of heat transfer during the third phase, conduction, is very small compared with the convective phases, so correlations are not made.

5.1 THE THERMAL PROPERTIES OF GAS

For gases, to a first approximation, many thermal properties can be regarded as independent of pressure, while changing with temperature. For correlating the data in this research, however, the effect of high pressure cannot be ignored. The thermal properties must therefore be considered as functions of both temperature and pressure. On the other hand, since the range of the gas temperature change was from 20 to 50 degree C, the thermal properties were treated as functions solely of pressure within this specific temperature range. The gas thermal properties concerned include dynamic viscosity μ, thermal conductivity $\mathbf{k}$ and specific heat $\mathbf{c}_p$ and $\mathbf{c}_p/\mathbf{c}_v$.

Viscosity μ The effect of high pressure on the viscosity may be calculated from the Kinetic theory of gases as presented by Comings et al.[7]. The effect of reduced pressure p/p_c and reduced temperature T/T_c (where p_c and T_c are critical gas pressure and critical gas temperature) on viscosity was determined. For air, we have

$$\frac{p}{p_c} = \frac{p}{3.77} \quad (MPa) \qquad (5\text{-}1)$$

and

$$\frac{T}{T_c} = \frac{T}{132} \quad (K) \qquad (5\text{-}2)$$

In the charging process, the range of gas temperature change is always within 20 to 60 degree C, so the range of T/T_c is

$$2.2 < \frac{T}{T_c} < 2.5 \qquad (5\text{-}3)$$

As shown in Coming's study [7], this is a very small T/T_c range in which μ/μ_1 only varies between 1 and 1.3. Therefore, the functional relation between the viscosity ratio μ/μ_1 and p/p_c may be curve fitted for this range and an equation can be derived by the least squares method. Based on the graph presented in Coming's study [7]. the equation obtained is

$$\frac{\mu}{\mu_1} = 0.00285\left(\frac{p}{p_c}\right)^2 + 0.0368\left(\frac{p}{p_c}\right) + 1.012 \qquad (5\text{-}4)$$

Where μ_1 refers to conditions at atmospheric pressure, which is assumed as a constant within this temperature range. The error of curve fit for this equation is within ±4%. As a result, the particular values of μ can be obtained during the charging process.

Thermal conductivity k The methodology to describe the thermal conductivity of the gas is exactly the same as that used above for determining the gas viscosity μ. Using the curve presented in Coming's study [8], according to the reduced pressure p/p_c and the reduced temperature T/T_c, for the range of T/T_c, the equations (5-9) was derived by curve fitting, using least squares method, for air:

$$\frac{k}{k_c} = 0.00857\left(\frac{p}{p_c}\right)^2 + 0.0366\left(\frac{p}{p_c}\right) + 1.006 \qquad (5\text{-}9)$$

The error of eq.(5-9) is within ±7%.

Specific heat According to the data obtained from the tables in references [9] and [12], the specific heat of high pressure gas is derived as a function of pressure, in relation to the particular range of the gas temperature change in the charging process. Using the least square method the specific heat can be estimated as below for air:

$$C_p = -0.000114p^2 + 0.015p + 1.003 \quad (p: MPa) \qquad (5\text{-}11)$$

and

$$\gamma = -0.0001962p^2 + 0.0191117p + 1.398 \quad (p: MPa) \qquad (5\text{-}12)$$

The error of eq.(5-11) is within ±0.6%, and the error of eq.(5-12) is within ±2%.

5.2 DIMENSIONLESS NUMBERS

The dimensionless numbers concerned include Nusselt number Nu, Fourier number Fo, Grashof number Gr, Prandtl number Pr and Rayleigh number Ra. Note that in determining the dimensionless numbers the value of T, Tw, p, and h_{in} are all average, so the dimensionless numbers used for the correlations reflect these values.

Nusselt number

$$Nu = \frac{h_{in} D}{k} \qquad (5\text{-}15)$$

Where the characteristic length, D, is the inside diameter of the tank and k is the thermal conductivity of the gas calculated by

equation (5-9) or (5-10). In Chapter 2, the heat transfer coefficient h has been derived, that is:

$$h_{in} = \frac{\dot{m}c_p T_i - c_v(\dot{m}T + \dot{T}m)}{A_{in}\,(T - T_w)} \qquad (5\text{-}16)$$

Fourier number

$$Fo = \frac{kt}{\rho c (\frac{D}{2})^2} \qquad (5\text{-}17)$$

Where k is thermal conductivity of the cylinder wall, t is time, ρ is density of the cylinder wall, c is specific heat of the cylinder wall and D is the cylinder diameter.

Grashof number

$$Gr = \frac{g\beta D^3 (T - T_w)}{\nu^2} \qquad (5\text{-}18)$$

Where $\nu=\mu/\rho$, μ is calculated by equation (5-8), T is the average gas temperature, T_w is the average tank wall temperature, β is the volume coefficient of expansion, and g is the acceleration due to gravity.

Prandtl number

$$Pr = \frac{C_p \mu}{k} \qquad (5\text{-}19)$$

Where c_p, μ and k are calculated in section 5.1.

Rayleigh number

$$Ra = GrPr \qquad (5\text{-}20)$$

5.3 CORRELATIONS FOR FORCED CONVECTION

The experimental results in this research strongly suggest the Nusselt number need be correlated only with time, because variations between each run are small, as shown in Fig.4.15 in chapter 4. Therefore, the forced convection phase may be correlated on a Fourier number-Nusselt number plot. The values of Fourier number are from 0 to 0.06 with t from 5 to 80 seconds during this period. The data is plotted in Fig.(5.1) and the correlation may be fitted within 7 percent by the equation

$$Nu = 9320.71\, e^{-26.62Fo} \qquad (5\text{-}21)$$
$$(0 < Fo < 0.06)$$

Equation (5-21) covers the whole forced convection phase except for the first 5 seconds. During the first 5 seconds of this phase the values of Nu are not well correlated because the heat transfer coefficient is increasing rapidly from a very low value to its maximum value rather than decreasing.

5.4 CORRELATION FOR FREE CONVECTION

In the free convection phase, the Nusselt number is a function of both time and free convection. It therefore appears relevant to attempt to correlate the data by some combination of Rayleigh number and Fourier number versus Nusselt number plot

$$Nu = f(Ra, Fo)$$

The form of correlation which fitted the experimental data within 6% was found to be

$$Nu = 387.6\, e^{-7.6\times10^{9}\left(\frac{Fo^{0.5}}{Ra}\right)} \qquad (5\text{-}22)$$

$$(3.8\times10^{11} < GrPr < 6.9\times10^{11})$$

$$(0.06 < Fo < 0.09)$$

The data correlation for free convection portion is shown in Fig.5.2. Correlation (5-22) is valid throughout the whole free convection phase except about the final 30 seconds, when Nu rapidly approaches unity.

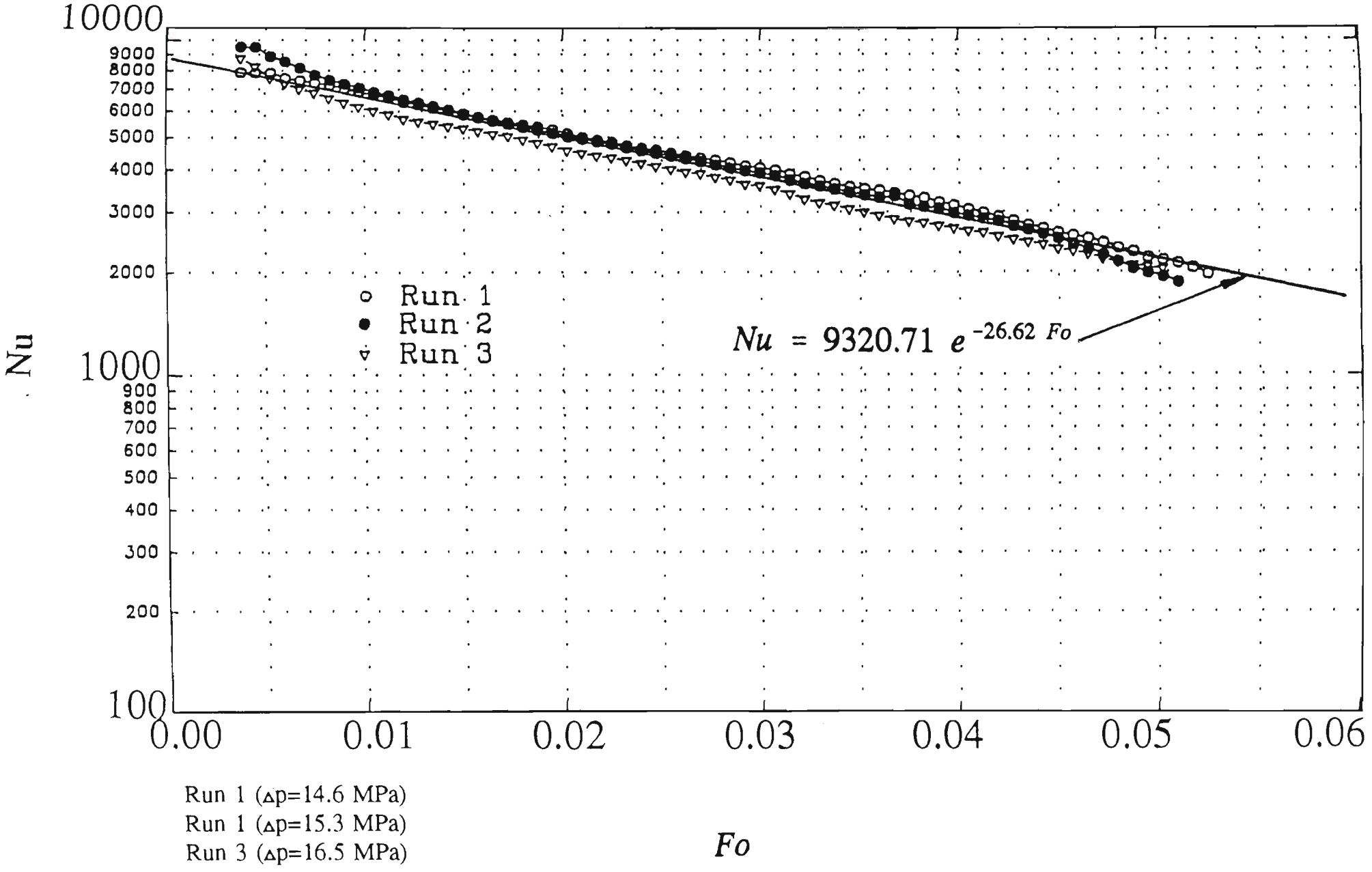

Fig.5.1 Forced convection data correlation

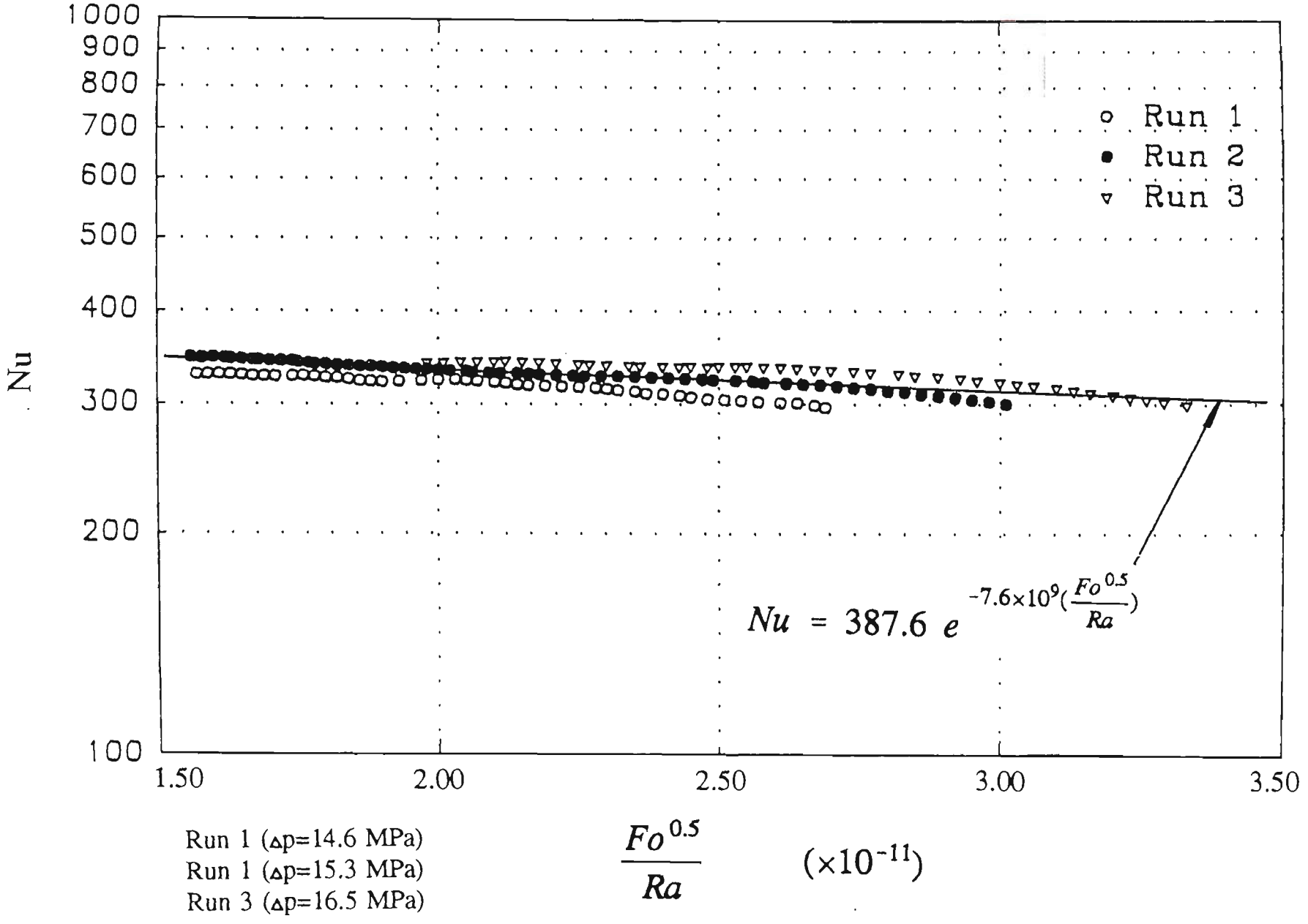

Fig.5.2 Free convection data correlation

5.5 CORRELATION FOR CONDUCTION

In next 30 seconds, the Nusselt number is close to unity, and the conduction mode is becoming predominant. In terms of total heat transfer, the conductive heat transfer is negligible. Curve fitting for this phase therefore has not been attempted. Since the Nusselt number change is from 2 to 30, a data correlation for estimating the heat transfer coefficients becomes less important.

5.6 SUMMARY

Since the data presented covered a gas pressure range from a starting pressure of 0.1 MPa to a final pressure between 14.5 MPa and 16.5 MPa in the cylinder, the range of applicability of the analysis is large.

The summary of the correlations are shown in table (5-1).

Table(5-1). Summary of correlations

	Forced convection	**Free convection**	**Conduction**
Time interval (s)	1 - 80	80-170	210-end
Fo	0.00 - 0.06	0.06 - 0.09	___
GrPr	---	3.8×10^{11}-6.9×10^{11}	---
Nu	>300	300-1	1
Correlation	eq.(5-21)	eq.(5-22)	---
p, T	increasing rapidly	p,T stable	stable
$\dot{m}$	increasing rapidly, then dropping	close 0	close 0

CHAPTER 6

SIMULATION AND COMPARISON WITH EXPERIMENTAL RESULTS

In previous chapters, the simple theoretical model was applied to calculate the heat transfer coefficient based on the experimental data, and the data correlations have been obtained.

In practice, during the refuelling process, pressure and mass flow rate are the two variables which were read from the gauges and the incoming gas temperature can be normally measured by a submerged thermocouple in the valve fitting of the cylinder with a threaded section. A simulation method designed to predict heat transfer parameters by monitoring gas pressure, mass flow rate and incoming gas temperature changes and environmental conditions as input variables was developed.

In this chapter, the detailed description of the simulation technique is given. The simulation results are plotted and are compared with the experimental results.

6.1 THEORETICAL SOLUTION

As we described before, the total heat transfer field of the charging system could be divided into three parts: inside cylinder, outside cylinder and cylinder wall. Based on these three parts of the heat transfer fields, system behaviour can be described by a set of simultaneous ordinary equations. To solve the simultaneous equation by computer program is the key to the simulation.

The variables we are going to derive are h_{in}, h_{∞}, T, T_w, E_w, q_{in}

and q_∞ in terms of average value. To solve these seven variables, there must be seven separate simultaneous equations. The set up of the simultaneous equations is presented as below.

6.1.1 Inside cylinder

For calculating the heat transfer coefficient, equation (2-11) can be used as

$$h_{in} = \frac{\dot{m}c_p T_1 + c_v(\dot{m}T + \dot{T}m)}{A_{in}\ (T - T_w)} \qquad (6-1)$$

For calculating the gas temperature values, we have

$$\frac{pV}{T} = mRZ \qquad (6-2)$$

Equation (6-2) is from the ideal gas equation by inserting compressibility Z. It has been proved to be applicable, provided Z could be derived precisely.

And also, Newton's law of cooling can be used as

$$q_{in} = h_{in}\, A_{in}(T - T_w) \qquad (6-3)$$

6.1.2 Outside cylinder

It is clear that the mechanism of heat transfer from cylinder wall to the atmosphere is free convection.

For laminar and turbulent free convection from a horizontal cylinder, reference [6] produced simple and empirical expressions for all Rayleigh Numbers Ra. A complex expression, for use over a

wide range of GrPr is given by :

$$Nu^{\frac{1}{2}} = 0.60 + 0.387 \left[\frac{GrPr}{\left[1 + \left(0.\frac{559}{Pr}\right)^{\frac{9}{16}}\right]^{\frac{16}{9}}} \right]^{\frac{1}{6}} \qquad (6-4)$$

$$(10^{-5} < GrPr < 10^{12})$$

Equation (6-4) is available for uniform heating as well as for uniform wall temperature, and for simultaneous mass and heat transfer. To apply equation (6-4), it is assumed that the heating and the wall temperature are constant within each time differential period. It is suitable to apply to the differential time period. By integration, the change of Nu and heat transfer coefficient h_m may therefore be calculated.

In addition, Newton's law of cooling can also be employed as

$$q_m = h_m A_m (T_w - T_m) \qquad (6-5)$$

6.1.3 Cylinder wall

The cylinder wall is the third part of the heat transfer path. It is noted that the temperature field of the cylinder wall varies with time, the analysis must take into account the resulting change in internal energy of the wall with time. In the charging process, transient heat conduction is connected with the convection boundary condition at the surface of the cylinder wall. In this case, the convection environment temperature is the gas temperature **T** inside cylinder, the wall temperature T_w is assumed to be uniform, as was assumed previously. The analysis is shown in Fig.6.1.

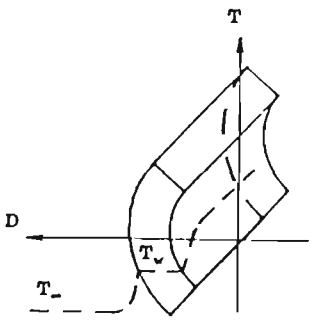

Fig.(6.1). Internal energy change of wall

A significant amount of the heat produced inside cylinder goes to increasing the cylinder wall temperature, while it is transferred to the outside. The change in internal energy of the wall is given by:

$$\frac{dE_w}{dt} = \rho c dr d\theta dz \frac{\partial T_w}{\partial t}$$

For the condition of lumped capacity,

$$\dot{E}_w = \frac{dE_w}{dt} = \rho C V \frac{dT_w}{dt} \qquad (6-6)$$

While V = volume of cylinder wall.

6.1.4 Energy balance

As the thermal capacitance of the cylinder has been "lumped", an energy balance on the capacitance is given by:

$$q_i = q_\infty + \frac{dE_w}{dt} \qquad (6-7)$$

Equation (6-7) implies that, in charging process, the heat which is generated in cylinder enters the cylinder wall and atmosphere; the heat transfer rate from gas to cylinder wall equals to the sum of the rate of energy change in the wall and the heat transfer rate from the wall to outside.

Equation (6-7) is the second energy balance equation following

equation (6-1). Equation (6-1) is from first law of thermodynamics, while equation (6-7) is the consideration of transient convection and unsteady conduction. And also, equation (6-7) is taken as a criterion in the simulation.

6.2 SIMULTANEOUS EQUATIONS

As a result a complete set of simultaneous equations have been established, which are expressed as

$$h = \frac{c_p(\dot{m}T_i + \dot{T}_i m) + c_v(\dot{m}T + \dot{T}m)}{A(T - T_w)}$$

$$\frac{PV}{T} = mRZ$$

$$q_i = h_i A_i (T - T_w)$$

$$Nu^{\frac{1}{2}} = 0.60 + 0.387 \left[\frac{GrPr}{\left[1 + \left(0.\frac{559}{Pr}\right)^{\frac{9}{16}}\right]^{\frac{16}{9}}} \right]^{\frac{1}{6}}$$

$$(10^{-5} < GrPr < 10^{12})$$

$$q_\infty = h_\infty A_\infty (T_w - T_\infty)$$

$$\dot{E}_w = \frac{dE_w}{dt} = \rho CV \frac{dT}{dt}$$

$$q_i = q_\infty + \frac{dE_w}{dt}$$

It is therefore possible to determine these seven variables by

solving the simultaneous equations.

6.3 COMPRESSIBILITY Z

In section 4.6, functional relations between Z and P were derived for calculating pressure values. In order to derive the temperature values, the functional relations between Z and temperature T are also needed.

As it is known, Z must be determined from experiments, and the experimental data has been curve fitted into charts (in reference [17]). Z factor is a function of temperature, pressure and gas composition.

From the chart for air, two observations can be made. The first is at temperatures from 15.6 to 93 degrees C., ie., room temperature and above, the compressibility factor is near unity for the pressures less than 10 MPa. This means that the ideal gas equation of state can be used for dry air over this range with good accuracy. When the pressure is above 10 MPa, the deviation from ideal gas behaviour may be considerable. In this region, there are thermodynamics tables and charts for a particular gas. It is noted that an equation of state that accurately describes the relation between pressure, temperature, and specific volume is rather cumbersome. However, Z factor could be predicted sufficiently accurately relative to different pressure value. In other words, in relation to any pressure value, Z is a function of the gas temperature

$$z=f(T) \qquad (6-8)$$

In this research, a computer program was made to curve fit the functions z=f(T) for air, depending on the chart in reference [17], in relation to different pressure values. As it is shown, the value of Z factor is changed from 1 to 1.006, within the range of pressure change from 0.101 MPa to 20 MPa. It is possible to divide the pressure change into many parts with reasonable accuracy. As a result, thirty equations of z=f(T) were derived relative to thirty differential pressure periods. They are all linear and of the form

$$z = ax+b. \qquad (6\text{-}9)$$

Appendix (C.1) shows the values of a and b relative to each different pressure range of these equations. The maximum error in these curve fits is ±0.012%. The functions are put back into equation (6-2). Therefore, equation (6-2) becomes a new PVT relationship as:

$$T=f(p,V,m,R) \qquad (6\text{-}10)$$

Linear curve fitting is not available for Z calculation of NGV. It is more accurate to express the curve fitting as the form below:

$$Z= at^2+bt+c \qquad (6\text{-}11)$$

The values of a, b, and c are listed in appendix (C-2).

6.4 SIMULATION PROCEDURE

The theoretical solution process has been developed. The further aim will be to solve the simultaneous equation by a computer program. In this research, computer programs have been written in Turbo C. The flow chart of the program is shown in Fig.6.2.

As described before, the preconditions for carrying out the simulations are that the data of mass flow rate $\dot{m}$, gas pressure p and gas incoming temperature T_i must be obtained first, the seven variables then could be rapidly calculated.

Fig.(6.2) Simulation program flow chart

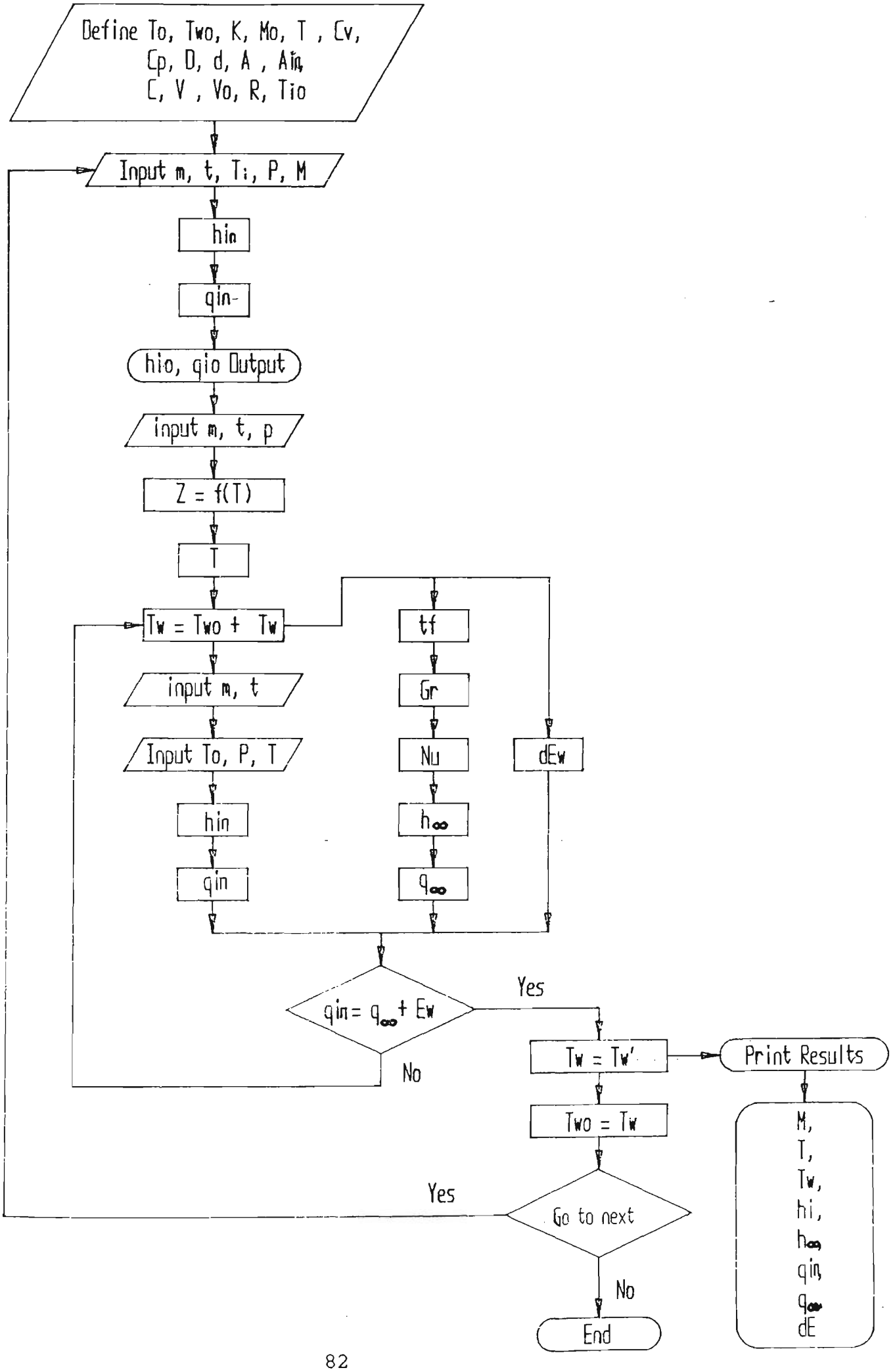

Step 1. Initial conditions

To simulate the heat transfer phenomenon, the initial conditions of cylinder charging process are required. Here initial conditions of gas both inside and outside cylinder are set. And also, the dimension and properties of cylinder are needed.

For gas, the initial conditions are:

1. Gas temperature T_o;
2. Cylinder wall temperature T_{wo};
3. Ambient T_∞;
4. Gas pressure p_o;
5. Gas mass m_o;

For cylinder wall, the parameters needed are:

6. External diameter D_o;
7. Internal diameter D_i;
8. External surface area A_∞;
9. Internal surface area A_i;
10. Density ρ and specific heat C.

Also in the initialisation phase an "accuracy" figure which determines the accuracy. This is included in order to speed up simulation time at the cost of a loss of accuracy.

Step 2. The average temperature change of gas T

The value of average pressure and mass are two known variables which are obtained by general measurement. Therefore, the temperature could be evaluated by the following equation

$$T=\frac{pV}{mRZ} \qquad (6-12)$$

While pressure given, the relationship between T and Z is specific and the function could be curve fitted by a computer program (in Appendix B.3). In relationship to any particular pressure value, the function is linear with the form:

$$Z=aT+b \qquad (6-13)$$

Appendix (C.1) and (C.2) show the values of **a** and **b** for air and natural gas relative to different pressure range of thirty equations. Combining equation (6-12) and equation (6-13), we obtain

$$aT^2+bT-\frac{PV}{mR}=0 \qquad (6-14)$$

Solving this second order equation, the average temperature change T is determined by

$$T=\frac{-b+(b^2+4a\frac{pV}{mRz})^{0.5}}{2a} \qquad (6-15)$$

Step 3. The variable time derivatives $\dot{p}$, $\dot{T}$ and $\dot{T}_i$

Since the whole simulation is based on mass flow rate and pressure at each particular time, it is better to derive the solutions of the variable time derivatives p, T and T_i before the simulation commences, in order to keep the continuity of the simulation. That is, the simulation would be carried out with each group of p, $\dot{m}$, T_i and T data after the equations of $\dot{p}$, $\dot{T}$ and $\dot{T}_i$ has been determined.

Calculations should be carried out in order to derive the pressure-time derivative $\dot{p}$, Z-time derivative $\dot{Z}$ and T_i- time

derivative $\dot{T}_i$. In this study, data for p,Z and T_i changes with time were curve fitted by the least square method to derive second order equations. The variables time derivative is going to be a first order equations with the form

$$\dot{p} = a_1 t + b_1$$
$$\dot{Z} = a_2 t + b_2$$
$$\dot{T}_i = a_3 t + b_3 \qquad (6\text{-}16)$$

The solution of $\dot{T}$ requires several steps. First of all, the T values could be calculated as described above. Relative to each particular time t, the function relationship between T and t could be derived by curve fitting, then the T time derivative $\dot{T}$ can be obtained.

Therefore, $\dot{p}$, $\dot{Z}$ and $\dot{T}_i$ values can be determined relative for any particular time t.

Step 4. Assumption of cylinder wall Temperature T_w

To start the simulation, the cylinder wall temperature T_w must be assumed as a initial value, then it is adjusted in each iteration. Finally, by equation(6-7), T_w can be confirmed to be a correct value. whence, in this step,

$$T_w = T_w' \qquad (6\text{-}17)$$

Ambient is usually settled as T_w' at the beginning of simulation.

Step 5. Heat transfer coefficient inside cylinder h_i

According to the equation

$$h_{in} = \frac{C_p \dot{m} T_1 - C_v (\dot{m} T - \dot{T} m)}{A_{in} (T - T_w)}$$

By applying the equation-of-state, pV/T = mRZ. Each term in this equation is determined as below. T_w has been assumed already. It has specific value whenever the coefficient hi is being calculated. The procedures for determining the specific heat c_p and c_v of both air and natural gas are described in Chapter 5-1. As a result, a value of h_i is obtained in this step.

Step 6. Heat transfer coefficient outside cylinder h_∞

For using equation (6-4),

$$Nu^{\frac{1}{2}} = 0.60 + 0.387 \left[\frac{GrPr}{\left[1 + \left(0.\frac{559}{Pr}\right)^{\frac{9}{16}}\right]^{\frac{16}{9}}} \right]^{\frac{1}{6}}$$

GrPr could be calculated with the wall temperature assumed.

Firstly, for free convection, Grashof number is:

$$Gr = \frac{g\beta (T_w - T_\infty) D_o^3}{\nu^2}$$

While D_o is the outside diameter of cylinder.

Secondly, Rayleigh number is calculated from

$$Ra = GrPr$$

whence, by applying equation (6-4), Nu is determined.

h_∞ is calculated easily from

$$h_\infty = \frac{N_u k}{D}$$

Step 7. Heat transfer rate q_{in} and q_{∞}

Now the heat transfer rate both inside and outside cylinder can be obtained from equation

$$q_{in}=h_{in}A_{in}(T-T_w)$$

$$q_{\infty}=h_{\infty}A_{\infty}(T_w-T_{\infty})$$

Step 8. Change in internal energy of wall $\dot{E}_w$

With the lumped capacitance method described before, the assumption in this step is that the specific heat of the wall is constant and the average temperature is used to present the internal energy change in the wall.

$$dE_w=\rho C\frac{dT_w}{dt}V_m$$

While dT_w is determined by assumed temperature difference of cylinder wall within a differential time dt, dE_w is calculated.

Step 9. Adjustment of parameters by energy balance

It is apparent that, apart from the prediction of gas temperature T, an assumed value of wall temperature is used in every step during a simulation. The way to confirm the variables derived is to check against equation (6-7) after each iteration.

$$q_{in}=q_{\infty}+\frac{dE_w}{dt}$$

T_w is adjusted up or down to make the equation balance. Simulation is completed when the equation is balance.

Step 10. Simulation output

When the parameters T, h_i, h_∞, $\dot{E}_w$, q_i and q_∞ are computed relative to particular values of time, mass flow rate, and pressure etc., the results are printed.

Step 11. Next simulation

The program continues to the next simulation by taking new input variables all steps in the first process are repeated.

6.5 COMPUTER PROGRAM

The whole simulation consists of two computer programs, which are written in Turbo C language. Copies of these two programs are included in Appendix B.

The data curve fitting program (Appendix B) is for the solutions of time derivatives of p, T, and T_i. The least squares method was employed in this program for quadratic curve fitting through fifteen points. Functional relations between these three variables and fill time were derived first, then the time derivative equations for p, T and T_i were obtained.

The simulation program (Appendix B.1) is for simulation and prediction of the heat transfer coefficients, and cylinder wall temperature. The input variables included measured data of pressure, mass flow rate, incoming temperature, as well as the predicted values of gas temperatures.

Since the gas used in this experiments of this research was

air instead of NGV, the simulation was carried out using air, in order to make the comparisons with the experimental results.

6.6 COMPARISON OF SIMULATION AND EXPERIMENT

As above, test 1, test 6 and test 8 are chosen for the comparison, because each of them presents a different kind of cylinder or thermocouple array position. The results of the comparison are shown in table (6.1-6.3).

All the comparisons of the experimental results and the simulations are satisfactory.

6.6.1 Heat Transfer Coefficient h_{in} and h_{∞} Comparison

The predicted value of heat transfer coefficient in cylinder h_i is simulated with converted value of the gas pressure, predicted cylinder wall temperature, as well as the measured data of mass flow rate and inlet temperature. The heat transfer coefficients values of the experimental results are calculated with measured data of T, T_i and m. The results are shown in Fig.6.3-6.5.

For the heat transfer coefficient between the external surface of the cylinder and its surrounding h_{∞}, the results of comparison are shown in Fig.6.6-6.8.

6.6.2 Wall Temperature Comparison

Based on the pressure value converted, T_w is predicted by the simulation program. Fig.6.9-6.11 show that it agreed well with the test data.

6.6.3 Gas Temperature Comparison

The temperature value is predicted by equation (6-15), while the Z factor is derived by a subroutine computer program based on Z=f(P,T) curve fitting. The comparisons are shown in Fig.6.12-6.14, with fill time as independent variable. The corrected experimental values of temperature by the thermocouple time constant are used in the comparison. The comparisons are also shown in table 6.6. The comparisons are for the duration after the first 80 seconds, because of the pressure lag in the measurement of first phase. The comparison shows good agreement and the trend is similar.

Table (6.1) Comparison of test 1

Time	Mass	Experiment			Simulation		
		hin	hoo	Tw	hin	hoo	Tw
(s)	(kg)	(W/M^2S)	(W/M^2S)	(℃)	(W/M^2S)	(W/M^2S)	(℃)
31	3.98	476.40	2.40	19.53	481.89	2.34	19.14
35	4.50	441.03	2.55	20.22	470.68	2.47	19.58
41	5.25	399.01	2.74	21.32	427.52	2.74	21.92
45	5.71	369.59	2.85	22.07	384.44	2.83	22.50
51	6.35	330.60	3.00	23.23	360.40	3.09	23.36
55	6.74	304.56	3.08	23.96	322.69	3.16	24.01
61	7.25	261.29	3.20	25.10	288.23	3.31	24.93
65	7.53	238.80	3.27	25.77	255.51	3.36	25.60
71	7.90	202.09	3.35	26.71	229.97	3.45	26.74
75	8.08	170.60	3.39	27.25	200.88	3.48	27.14
81	8.28	124.23	3.46	28.08	152.40	3.51	27.56
85	8.36	104.05	3.50	28.62	130.26	3.54	28.99
86	8.37	99.42	3.51	28.70	127.39	3.56	29.21
91	8.42	30.60	3.54	29.14	35.95	3.59	29.71
93	8.43	30.74	3.55	29.37	40.22	3.58	29.45
99	8.45	31.22	3.59	29.93	41.44	3.62	30.56
105	8.47	31.46	3.62	30.35	41.74	3.60	30.78
110	8.49	31.23	3.64	30.57	31.09	3.63	31.35
113	8.50	31.24	3.64	30.72	31.03	3.61	30.99
119	8.52	30.74	3.66	30.97	30.38	3.64	31.49
125	8.54	30.83	3.69	31.41	30.37	3.62	31.08
130	8.56	30.38	3.69	31.45	30.28	3.64	31.50
133	8.57	30.20	3.70	31.59	30.03	3.62	31.57

Table (6.2) Comparison of test 6

Time	Mass	Experiment			Simulation		
		hin	hoo	Tw	hin	hoo	Tw
(s)	(kg)	(W/M^2S)	(W/M^2S)	(℃)	(W/M^2S)	(W/M^2S)	(℃)
21.00	2.95	546.37	2.73	21.41	566.31	2.83	22.27
26.00	3.71	489.24	2.87	22.37	510.16	2.95	23.54
31.00	4.52	444.26	2.99	23.40	455.20	3.09	24.69
36.00	5.35	403.03	3.10	24.44	423.30	3.17	25.52
41.00	6.14	365.15	3.21	25.49	386.41	3.23	26.61
46.00	6.87	327.26	3.31	26.61	345.43	3.37	27.98
51.00	7.50	295.94	3.39	27.64	310.44	3.43	29.17
56.00	8.01	268.47	3.46	28.58	285.15	3.52	30.01
61.00	8.45	229.75	3.54	29.65	233.70	3.63	30.55
66.00	8.82	189.50	3.61	30.66	218.45	3.74	31.57
71.00	9.11	160.14	3.67	31.63	185.01	3.75	32.89
76.00	9.31	157.22	3.71	32.36	149.85	3.79	33.92
77.00	9.33	133.57	3.72	32.48	140.00	3.80	33.96
81.00	9.42	91.50	3.75	33.08	101.14	3.83	34.19
84.00	9.44	78.31	3.78	33.51	90.41	3.85	34.13
88.00	9.45	69.52	3.80	33.98	81.87	3.86	34.25
94.00	9.46	33.16	3.83	34.51	36.15	3.85	35.08
100.00	9.47	33.16	3.86	35.00	35.61	3.87	35.68
105.00	9.48	32.87	3.87	35.37	34.96	3.88	36.14
111.00	9.49	32.49	3.89	35.62	32.98	3.91	36.23
115.00	9.49	32.26	3.90	35.83	32.45	3.91	35.90
120.00	9.50	32.01	3.91	36.13	32.41	3.93	36.20

Table (6.3) Comparison of test 8

Time	M	hin	hoo	Tw	hin	hoo	Tw
(s)	(kg)	(W/M^2S)	(W/M^2S)	(℃)	(W/M^2S)	(W/M^2S)	(℃)
20.00	3.26	522.37	2.54	20.32	597.65	2.57	20.92
25.00	4.09	480.20	2.62	20.75	492.52	2.65	21.08
30.00	4.89	426.99	2.75	21.54	449.60	2.83	22.30
35.00	5.65	391.32	2.85	22.26	420.86	2.98	23.49
40.00	6.35	354.83	2.93	22.89	375.48	3.07	24.62
45.00	7.00	318.60	3.04	23.82	332.59	3.12	25.06
50.00	7.59	285.33	3.14	24.75	312.85	3.20	26.05
55.00	8.10	260.14	3.23	25.70	283.91	3.35	27.31
60.00	8.55	238.16	3.31	26.68	268.64	3.43	28.71
65.00	8.91	214.67	3.38	27.54	258.92	3.49	28.90
70.00	9.20	194.14	3.44	28.22	219.20	3.53	29.64
75.00	9.42	140.84	3.49	28.91	164.64	3.56	30.17
80.00	9.55	40.97	3.53	29.60	55.49	3.61	31.34
85.00	9.62	31.90	3.59	30.43	47.35	3.64	31.48
90.00	9.66	32.31	3.63	31.12	38.81	3.75	31.71
95.00	9.68	32.66	3.66	31.58	33.69	3.78	32.85
100.00	9.70	32.74	3.71	32.36	33.51	3.74	33.78
107.00	9.73	32.28	3.79	33.73	32.94	3.83	35.28
117.00	9.76	32.08	3.84	34.62	32.86	3.89	35.33
130.00	9.77	30.20	3.90	35.91	32.88	3.95	35.74

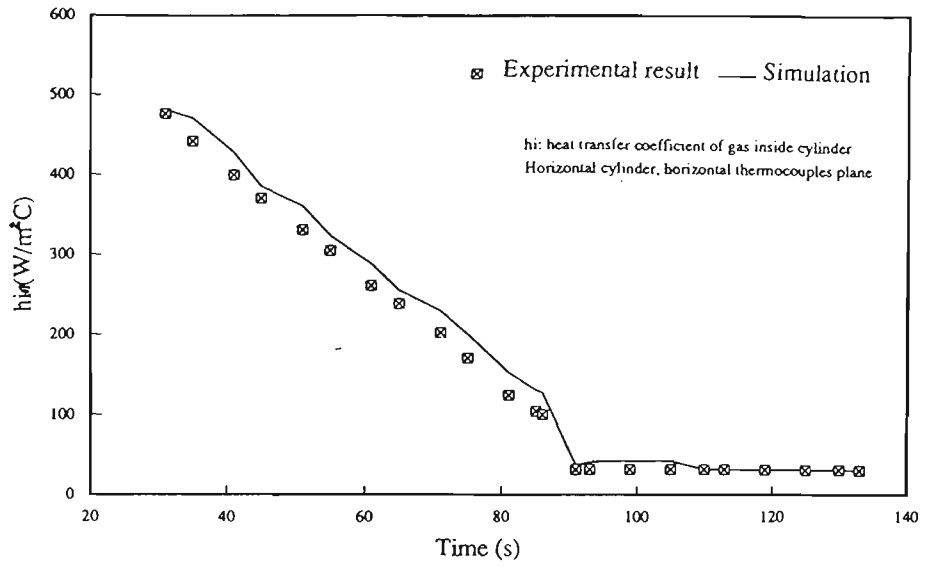

Fig 6.3 heat transfer coefficient hi comparison of run 1

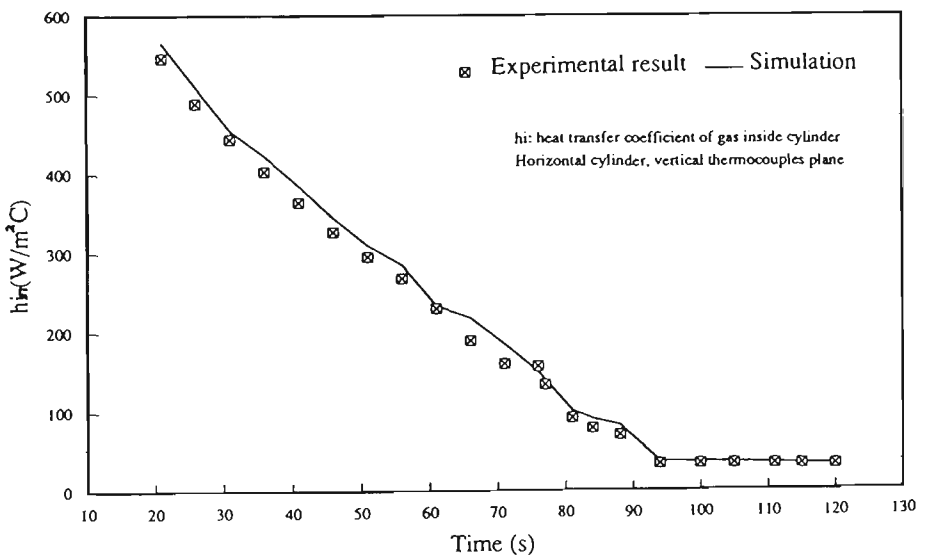

Fig 6.4 heat transfer coefficient hi comparison of run 6

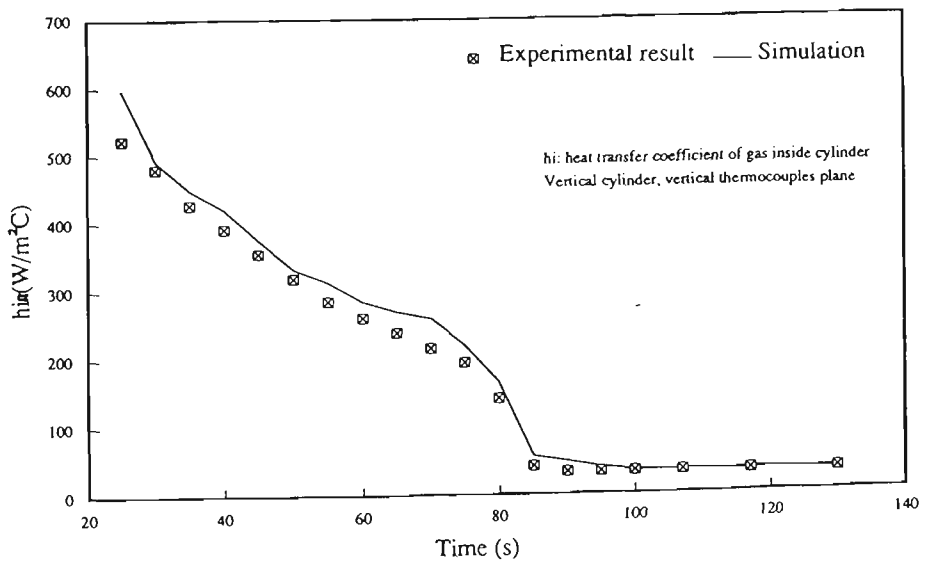

Fig 6.5 heat transfer coefficient hi comparison of run 8

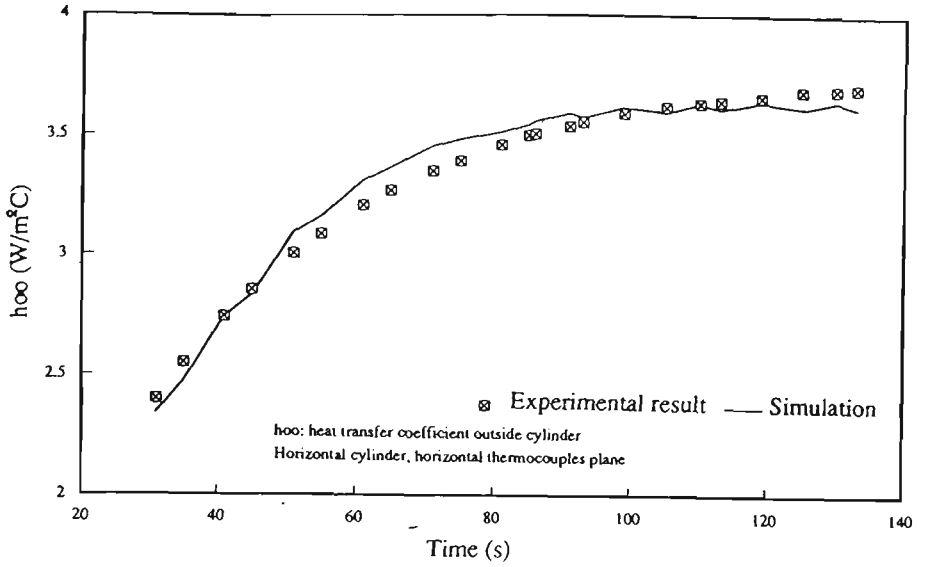

Fig 6.6 heat transfer coefficient h_∞ comparison of run 1

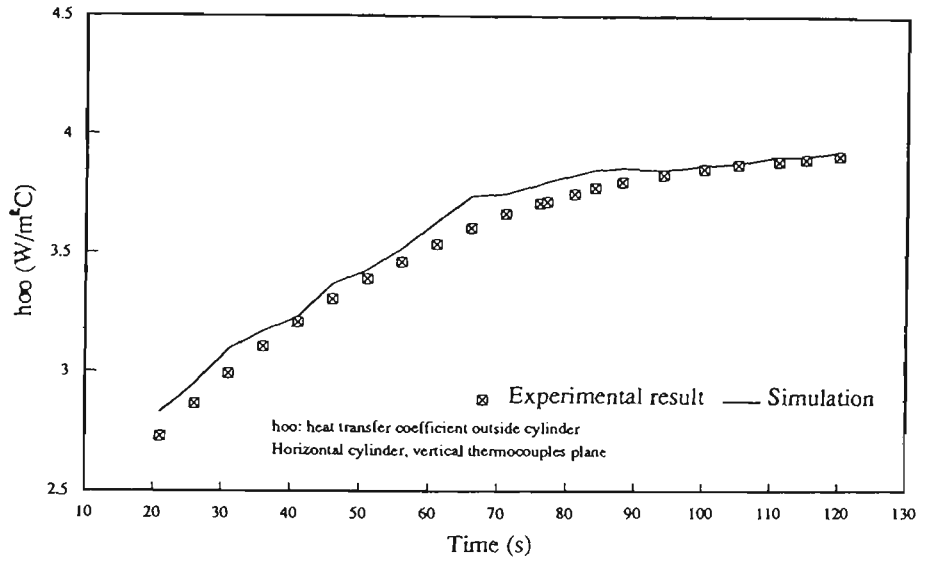

Fig 6.7 heat transfer coefficient h_∞ comparison of run 6

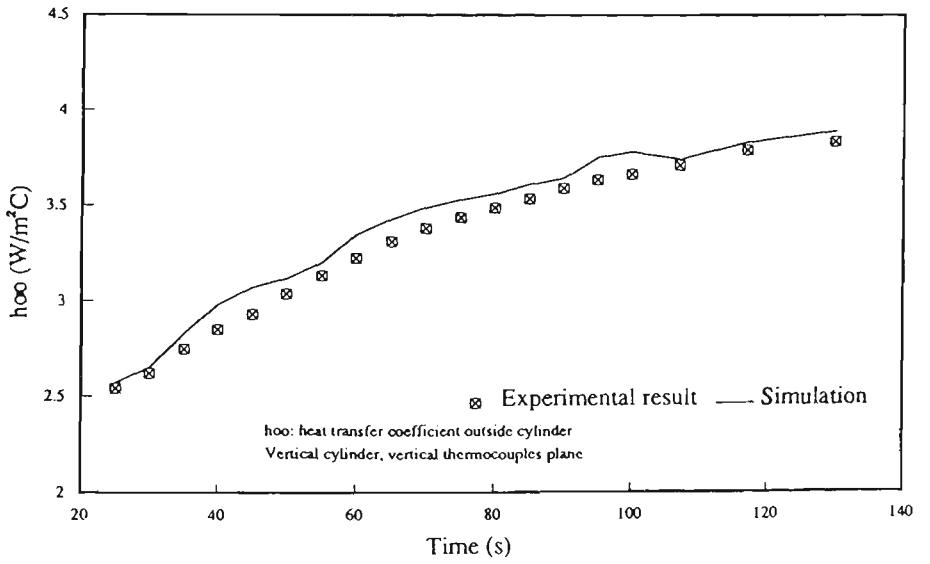

Fig 6.8 heat transfer coefficient h_∞ comparison of run 8

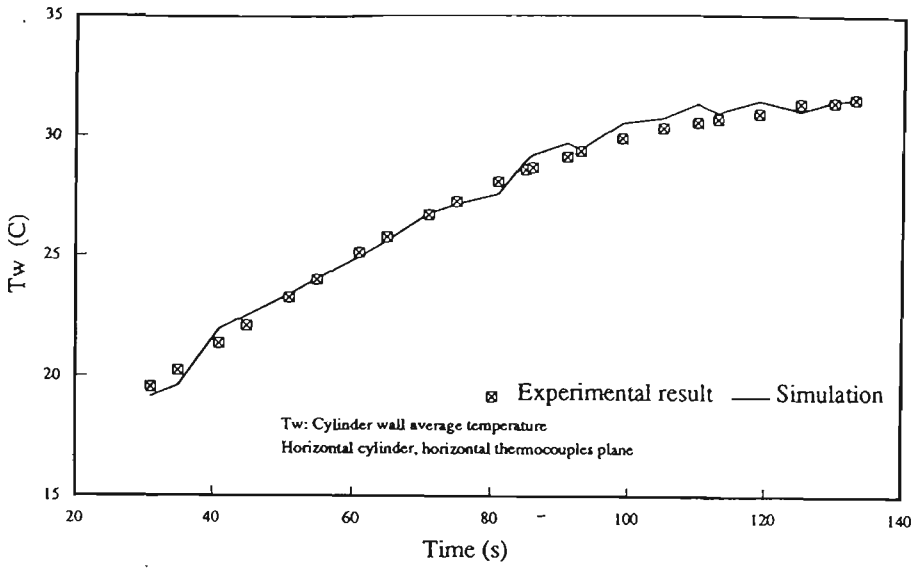

Fig. 6.9 Cylinder wall temperature T_w comparison of run 1

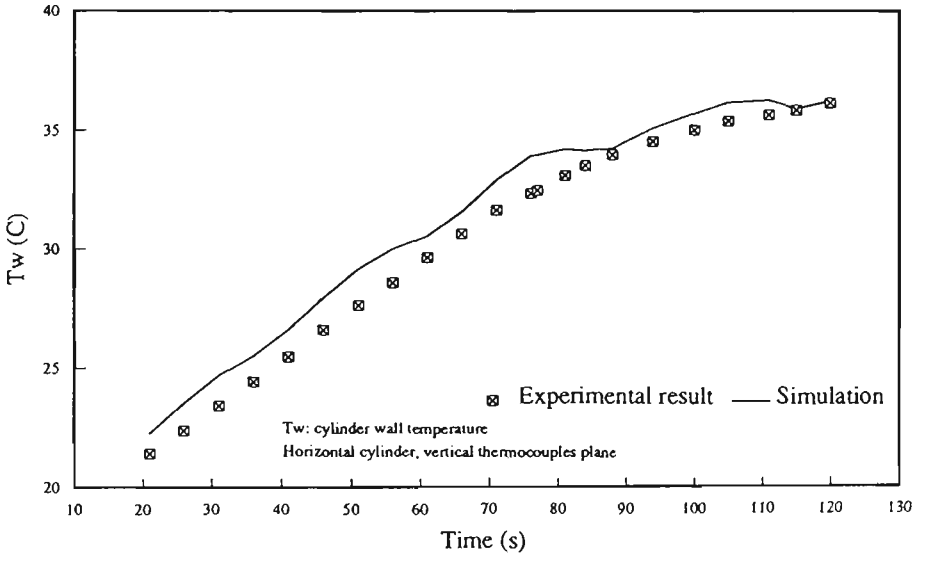

Fig. 6.10 Cylinder wall temperature T_w comparison of run 6

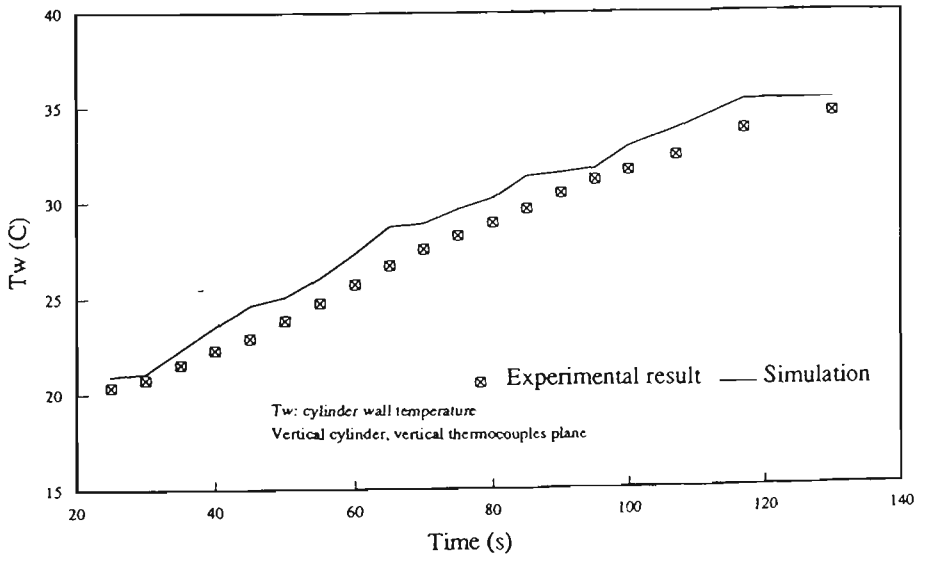

Fig. 6.11 Cylinder wall temperature T_w comparison of run 8

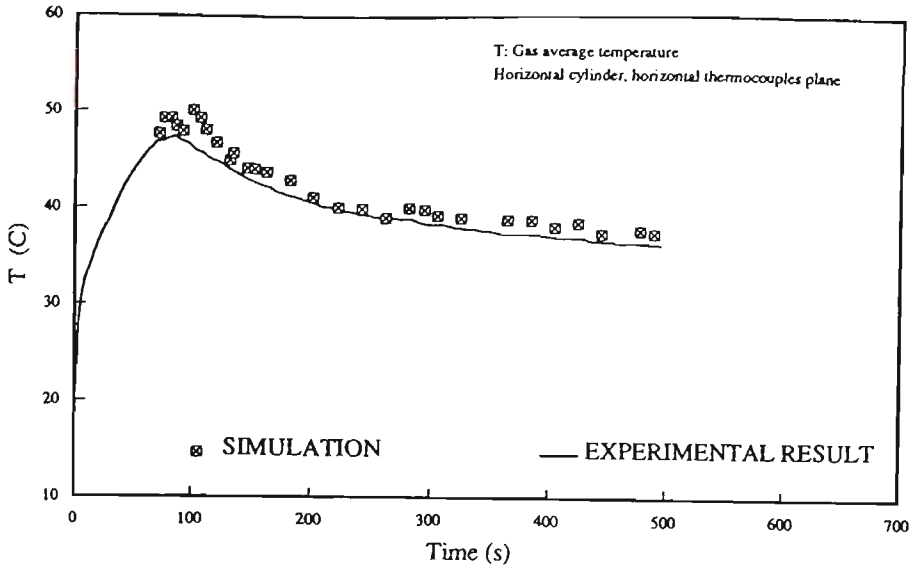

Fig. 6.12 Gas temperature T comparison of run 1

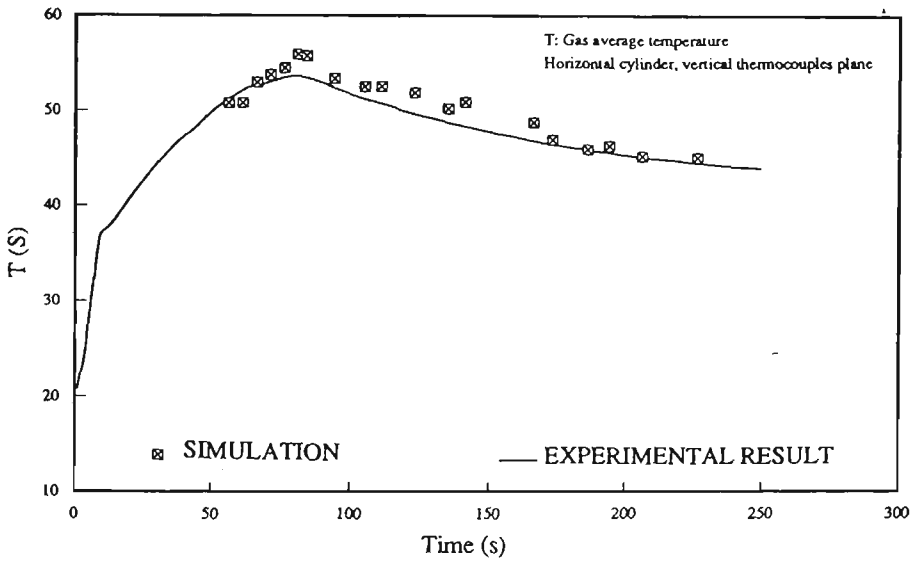

Fig. 6.13 Gas temperature T comparison of run 6

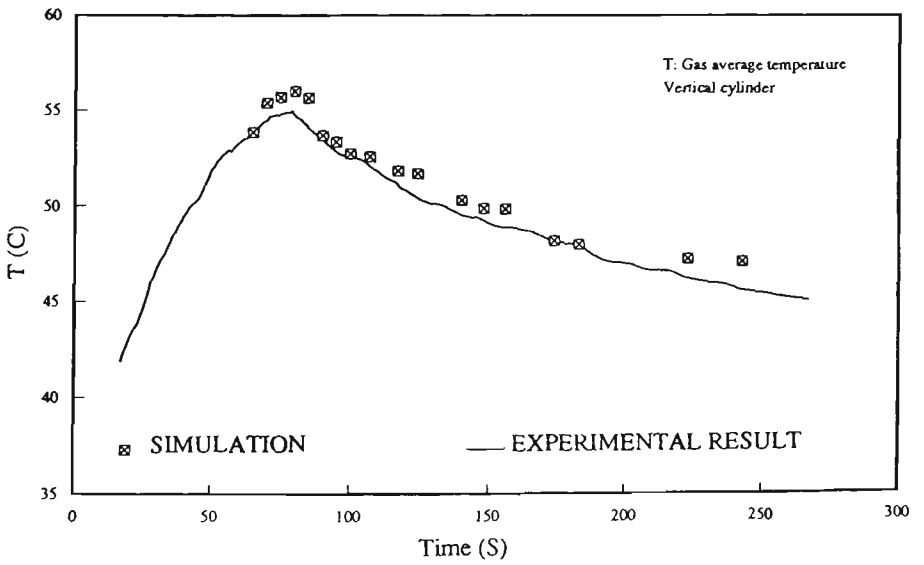

Fig. 6.14 Gas temperature T comparison of run 8

Table 6.6 Gas temperature comparison of run 1, 2 and 8

run 1

Time (s)	T (C)	Tp (C)	Time (s)	T (C)	Tp (C)
71	46.88	47.70	145	43.05	44.15
75	46.95	49.34	151	42.77	44.07
81	47.30	49.30	161	42.28	43.76
85	47.40	48.50	181	41.26	42.87
91	46.94	47.97	200	40.58	41.15
99	46.31	50.09	221	39.80	40.04
105	45.81	49.30	241	39.31	39.97
110	45.49	48.14	261	39.00	38.94
119	44.91	46.80	281	38.89	40.02
130	44.05	44.95	294	38.37	39.77
133	43.86	45.70	305	38.24	39.14

run 6

Time (s)	T (C)	Tp (C)	Time (s)	T (C)	Tp (C)
56	51.22	50.77	111	50.72	52.50
61	52.11	50.80	123	49.61	51.90
66	52.60	52.97	135	48.73	50.20
71	53.04	53.80	141	48.33	50.90
76	53.47	54.45	166	46.81	48.72
81	53.61	55.88	173	46.50	46.99
84	53.47	55.76	186	45.86	45.90
94	52.37	53.37	194	45.54	46.30
105	51.21	52.50	206	45.06	45.20

run 8

Time (s)	T (C)	Tp (C)	Time (s)	T (C)	Tp (C)
65.00	53.84	53.87	117.00	51.12	51.86
70.00	54.45	55.39	124.00	50.43	51.71
75.00	54.84	55.70	140.00	49.54	50.30
80.00	54.74	56.03	148.00	49.26	49.89
85.00	54.10	55.65	156.00	48.89	49.83
90.00	53.55	53.70	174.00	48.07	48.16
95.00	52.88	53.37	183.00	47.95	47.98
100.00	52.56	52.75	223.00	46.19	47.23
107.00	52.06	52.58	243.00	45.56	47.06

Tp: Predicted temperature
T: Measured temperature

CHAPTER 7

CONCLUSIONS

1) Based on the energy balance of the system, a simple model has been developed. The values of the heat transfer coefficient were derived from the model, using measured experimental data.

2) In the charging process, the temperature increase rapidly in the first 1 minute until it is 20 to 30 degree C above ambient. The cylinder pressure increases from atmospheric to its maximum values of 14 MPa to 17 MPa. During this period, the mass flow rate increases to the maximum value, then drops to a small value. In the meantime, the heat transfer coefficient inside the cylinder is initially very high and then falls quickly.

3) Beyond this 60 minutes the mass flow rate is close to zero. Heat transfer within the cylinder is by conduction. There is always 4-7 degree C temperature difference between top and bottom in side the cylinder, with the higher temperature at the top. The temperature difference between charging of horizontally and vertically oriented cylinder is slight, and the difference is small along the horizontal direction inside the tank.

4) The whole charging process can be divided into three heat transfer phases: forced convection, free convection and conduction. For these tests, the forced convection phase lasts about 80 seconds, while the free convection phase takes about 130 seconds. Data from both phases may be fitted by

$$Nu = 9320.71\ e^{-26.62\ Fo}$$

$$(\ 0.00 < Fo < 0.06)$$

$$Nu = 387.6\ e^{-7.6\times10^{9}\left(\frac{Fo^{0.5}}{Ra}\right)}$$

$$(\ 3.8\times10^{11} < Ra < 6.9\times10^{11})$$

$$(0.06 < Fo < 0.09)$$

The Heat transfer coefficient in the conduction phase is close to zero.

The correlations almost cover the whole range of convective heat transfer during the charging process, and therefore may be employed to predict the heat transfer coefficients within the relevant ranges.

5) A simulation method was developed for predicting the change in heat transfer coefficients inside and outside the cylinder, the temperature of the cylinder wall, and the gas temperature during the charging process. The comparisons of experimental and theoretical results agree well. The simulation method was shown to be a successful method for predicting the heat transfer coefficient in a tank during the charging process, provided accurate values of pressure and mass flow rate can be obtained as the input variables.

6) Either the heat transfer data correlations or the computer simulation method presented in this research could be used to predict the heat transfer coefficients appropriate to the process. Owing to its accuracy and convenience, the data correlations are particularly recommended for prediction and calculation. The simulation method is very useful when only considering gas pressure, inlet temperature and mass flow rate as input variables provided the

resulting correlation are within the range of validity.

7) A method of experimentally measuring the gas temperature during the charging process has been developed, in spite of the transient conditions and the high pressure. A satisfactory time response (τ=1.5 seconds when V=24.9 m/s) of the type T thermocouples can be obtained, providing low mass thermocouples are used. The thermocouple array assembly has proved to be an excellent test device to measure the gas temperature and its stratification. Gas tight sealing of the multiple thermocouple cables was difficult, but a successful technique was developed, utilising silver soldered connections. The thermocouple array assembly which has been designed for this project can be used in further experimental work.

8) The properties used in the theoretical analysis are those for air, the fluid used in the experiments and the coefficients of the equations in (7.1.2) are therefore for air. Further experiments with natural gas could yield the appropriate coefficients for CNG.

7.2 RECOMMENDATIONS

This thesis has opened up a number of avenues for further research. Presented below are some recommendations suggesting several areas needing research effort.

More advanced simulation The further simulations of flow and heat transfer fields could be carried out, based on the phenomena demonstrated in this thesis. The procedure outlined in this thesis computes the average heat transfer coefficient between the gas and the tank wall. Studies of local heat transfer coefficients should be

made. Initially these simulations could be on a two-dimensional axi-symmetric basis, later they should include three-dimensional flow. Computational Flow Dynamics (CFD) studies, using packages such as PHOENICS, may be appropriate.

Gas pressure measurement A better means for measuring gas pressure is needed. Perhaps the best location of pressure transducer should be in the middle of the tank space, additional to the other pressure transducer at the inlet.

Velocity and vorticity Velocity profiles and vorticity should be measured for the different flow fields which can be established in a closed container. There are several ways to accomplish this, perhaps the best way would be with hot wire anemometers, or with a laser doppler velocity meter.

Heat flux Studies of local heat transfer coefficients could be accomplished by installing heat flux meters in the cylinder wall.

Different geometries A wide range of inlet nozzle geometries should be tested. Further, studies should be made to determine the proper characteristic length to be made in an analysis such as this.

Pulse injection Experiments to repeatedly inject short pulses of gas in charging process should be carried out. Since this would keep the gas in the cylinder agitated continually, one would expect that heat transfer coefficient would be very high. Investigation of this possibility would be useful.

Filling silencer It would be useful to examine the heat

transfer consequences of the silencer tube used in some cylinder applications.

Natural gas Currently available results are all with dry ambient air. It would be desirable to obtain similar data correlations for NGV charging process. Also, the differences introduced by greatly different gases, such as He and H_2, should be studied. Tests with combustible gases will require safety measures to avoid ignition.

REFERENCES

1. American Gas Association, *Manual for the Determination of Super Compressibility Factors for Natural Gas*, December.

2. Amstrong, G. and McEwen,R., *Heat Transfer and Temperature Measurement in a NGV Cylinder During a Fast Refuelling Process*, Student Thesis, Dept. of Mechanical Engineering, University of Melbourne.(1990)

3. Baumeister, T. and Marks, L.S., *Standard Handbook for Mechanical Engineers*, McGraw-Hill, New York, 1967, Section 12:17.(1967)

4. Bayley, F.J., Owen, J.M., and Turner, A.B., *Heat Transfer*, William Clowes & Sons, Limited, London.(1972)

5. Chase, P., *High speed Natural Gas Refuelling by Computer Simulation*, Student Thesis, Dept. of Mechanical Engineering, University of Melbourne. (1989)

6. Churchill, S.W., and Chu, H.H.S., *Correlations Equations for Laminar and Turbulent Free Convection from a Horizontal Cylinder*, J. Heat Mass Transfer, Vol.18. pp.1049-1053.(1975)

7. Comings, E.W., Mayland, B.J., and Egly, R.S., *The Viscosity of Gases at High Pressure*, Univ. Ill. Bull., Series No.354. (1944)

8. Comings, E.W. and Nathan, M.F., *Thermal Conductivity of Gases at High Pressure*, Ind. Engng Chem., 1947, 39, 964.(1947)

9. Din, F., *Thermodynamic Functions of Gases*, Butterworths, London. (1962).

10. Gauthier,S.W., *Natural Gas Vehicle Developments-- a Gas Industry and Original Equipment Manufacturer Cooperative*, Proc. of 25th Intersociety Energy Conversion Engineering Conference,IECEC'90, pp.230-239.(1990)

11. *Handbook of Supersonic Aerodynamics*, vol.5, Bureau of Ordnance, Dept. of U.S. Navy. (1953).

12. Hilsenrath, J., et al., *Table of Thermal Properties of Gases*, U.S.N.B.S. Circular 564, Pergamon Press, Oxford.(1960).

13. Holman, J.P., *Heat Transfer*, SI Metric Edition, McGraw-Hill Book Company. (1989)

14. Incropera, F.P. and DeWitt, D.P., *Fundamentals of Heat and Mass Transfer*, 2nd.edn, John Wiley & Sons, London.(1985)

15. Lee, I., *What Is It Like To Drive a Natural Gas Powered Car*, Energy, Vol.2/No.7.1992, pp.20-23. (1992)

16. Li, H., Milkins, E. and Hunt, K., *A Heat Transfer Model of Refuelling Process for Natural Gas Vehicle Storage Tanks*, Presentation and Publication at the 6th International Symposium on Transport and Phenomena in Thermal Engineering, Seoul, Korea, May 9-13, 1993

17. Loomis, A.W., *Compressed Air and Data*, 3rd.edn, Ingersoll-Rand Company.(1982)

18. McAdam, W.H., *Heat Transmission*, 3rd.edn, McGraw-Hill Book Company.(1954)

19. Means, J.D. & Ulrich, R.D., *Transient Convective Heat Transfer During and After Gas Injection into Containers*, Transactions of ASME, May, 1975, pp.282-287. (1975)

20. Metais, B. & Eckert, E.R.G., *Forced, Mixed, and Free Convection Regimes*, J. Heat Transfer, ser. C, Vol.86, p.295.(1964)

21. Perry, R.H. & Green, D., *Perry's Chemical Engineer's Handbook*, 6th edn. McGraw-Hill, New York. (1984).

22. Reid, R.C., Prensnitz J.M, & Sherwood, T.K., *Properties of Gases and Liquids*, McGraw-Hill Inc. (1977)

23. Reynolds, W.C., & Kays, W.M., *Blowdown and Charging Process in a Single Gas Receiver with Heat Transfer*, Transactions of ASME, July, 1958, pp.1160-1168. (1958)

24. Ring, E., *Rocket Propellant and Pressurising System*, Prentice-Hall, Inc., Englewood Cliffs, N.J. (1964)

25. Ulrich, R.D., Wirtz, D.P., & Numn, R.H., *Transient Heat Transfer in Closed Containers After Gas Injection*, J. Heat Transfer, Transactions of ASME, ser. C, Vol.91. Aug.(1969)

26. Van Wylen, G.J. & Sontag, R.E., *Fundamentals of Classical Thermodynamics*, John Wiley and Son, Inc. (1973)

27. Walker, I.J & Lyall, K.D., *Natural Gas Vehicles (NGV)-Research and Development*, EPD Discussion Paper

No.4, Energy Programs Division, Department of Primary Industries and Energy, Canberra. (1991)

28. Wark, K., Jr. *Thermodynamics*, 5th Edition, McGraw-Hill Book Company. (1988)

29. Wyman, R.P., *CNG Measurement Using PVT Relationships*, SAE Technical Paper Series No.831067, pp.13-26. (1983)

BIBLIOGRAPHY

Alamdari, F. & Hammond, G.P., *Improved Data Correlation for Buoyancy-Driven Convection*, BSER & T, 4 pp.106-120. (1983)

American Gas Association, *Manual for the Determination of Super Compressibility Factors for Natural Gas*, December.

Amstrong, G. & McEwen,R., *Heat Transfer and Temperature Measurement in a NGV Cylinder During a Fast Refuelling Process*, Student Thesis, Dept. of Mechanical Engineering, University of Melbourne.(1990)

Baumeister, T. & Marks, L.S., *Standard Handbook for Mechanical Engineers*, McGraw-Hill, New York, 1967, Section 12:17.(1967)

Bayley, F.J., Owen, J.M., & Turner, A.B., *Heat Transfer*, William Clowes & Sons, Limited, London.(1972)

Bontoux, P., Roux, B., Shiroky, G.H., Markham, B.L. & Rosenberger, F., *Convection in the Vertical Midplane of a Horizontal Cylinder. Comparison of Two-Dimensional Approximations with Three-Dimensional Results*, Int.J. Heat Mass Transfer, Vol.29, No.2, pp.227-240.(1986).

Catton, I., *Natural Convection in enclosures*, Proc. 6th Int. Heat Transfer Conf., Vol.6, pp.13-31. (1978)

Chase, P., *High speed Natural Gas Refuelling by Computer Simulation*, Student Thesis, Dept. of Mechanical Engineering, University of Melbourne. (1989)

Churchill, S.W., & Chu, H.H.S., *Correlations Equations for Laminar and Turbulent Free Convection from a Horizontal Cylinder*, J. Heat Mass Transfer, Vol.18. pp.1049-1053.(1975)

Comings, E.W., Mayland, B.J., & Egly, R.S., *The Viscosity of Gases at High Pressure*, Univ. Ill. Bull., Series No.354. (1944)

Comings, E.W. & Nathan, M.F., *Thermal Conductivity of Gases at High Pressure*, Ind. Engng Chem., 1947, 39, 964.(1947)

Din, F., *Thermodynamic Functions of Gases*, Butterworths, London. (1962).

Fahmy, M.F.M. & Abdel, S.M., *On the Dynamic Behaviour of Hot Water Systems with Tanks in Series*, Energy Conversion and Management V.30, No.3, pp.287-296. (1990)

Farouk, B. & Guceri, S.I., *Natural Convection from a Horizontal Cylinder-Laminar Regime*, Transactions of ASME, Vol.103, Aug. 1981, pp.522-527.(1981)

Faw, R.E., Ismuntoyo, R.P.H. & Lester, T.W., *Transition from Conduction to Convection Around a Horizontal Cylinder Experiencing a Ramp Excursion in Internal Heat Generation*, Int.J. Heat Mass Transfer, Vol.27, No.7, pp.1087-1097.(1984)

Franke, M.E & Hutson, K.E., *Effects of Corona Discharge on Free-Convection Heat Transfer inside a Vertical Hollow Cylinder*, Transactions of ASME, Vol.106, May, pp.346-351. (1984)

Gauthier,S.W., *Natural Gas Vehicle Developments-- a Gas Industry and Original Equipment Manufacturer Cooperative*, Proc. of 25th Intersociety Energy Conversion Engineering Conference,IECEC'90, pp.230-239.(1990)

Grace, H.P. & Lapple, C.E., *Discharge Coefficients of Small-Diameter Orifices and Flow Nozzles*, Transactions of ASME, July, 1951, pp.639-648. (1951)

Handbook of Supersonic Aerodynamics, vol.5, Bureau of Ordnance, Dept. of U.S. Navy. (1953).

Hanzawa, T., Huang, X.J., Kamata, S & Sakai, N., 1991, *Heat Transfer by Natural Convection in a Enclosed Flat Cylinder*, J. of Chemical Engineering of Japan, V 23, No.3, Jun., pp.378-381. (1991)

Hilsenrath, J., et al., *Table of Thermal Properties of Gases*, U.S.N.B.S. Circular 564, Pergamon Press, Oxford.(1960).

Holman, J.P., *Heat Transfer*, SI Metric Edition, McGraw-Hill Book Company. (1989)

Incropera, F.P. & DeWitt, D.P., *Fundamentals of Heat and Mass Transfer*, 2nd, John Wiley & Sons, London.(1985)

Jourda, P. & Probert, S.D., *Heat Transfer Consideration for Large Liquefied-Natural-Gas Storage Tanks*, Applied Energy, pp.263-282. (1991)

Kalhori, B. & Ramadhyani, R., *Studies on Heat Transfer from a Vertical Cylinder, with or without Fins, Embedded in a Solid Phase Change Medium*, Transactions of ASME, Vol.107, Feb., 1985, pp.44-51.(1985)

Kalinin, E.K. & Dreitser, G.A., *Unsteady Convective Heat Transfer for Turbulent Flows of Gases and Liquids in Tubes*, Int.J. Heat Mass Transfer, Vol.28, No.2, pp.361-369.(1985)

Kelley, A. & Pohl, I., *A Book on C*, The Benjamin/Cummings Publishing Company, Inc.(1984)

Kimura, K. & Bejan, A., *Experimental Study of Natural Convection in a Horizontal Cylinder with Different End Temperatures*, Int.J. Heat Mass Transfer 23, pp.1117-1126.(1980)

Krepec, T., Miele, D. & Lisio, C., *Improved Concept of Hydrogen On-Board Storage and Supply for Automotive Applications*, Int.J. Hydrogen Energy, Vol.15, No 1, pp.27-32.(1990)

Landram, C.S., *Heat Transfer During Vessel Discharge: Mean and Fluctuating Gas Temperature*, Transactions of ASME, J. Heat Transfer, Feb.,1973, pp.101-106.(1973)

Leaver, R.H. & Thomas, T.R., *Analysis and Presentation of Experimental Results*, The Macmillan Press Ltd.(1974)

Lee, I., *What Is It Like To Derive a Natural Gas Powered Car*, Energy, Vol.2/No.7.1992, pp.20-23. (1992)

Lin, Y.S. & Akins, R.G., *Thermal Description of Pseudosteady-State Natural Convection Inside a Vertical Cylinder*, Int.J. Heat Mass Transfer, Vol.29, No.2, pp.301-307.(1986)

Loomis, A.W., *Compressed Air and Data*, 3rd, Ingersoll-Rand Company.(1982)

Maillet, D., Degiovanni, A. & Pasquetti, R., *Inverse Heat Conduction Applied to the Measurement of Heat Transfer Coefficient on a Cylinder*, J. Heat Transfer, Transactions ASME V.113, No.3, Aug., pp.549-557. (1991)

Maxson, J.A., Ezekoye, O.A., Hensinger, D.M., Greif, R. & Oppenheim, A.K., *Heat Transfer from Combustion in an Enclosure*, Lawrence Berkeley Laboratory, University of California, Berkeley. (1990)

McAdam, W.H., *Heat transmission*, 3rd, McGraw-Hill Book Company.(1954)

Means, J.D. & Ulrich, R.D., *Transient Convective Heat Transfer During and After Gas Injection into Containers*, Transactions of ASME, May, 1975, pp.282-287. (1975)

Metais, B. & Eckert, E.R.G., *Forced, Mixed, and Free Convection Regimes*, J. Heat Transfer, ser. C, Vol.86, p.295.(1964)

Muller, W, Leland, T., R.Kobayashi, R., *Volumetric Properties of Gas Mixtures at Low Temperature and High Pressures by the Burnett Method: The Hydrogen-Methane System*, AICHE J. Vol.7, No.2. (1961).

Ostrach, S., *Natural Convection in Enclosures*, Adv. Heat Transfer 8, pp.161-227. (1972)

Paolucci, S., *Heat Transfer During the Early Expansion of Gas in Pressurised Vessels*, Int. J. Heat Mass Transfer, Vol. 28, No.8, pp.1525-1537. (1985)

Parsons, J.R. & Mulligan, J.C., *Onset of Natural Convective from a Suddenly Heated Horizontal Cylinder*, Transactions of ASME, Vol.102, November, pp.636-639. (1980)

Paul, S., *Tanks for Everything*, Process Engineer, Vol.71, No.6, Jun.(1990)

Pehchka, W., *New Status of Handling and Storage Techniques for Liquid Hydrogen in Motor Vehicles*, Int.J. Hydrogen Energy 12, 1987, pp.753-764. (1987)

Peng,D.Y., & Robinson, D.B., *A New Two-Constant Equation of State, Ind. Eng. Chem. Fundamentals*, Vol. 15, No.1. (1976).

Perry, R.H. & Green, D., *Perry's Chemical Engineer's Handbook*, 6th edn. McGraw-Hill, New York. (1984).

Probert, S.D. & Giani, S., *Thermal Insulants*, Applied Energy, 2, pp.83-115. (1976)

Reid, R.C., Prensnitz J.M, & Sherwood, T.K., *Properties of Gases and Liquids*, McGraw-Hill Inc. (1977)

Reynolds, W.C., & Kays, W.M., *Blowdown and Charging Process in a Single Gas Receiver with Heat Transfer*, Transactions of ASME, July, 1958, pp.1160-1168. (1958)

Ring, E., *Rocket Propellant and Pressurising System*, Prentice-Hall, Inc., Englewood Cliffs, N.J. (1964)

Schiroky, G.H. & Roseberger, F., *Free Convection of Gases in a Horizontal Cylinder with Differentially Heated End Walls*, Int.J Heat Mass Transfer, Vol.27, No.4, pp.587-598.(1984).

Schiroky, G.H & Roseberger, F., *High Rayleigh Number Heat Transfer In a Horizontal Cylinder with Adiabatic Wall*, Int.J. Heat Mass Transfer, Vol.27, pp.630-633. (1984)

Shashkov, A.G., Volokhov, G.M. & Lipovtsey, V.N., *Exchange of Heat in an Orthotropic Bounded Cylinder under Combined Boundary Conditions of the First, Second, and Third Kinds*, J. of Engineering Physics, V.57, No.6, Jun., pp.1475-1483. (1983)

Storesletten, L. & Tveitereid, M., *Natural Convection in a Horizontal Porous Cylinder*, Int. J. Heat and Mass Transfer, V 34, No. 8, Aug., pp.1959-1968.(1991)

Strance,C.L., *Guaging, Testing, and Running of Lease Tanks*, 1991, Proc. of 66th International School of Hydrocarbon Measurement, Conference No. 15053, pp.426-431. (1991)

Ulrich, R.D., Wirtz, D.P., & Numn, R.H., *Transient Heat Transfer in Closed Containers After Gas Injection*, J. Heat transfer, Transactions of ASME, ser. C, Vol.91. Aug.(1969)

Van Wylen, G.J. & Sonntag, R.E., *Fundamentals of Classical Thermodynamics*, John Wiley and Son, Inc. (1973)

Walker, I.J & Lyall, K.D., *Natural Gas Vehicles (NGV)-Research and Development*, EPD Discussion Paper No.4, Energy Programs Division, Department of Primary Industries and Energy, Canberra. (1991)

Watson, H.C. & Milkins, E.E., *Future Fuels and Engines*, 2nd Automotive Eng. Conference, S.A.E.-A and S.A.E - J., Paper 26.

Wyman, R.P., *CNG Measurement Using PVT Relationships*, SAE Technical Paper Series No.831067, pp.13-26. (1983)

Yu, W.C., Lee, H.M. & Logon, R.M., *Prediction of High Pressure Properties*, Hydrocarbon Processing,

Jan.(1982)

Zwemmer, A., *Compact High Pressure Natural Gas Compressors for CNG Refuelling System*, Sulzer Technical Review, V.69, No.2, pp.3-7. (1987)

APPENDIX A

EXPERIMENTAL RESULTS OF THREE TESTS

TABLE A.1 EXPERIMENTAL RESULT OF TEST 1

Parameters Measured: T, P, $\dot{m}$, Tw, and T1;
Ambient= 17.5 C, Po=0.101 MPa, Storage Pressure= 17 MPa, Horizintal Cylinder, Horizontal Thermocouples Array Plane
TC- Thermocouple, relative to the numbers in Fig.(4.3).

TIME	TEMPERATURE (C)													P	$\dot{m}$	MASS
(s)	TC.1	TC.2	TC.3	TC.4	TC.5	TC.6	TC.7	TC.8	TC.9	TC.10	TC.11	TC.12	TC.13	MPa	kg/min	kg
1	19.64	20.21	19.84	20.15	19.57	20.15	20.77	19.08	18.53	19.39	16.24	15.99	15.63	15.49	1.34	0.02
2	23.38	24.16	23.58	24.31	22.90	24.31	24.51	22.62	22.49	23.55	16.24	16.20	15.24	15.05	2.42	0.06
3	26.71	27.08	26.91	27.22	25.81	27.22	27.42	25.94	24.98	26.88	16.24	16.20	14.48	12.43	4.12	0.13
4	28.37	28.95	28.57	29.30	27.89	29.30	28.67	28.02	27.48	30.00	16.24	16.20	13.32	11.31	5.84	0.23
5	29.41	29.57	29.61	30.14	29.14	30.14	29.71	29.27	28.52	30.41	16.24	16.41	12.56	10.52	6.64	0.34
6	30.45	30.61	30.65	30.97	29.97	30.97	30.75	30.10	29.14	31.04	16.66	16.41	11.79	9.44	7.16	0.46
7	31.08	31.44	31.28	31.80	30.81	31.80	31.38	30.94	29.97	31.87	16.66	16.20	10.64	7.50	8.03	0.59
8	31.70	32.07	31.90	32.22	31.64	32.22	32.00	31.35	30.81	32.08	16.66	16.41	9.87	7.62	8.18	0.73
9	32.53	32.48	32.73	32.63	31.64	32.63	32.42	31.98	31.22	32.49	16.87	16.41	9.87	7.40	8.52	0.87
10	32.78	32.90	32.98	32.96	32.18	32.96	32.79	32.39	31.64	32.87	16.95	16.45	9.98	7.38	8.68	1.02
11	33.20	33.27	33.40	33.38	32.51	33.38	33.12	32.85	32.01	33.24	17.03	16.45	10.06	7.21	8.60	1.16
12	33.53	33.69	33.73	33.71	32.84	33.71	33.41	33.22	32.43	33.62	17.16	16.49	10.10	7.09	8.68	1.30
13	33.90	34.02	34.10	34.00	33.01	34.00	33.75	33.56	32.80	33.99	17.28	16.57	10.10	7.11	8.72	1.45
14	34.24	34.36	34.44	34.34	33.26	34.20	34.04	33.85	33.22	34.32	17.41	16.66	10.06	7.32	8.77	1.60
15	34.61	34.61	34.81	34.67	33.55	34.39	34.37	34.18	33.55	34.66	17.53	16.70	9.94	7.32	8.76	1.74
16	35.03	34.94	35.23	34.88	33.80	34.46	34.70	34.47	33.93	34.99	17.78	16.82	9.79	7.34	8.76	1.89
17	35.40	35.19	35.60	35.13	34.13	34.57	35.00	34.76	34.26	35.32	17.95	16.95	9.68	7.37	8.74	2.03
18	35.74	35.52	35.94	35.42	34.47	34.72	35.24	35.10	34.63	35.57	18.12	17.03	9.60	7.41	8.70	2.18
19	36.11	35.77	36.31	35.63	34.88	34.93	35.58	35.39	34.88	35.86	18.32	17.16	9.45	7.47	8.62	2.32
20	36.44	36.19	36.64	35.96	35.22	35.26	35.74	35.72	35.22	36.19	18.49	17.28	9.33	7.55	8.62	2.46
21	36.69	36.48	36.89	36.25	35.47	35.55	35.99	35.97	35.51	36.49	18.57	17.41	9.25	7.63	8.57	2.61
22	36.98	36.77	37.18	36.58	35.71	35.88	36.33	36.30	35.84	36.78	18.74	17.49	9.14	7.72	8.56	2.75
23	37.27	37.02	37.47	36.83	36.05	36.13	36.58	36.55	36.09	37.11	18.95	17.61	8.98	7.82	8.46	2.89
24	37.44	37.35	37.64	37.12	36.21	36.42	36.78	36.84	36.38	37.44	19.07	17.74	8.91	7.91	8.42	3.03
25	37.61	37.60	37.81	37.29	36.38	36.59	37.03	37.09	36.71	37.69	19.24	17.91	8.83	8.02	8.34	3.17
26	37.86	37.85	38.06	37.54	36.71	36.84	37.28	37.43	37.05	37.98	19.49	18.07	8.75	8.14	8.29	3.31
27	38.02	38.14	38.22	37.79	36.96	37.09	37.49	37.63	37.30	38.23	19.66	18.24	8.72	8.27	8.21	3.45
28	38.23	38.43	38.43	38.08	37.21	37.38	37.82	37.88	37.63	38.48	19.78	18.40	8.64	8.39	8.18	3.58
29	38.52	38.68	38.72	38.33	37.55	37.63	38.12	38.09	37.92	38.73	19.99	18.57	8.60	8.53	8.11	3.72
30	38.86	38.93	39.06	38.66	37.88	37.96	38.36	38.34	38.17	39.06	20.15	18.70	8.56	8.66	8.04	3.85
31	39.10	39.26	39.30	38.96	38.13	38.26	38.61	38.55	38.46	39.36	20.24	18.82	8.52	8.81	7.95	3.98
32	39.44	39.60	39.64	39.16	38.46	38.46	38.91	38.80	38.71	39.65	20.40	18.99	8.52	8.95	7.89	4.12
33	39.73	39.89	39.93	39.37	38.79	38.67	39.11	39.05	38.92	39.98	20.65	19.11	8.60	9.08	7.84	4.25
34	39.98	40.14	40.18	39.70	39.04	39.00	39.45	39.34	39.25	40.27	20.82	19.24	8.64	9.22	7.76	4.38
35	40.23	40.39	40.43	40.04	39.29	39.34	39.78	39.59	39.50	40.60	21.07	19.36	8.72	9.35	7.68	4.50
36	40.48	40.64	40.68	40.33	39.54	39.63	40.07	39.96	39.75	40.90	21.32	19.53	8.79	9.46	7.64	4.63
37	40.73	40.80	40.93	40.62	39.87	39.92	40.32	40.21	40.08	41.19	21.49	19.65	8.83	9.59	7.54	4.76
38	40.94	41.05	41.14	40.91	40.12	40.21	40.61	40.42	40.37	41.48	21.65	19.82	8.87	9.73	7.48	4.88
39	41.18	41.30	41.38	41.16	40.37	40.46	40.78	40.71	40.62	41.85	21.82	19.99	8.95	9.86	7.43	5.00
40	41.43	41.47	41.63	41.33	40.71	40.63	40.99	40.92	40.96	42.06	22.03	20.19	8.98	10.01	7.34	5.13
41	41.68	41.68	41.88	41.53	41.04	40.83	41.15	41.09	41.21	42.31	22.28	20.36	9.02	10.16	7.25	5.25
42	41.85	41.93	42.05	41.78	41.12	41.08	41.40	41.34	41.37	42.60	22.53	20.53	9.14	10.31	7.13	5.37
43	42.02	42.18	42.22	42.08	41.29	41.38	41.57	41.59	41.58	42.85	22.73	20.69	9.22	10.45	7.05	5.48
44	42.22	42.34	42.42	42.20	41.50	41.50	41.82	41.75	41.83	43.02	22.98	20.82	9.29	10.60	6.94	5.60
45	42.39	42.59	42.59	42.37	41.75	41.67	42.03	42.04	42.00	43.27	23.19	20.94	9.37	10.74	6.79	5.71
46	42.64	42.80	42.84	42.53	41.91	41.83	42.32	42.29	42.25	43.52	23.36	21.07	9.45	10.87	6.70	5.82
47	42.89	43.05	43.09	42.78	42.16	42.08	42.48	42.54	42.50	43.72	23.52	21.28	9.45	11.00	6.55	5.93
48	43.14	43.22	43.34	42.95	42.41	42.25	42.69	42.79	42.75	43.93	23.73	21.44	9.56	11.14	6.43	6.04
49	43.35	43.47	43.55	43.16	42.62	42.46	42.94	43.04	42.91	44.10	23.94	21.65	9.64	11.30	6.31	6.15
50	43.51	43.67	43.71	43.41	42.75	42.71	43.19	43.25	43.08	44.31	24.15	21.86	9.75	11.45	6.21	6.25
51	43.60	43.92	43.80	43.70	42.91	43.00	43.44	43.37	43.24	44.56	24.36	22.11	9.91	11.59	6.11	6.35
52	43.76	44.09	43.96	43.86	43.12	43.16	43.69	43.54	43.49	44.76	24.61	22.27	10.06	11.74	5.99	6.45
53	43.93	44.26	44.13	44.03	43.37	43.33	43.90	43.67	43.70	44.97	24.86	22.44	10.21	11.88	5.87	6.55
54	44.06	44.51	44.26	44.28	43.62	43.58	44.06	43.87	43.87	45.18	25.06	22.61	10.37	12.00	5.75	6.64
55	44.30	44.71	44.50	44.40	43.83	43.70	44.23	44.08	44.12	45.30	25.19	22.73	10.48	12.14	5.59	6.74
56	44.55	44.80	44.75	44.57	44.08	43.87	44.36	44.33	44.28	45.39	25.44	22.81	10.56	12.26	5.47	6.83
57	44.72	44.92	44.92	44.74	44.24	44.04	44.48	44.58	44.45	45.51	25.65	22.98	10.64	12.39	5.30	6.92
58	44.89	45.09	45.09	44.90	44.41	44.20	44.60	44.83	44.62	45.60	25.81	23.15	10.67	12.53	5.15	7.00
59	45.10	45.17	45.30	44.99	44.58	44.29	44.77	44.96	44.78	45.80	26.06	23.31	10.75	12.67	5.01	7.09
60	45.18	45.26	45.38	45.15	44.74	44.45	44.94	45.04	44.87	46.01	26.31	23.52	10.83	12.81	4.85	7.17
61	45.34	45.38	45.54	45.24	44.83	44.54	45.06	45.16	45.12	46.18	26.52	23.69	10.98	12.93	4.68	7.25
62	45.43	45.42	45.63	45.40	45.03	44.70	45.19	45.25	45.28	46.34	26.73	23.81	11.14	13.05	4.53	7.32
63	45.59	45.46	45.79	45.57	45.12	44.87	45.35	45.33	45.45	46.51	26.89	23.98	11.25	13.15	4.38	7.39
64	45.68	45.63	45.88	45.74	45.20	45.04	45.44	45.50	45.62	46.55	27.06	24.10	11.33	13.24	4.26	7.47
65	45.80	45.80	46.00	45.86	45.37	45.16	45.52	45.66	45.78	46.68	27.27	24.27	11.40	13.33	4.14	7.53
66	45.93	45.92	46.13	46.03	45.57	45.33	45.60	45.75	45.78	46.84	27.43	24.44	11.40	13.42	3.99	7.60
67	46.18	46.09	46.38	46.07	45.70	45.37	45.77	45.91	45.87	46.89	27.60	24.64	11.44	13.50	3.82	7.66
68	46.26	46.25	46.46	46.11	45.78	45.41	45.94	46.08	45.95	47.01	27.77	24.81	11.52	13.58	3.69	7.73
69	46.38	46.25	46.58	46.19	45.87	45.49	46.10	46.16	46.07	47.18	27.93	24.98	11.60	13.66	3.51	7.78
70	46.43	46.25	46.63	46.32	45.95	45.62	46.19	46.24	46.16	47.26	28.06	25.06	11.75	13.75	3.40	7.84
71	46.43	46.34	46.63	46.36	45.91	45.66	46.27	46.37	46.32	47.34	28.18	25.23	11.90	13.84	3.27	7.90
72	46.34	46.50	46.54	46.57	45.91	45.87	46.19	46.45	46.41	47.47	28.35	25.31	12.02	13.94	3.11	7.95
73	46.34	46.63	46.54	46.86	45.99	46.16	46.14	46.54	46.49	47.47	28.52	25.39	12.10	14.02	2.91	8.00
74	46.38	46.84	46.58	47.11	46.16	46.41	46.06	46.62	46.53	47.43	28.60	25.56	12.17	14.10	2.70	8.04
75	46.47	47.04	46.67	47.23	46.24	46.53	46.14	46.70	46.61	47.43	28.77	25.73	12.17	14.19	2.54	8.08

TABLE A.1 EXPERIMENTAL RESULT OF TEST 1

TIME	TEMPERATURE (C)													P	$\dot{m}$	MASS
(s)	TC.1	TC.2	TC.3	TC.4	TC.5	TC.6	TC.7	TC.8	TC.9	TC.10	TC.11	TC.12	TC.13	MPa	kg/min	kg
76	46.59	47.21	46.79	47.32	46.41	46.62	46.19	46.74	46.61	47.43	28.97	25.81	12.21	14.27	2.40	8.12
77	46.76	47.25	46.96	47.23	46.53	46.53	46.31	46.74	46.61	47.47	29.14	25.98	12.29	14.35	2.23	8.16
78	46.84	47.25	47.04	47.11	46.61	46.41	46.39	46.74	46.66	47.55	29.31	26.10	12.36	14.43	2.07	8.19
79	46.84	47.21	47.04	46.98	46.57	46.28	46.56	46.74	46.70	47.59	29.47	26.18	12.44	14.50	1.88	8.23
80	46.93	47.17	47.13	46.90	46.57	46.20	46.64	46.74	46.74	47.59	29.56	26.35	12.52	14.57	1.69	8.25
81	46.93	47.09	47.13	46.86	46.57	46.16	46.77	46.74	46.74	47.68	29.64	26.52	12.56	14.62	1.52	8.28
82	46.93	47.04	47.13	46.86	46.61	46.16	46.85	46.79	46.74	47.76	29.72	26.60	12.56	14.64	1.36	8.30
83	46.93	46.96	47.13	46.79	46.61	46.24	46.85	46.87	46.61	47.84	29.85	26.81	12.63	14.65	1.26	8.32
84	46.93	46.79	47.13	46.71	46.66	46.28	46.85	46.95	46.49	47.97	30.01	26.97	12.71	14.65	1.12	8.34
85	46.76	46.63	47.04	46.67	46.66	46.37	46.85	47.04	46.36	48.05	30.18	27.06	12.79	14.66	1.00	8.36
86	46.59	46.46	46.96	46.62	46.66	46.37	46.85	47.12	46.28	47.97	30.26	27.14	12.86	14.68	0.87	8.37
87	46.41	46.30	46.83	46.56	46.61	46.37	46.89	47.16	46.16	47.93	30.35	27.31	12.94	14.70	0.79	8.39
88	46.31	46.25	46.79	46.53	46.61	46.24	46.98	47.16	46.07	47.93	30.39	27.39	12.94	14.73	0.66	8.40
89	46.16	46.25	46.71	46.50	46.53	46.16	46.98	47.12	45.99	47.84	30.39	27.47	12.94	14.76	0.53	8.41
90	46.09	46.25	46.63	46.46	46.45	45.99	46.98	47.04	45.91	47.84	30.47	27.56	12.94	14.78	0.42	8.41
91	45.99	46.25	46.50	46.41	46.36	45.83	46.89	46.95	45.82	47.88	30.60	27.68	12.94	14.79	0.35	8.42
92	45.90	46.24	46.42	46.34	46.28	45.64	46.81	46.83	45.78	47.93	30.72	27.76	12.94	14.81	0.34	8.42
93	45.78	46.19	46.29	46.24	46.20	45.44	46.73	46.70	45.78	47.84	30.89	27.85	12.94	14.84	0.34	8.43
94	45.71	46.17	46.25	46.15	46.20	45.19	46.64	46.58	45.78	47.84	31.05	28.01	12.94	14.88	0.33	8.43
95	45.58	46.14	46.17	46.07	46.20	45.02	46.52	46.49	45.78	47.88	31.14	28.18	12.94	14.92	0.32	8.43
96	45.47	46.11	46.13	45.99	46.16	44.94	46.48	46.53	45.78	47.84	31.18	28.31	12.94	14.98	0.31	8.44
97	45.43	46.09	46.09	45.95	46.11	44.87	46.39	46.60	45.78	47.72	31.30	28.39	12.94	15.02	0.30	8.44
98	45.28	46.06	46.09	45.93	46.03	44.81	46.31	46.55	45.78	47.59	31.30	28.47	12.94	15.03	0.30	8.44
99	45.24	46.05	46.00	45.91	45.95	44.81	46.14	46.50	45.78	47.38	31.39	28.47	12.94	15.03	0.29	8.45
100	45.26	46.05	45.96	45.89	45.87	44.80	46.02	46.37	45.78	47.09	31.39	28.51	12.94	15.03	0.28	8.45
101	45.26	46.05	45.92	45.80	45.82	44.79	45.85	46.12	45.78	46.89	31.39	28.60	12.94	15.02	0.27	8.45
102	45.27	46.05	45.84	45.70	45.78	44.78	45.69	45.87	45.78	46.68	31.39	28.68	12.94	15.01	0.26	8.46
103	45.27	46.05	45.75	45.70	45.78	44.85	45.52	45.66	45.70	46.55	31.55	28.76	12.94	15.01	0.26	8.46
104	45.23	45.92	45.71	45.61	45.78	44.84	45.44	45.50	45.62	46.47	31.55	28.93	12.94	15.02	0.25	8.46
105	45.19	45.80	45.67	45.53	45.78	44.83	45.35	45.41	45.49	46.43	31.64	29.05	12.94	15.01	0.24	8.47
106	45.16	45.63	45.63	45.36	45.78	44.66	45.31	45.33	45.32	46.34	31.72	29.10	12.98	15.00	0.23	8.47
107	45.14	45.47	45.59	45.20	45.78	44.50	45.31	45.25	45.16	46.30	31.76	29.18	12.98	14.99	0.22	8.48
108	45.06	45.30	45.50	44.95	45.78	44.25	45.31	45.16	45.07	46.22	31.72	29.26	12.98	14.98	0.22	8.48
109	45.00	45.26	45.42	44.78	45.78	44.08	45.31	45.04	44.99	46.14	31.80	29.26	13.02	14.96	0.21	8.48
110	44.93	45.05	45.34	44.62	45.78	43.92	45.23	44.96	44.95	46.05	31.89	29.26	13.06	14.96	0.20	8.49
111	44.82	44.88	45.25	44.62	45.70	43.92	45.15	44.87	44.95	45.97	31.97	29.30	13.02	14.98	0.19	8.49
112	44.70	44.72	45.21	44.62	45.62	43.92	45.15	44.75	44.87	45.89	32.01	29.35	13.06	14.99	0.18	8.49
113	44.62	44.43	45.21	44.53	45.53	43.83	45.06	44.71	44.78	45.85	32.05	29.39	13.09	15.01	0.18	8.50
114	44.50	44.13	45.13	44.45	45.41	43.75	44.98	44.71	44.70	45.85	32.05	29.43	13.09	15.02	0.17	8.50
115	44.36	44.01	45.00	44.28	45.28	43.58	44.98	44.62	44.62	45.80	32.05	29.51	13.09	15.02	0.16	8.50
116	44.26	43.84	44.88	44.12	45.20	43.42	44.94	44.54	44.53	45.85	32.05	29.60	13.13	15.00	0.15	8.51
117	44.16	43.68	44.71	43.95	45.12	43.25	44.81	44.50	44.53	45.85	32.05	29.64	13.13	14.98	0.14	8.51
118	44.07	43.64	44.55	43.74	45.03	43.04	44.73	44.46	44.49	45.85	32.05	29.76	13.13	14.97	0.14	8.51
119	44.01	43.55	44.46	43.53	44.99	42.83	44.65	44.37	44.41	45.80	32.14	29.80	13.17	14.94	0.13	8.52
120	43.97	43.43	44.42	43.41	44.91	42.71	44.56	44.29	44.37	45.76	32.26	29.89	13.17	14.92	0.12	8.52
121	43.91	43.34	44.38	43.28	44.83	42.58	44.52	44.17	44.28	45.68	32.38	29.97	13.21	14.90	0.11	8.52
122	43.86	43.26	44.38	43.16	44.74	42.46	44.48	44.00	44.20	45.60	32.51	30.05	13.25	14.87	0.10	8.53
123	43.80	43.18	44.38	43.12	44.66	42.42	44.48	43.83	44.16	45.51	32.63	30.05	13.29	14.84	0.10	8.53
124	43.75	43.14	44.38	43.08	44.58	42.38	44.48	43.71	44.16	45.43	32.68	30.14	13.29	14.82	0.09	8.53
125	43.69	43.14	44.30	43.04	44.53	42.34	44.40	43.54	44.12	45.30	32.68	30.14	13.32	14.80	0.08	8.54
126	43.66	43.09	44.21	42.99	44.49	42.29	44.31	43.38	44.12	45.14	32.68	30.14	13.40	14.79	0.07	8.54
127	43.61	43.01	44.13	42.87	44.41	42.17	44.23	43.25	44.12	45.01	32.68	30.14	13.40	14.79	0.06	8.54
128	43.57	42.93	44.05	42.79	44.33	42.09	44.11	43.13	44.03	44.89	32.68	30.14	13.48	14.79	0.06	8.55
129	43.49	42.84	43.96	42.70	44.24	42.00	43.94	42.96	43.91	44.81	32.72	30.14	13.48	14.77	0.05	8.55
130	43.38	42.68	43.88	42.58	44.16	41.88	43.86	42.88	43.79	44.72	32.76	30.14	13.55	14.75	0.04	8.56
131	43.27	42.51	43.80	42.45	44.12	41.75	43.77	42.84	43.66	44.72	32.80	30.18	13.48	14.75	0.03	8.56
132	43.18	42.35	43.71	42.41	44.12	41.71	43.69	42.79	43.54	44.64	32.88	30.18	13.48	14.75	0.02	8.56
133	43.08	42.18	43.63	42.33	44.12	41.63	43.65	42.75	43.49	44.64	32.93	30.26	13.48	14.76	0.02	8.57
134	43.02	41.93	43.55	42.24	44.03	41.54	43.65	42.75	43.45	44.56	32.93	30.30	13.55	14.78	0.02	8.57
135	42.98	41.76	43.55	42.20	43.95	41.50	43.65	42.75	43.41	44.51	32.93	30.39	13.55	14.81	0.02	8.57
136	42.91	41.64	43.55	42.08	43.87	41.38	43.65	42.75	43.37	44.43	32.93	30.43	13.63	14.81	0.02	8.58
137	42.82	41.56	43.46	41.95	43.79	41.25	43.65	42.71	43.33	44.43	32.88	30.51	13.71	14.81	0.02	8.58
138	42.72	41.47	43.38	41.83	43.66	41.13	43.56	42.67	43.29	44.31	32.88	30.51	13.71	14.79	0.02	8.58
139	42.62	41.39	43.26	41.70	43.62	41.00	43.48	42.59	43.29	44.26	32.88	30.55	13.71	14.77	0.01	8.59
140	42.53	41.31	43.13	41.54	43.58	40.84	43.36	42.50	43.29	44.22	32.88	30.55	13.71	14.76	0.01	8.59
141	42.47	41.22	42.97	41.45	43.54	40.75	43.23	42.42	43.29	44.18	32.97	30.55	13.71	14.77	0.01	8.59
142	42.41	41.14	42.88	41.37	43.45	40.67	43.07	42.29	43.29	44.10	33.05	30.55	13.71	14.76	0.01	8.60
143	42.35	41.06	42.84	41.33	43.41	40.63	43.02	42.17	43.29	44.06	33.09	30.64	13.71	14.78	0.01	8.60
144	42.30	41.06	42.80	41.29	43.37	40.59	42.94	42.09	43.29	43.97	33.13	30.68	13.71	14.79	0.01	8.60
145	42.24	41.06	42.76	41.29	43.33	40.59	42.90	42.00	43.29	43.85	33.18	30.68	13.71	14.79	0.01	8.61
146	42.20	41.06	42.76	41.29	43.29	40.59	42.86	41.92	43.24	43.72	33.18	30.76	13.71	14.78	0.01	8.61
147	42.17	41.06	42.76	41.29	43.29	40.59	42.86	41.92	43.16	43.64	33.13	30.84	13.71	14.78	0.01	8.61
148	42.16	41.06	42.72	41.29	43.20	40.59	42.82	41.92	43.08	43.56	33.18	30.84	13.71	14.79	0.01	8.62
149	42.16	41.06	42.67	41.20	43.12	40.50	42.82	41.88	42.99	43.52	33.22	30.88	13.71	14.80	0.01	8.62
150	42.11	40.93	42.59	41.20	43.04	40.50	42.82	41.80	42.91	43.52	33.26	30.97	13.71	14.81	0.01	8.62
151	42.06	40.81	42.51	41.12	42.95	40.42	42.73	41.71	42.87	43.47	33.26	30.97	13.71	14.82	0.01	8.63
152	41.97	40.64	42.42	41.04	42.83	40.34	42.65	41.63	42.87	43.43	33.30	30.97	13.71	14.82	0.01	8.63
153	41.89	40.47	42.34	40.96	42.83	40.26	42.65	41.55	42.87	43.43	33.30	30.97	13.71	14.81	0.01	8.63
154	41.80	40.31	42.30	40.96	42.75	40.26	42.57	41.46	42.87	43.39	33.38	30.97	13.71	14.80	0.01	8.64
155	41.76	40.27	42.30	40.83	42.66	40.13	42.48	41.42	42.79	43.35	33.42	30.97	13.78	14.80	0.01	8.64
156	41.71	40.22	42.26	40.75	42.58	40.05	42.48	41.38	42.70	43.35	33.51	30.97	13.82	14.81	0.01	8.64
157	41.65	40.22	42.18	40.66	42.54	39.96	42.48	41.30	42.62	43.31	33.59	30.97	13.90	14.80	0.01	8.65

TABLE A.1 EXPERIMENTAL RESULT OF TEST 1

TIME	TEMPERATURE (C)													P	$\dot{m}$	MASS
(s)	TC.1	TC.2	TC.3	TC.4	TC.5	TC.6	TC.7	TC.8	TC.9	TC.10	TC.11	TC.12	TC.13	MPa	kg/min	kg
158	41.59	40.22	42.09	40.58	42.45	39.88	42.40	41.21	42.54	43.27	33.63	30.97	13.94	14.81	0.01	8.65
159	41.53	40.22	42.01	40.50	42.45	39.80	42.40	41.17	42.45	43.22	33.63	31.01	13.98	14.82	0.01	8.65
160	41.47	40.14	41.93	40.46	42.45	39.76	42.36	41.13	42.45	43.18	33.63	31.01	13.98	14.82	0.01	8.66
161	41.43	40.06	41.88	40.37	42.45	39.67	42.28	41.09	42.45	43.14	33.63	31.05	14.02	14.82	0.01	8.66
162	41.40	39.97	41.88	40.29	42.45	39.59	42.19	41.09	42.33	43.14	33.55	31.09	14.02	14.82	0.01	8.66
163	41.38	39.89	41.88	40.21	42.45	39.51	42.11	41.00	42.20	43.10	33.59	31.13	14.05	14.83	0.01	8.67
164	41.36	39.81	41.88	40.12	42.45	39.42	42.03	40.92	42.08	43.02	33.55	31.13	14.09	14.84	0.01	8.67
165	41.34	39.81	41.88	40.04	42.45	39.34	41.98	40.84	41.95	42.85	33.59	31.18	14.09	14.86	0.01	8.67
166	41.32	39.81	41.88	40.04	42.45	39.34	41.98	40.76	41.79	42.73	33.59	31.18	14.09	14.89	0.01	8.68
167	41.31	39.77	41.88	40.04	42.45	39.34	41.98	40.67	41.79	42.60	33.67	31.18	14.09	14.91	0.01	8.68
168	41.22	39.72	41.88	40.00	42.33	39.30	41.98	40.63	41.79	42.48	33.67	31.18	14.09	14.92	0.01	8.68
169	41.13	39.68	41.76	39.96	42.20	39.26	41.98	40.63	41.79	42.43	33.72	31.18	14.09	14.92	0.01	8.69
170	41.04	39.60	41.68	39.96	42.08	39.26	41.98	40.59	41.75	42.43	33.72	31.22	14.09	14.90	0.01	8.69
171	40.95	39.52	41.55	39.92	41.95	39.22	41.98	40.55	41.75	42.43	33.72	31.26	14.09	14.88	0.01	8.69
172	40.83	39.48	41.43	39.83	41.83	39.13	41.98	40.46	41.71	42.43	33.72	31.30	14.09	14.87	0.01	8.70
173	40.76	39.43	41.30	39.79	41.79	39.09	41.90	40.42	41.66	42.43	33.72	31.34	14.17	14.86	0.01	8.70
174	40.68	39.39	41.26	39.75	41.75	39.05	41.82	40.34	41.62	42.43	33.72	31.38	14.17	14.85	0.01	8.70
175	40.60	39.39	41.18	39.67	41.71	38.97	41.73	40.30	41.58	42.48	33.72	31.38	14.25	14.85	0.01	8.71
176	40.54	39.39	41.14	39.62	41.66	38.92	41.61	40.26	41.58	42.43	33.72	31.38	14.32	14.86	0.01	8.71
177	40.50	39.39	41.09	39.62	41.62	38.92	41.48	40.26	41.58	42.35	33.72	31.38	14.40	14.84	0.01	8.71
178	40.49	39.31	41.05	39.62	41.62	38.92	41.44	40.26	41.58	42.27	33.72	31.47	14.36	14.81	0.01	8.72
179	40.49	39.23	41.05	39.62	41.62	38.92	41.40	40.26	41.50	42.18	33.80	31.47	14.44	14.80	0.01	8.72
180	40.48	39.14	41.05	39.62	41.62	38.92	41.36	40.26	41.46	42.10	33.88	31.47	14.44	14.79	0.01	8.72
181	40.45	39.02	41.05	39.62	41.62	38.92	41.36	40.17	41.37	42.06	33.97	31.55	14.44	14.78	0.01	8.73
182	40.44	38.89	41.05	39.54	41.58	38.84	41.36	40.09	41.29	42.06	34.05	31.55	14.44	14.79	0.01	8.73
183	40.44	38.81	41.05	39.54	41.58	38.84	41.32	40.01	41.21	42.02	34.13	31.55	14.48	14.81	0.01	8.73
184	40.43	38.77	41.05	39.46	41.58	38.76	41.28	39.92	41.21	41.98	34.13	31.55	14.48	14.83	0.01	8.74
185	40.42	38.73	41.05	39.37	41.50	38.67	41.24	39.84	41.21	41.89	34.05	31.63	14.48	14.83	0.01	8.74
186	40.41	38.73	41.01	39.29	41.41	38.59	41.19	39.80	41.16	41.81	33.97	31.63	14.48	14.83	0.01	8.74
187	40.40	38.73	40.97	39.29	41.37	38.59	41.15	39.72	41.12	41.73	33.92	31.72	14.48	14.84	0.01	8.75
188	40.37	38.73	40.93	39.21	41.29	38.51	41.15	39.63	41.08	41.69	33.84	31.72	14.48	14.83	0.01	8.75
189	40.32	38.68	40.84	39.21	41.16	38.51	41.15	39.55	41.04	41.64	33.84	31.72	14.48	14.82	0.01	8.75
190	40.27	38.64	40.76	39.17	41.16	38.47	41.15	39.47	40.96	41.60	33.92	31.68	14.48	14.83	0.01	8.76
191	40.21	38.60	40.72	39.08	41.16	38.38	41.15	39.42	40.96	41.60	33.97	31.68	14.48	14.84	0.01	8.76
192	40.16	38.56	40.68	39.04	41.12	38.34	41.07	39.42	40.91	41.60	34.01	31.68	14.48	14.83	0.01	8.76
193	40.13	38.56	40.64	38.96	41.08	38.26	40.99	39.42	40.87	41.60	34.09	31.68	14.48	14.83	0.01	8.77
194	40.07	38.56	40.64	38.88	41.04	38.18	40.90	39.42	40.83	41.60	34.13	31.76	14.48	14.83	0.01	8.77
195	40.01	38.56	40.59	38.83	40.96	38.13	40.82	39.42	40.83	41.64	34.13	31.80	14.48	14.82	0.01	8.77
196	39.94	38.56	40.51	38.83	40.87	38.13	40.74	39.42	40.79	41.64	34.17	31.80	14.48	14.83	0.01	8.78
197	39.84	38.56	40.43	38.79	40.83	38.09	40.74	39.42	40.79	41.64	34.22	31.80	14.48	14.84	0.01	8.78
198	39.75	38.56	40.39	38.79	40.79	38.09	40.74	39.42	40.79	41.60	34.26	31.80	14.48	14.87	0.01	8.78
199	39.69	38.56	40.30	38.79	40.79	38.09	40.74	39.42	40.79	41.56	34.30	31.80	14.48	14.89	0.01	8.79
200	39.65	38.48	40.26	38.79	40.79	38.09	40.69	39.34	40.79	41.52	34.30	31.80	14.48	14.90	0.01	8.79
201	39.62	38.39	40.26	38.79	40.79	38.09	40.65	39.26	40.79	41.48	34.34	31.80	14.48	14.90	0.01	8.79
202	39.62	38.31	40.26	38.79	40.79	37.99	40.57	39.17	40.79	41.35	34.34	31.80	14.48	14.90	0.01	8.80
203	39.60	38.23	40.22	38.79	40.79	37.88	40.49	39.09	40.79	41.27	34.38	31.80	14.48	14.90	0.01	8.80
204	39.57	38.14	40.22	38.79	40.79	37.88	40.40	39.01	40.71	41.19	34.34	31.80	14.48	14.91	0.01	8.80
205	39.54	38.10	40.22	38.79	40.79	37.88	40.36	39.01	40.58	41.10	34.38	31.80	14.48	14.92	0.01	8.81
206	39.50	38.02	40.22	38.71	40.79	37.80	40.32	39.01	40.46	40.98	34.38	31.80	14.51	14.95	0.01	8.81
207	39.42	37.94	40.22	38.63	40.79	37.82	40.32	39.01	40.33	40.98	34.42	31.80	14.55	14.97	0.01	8.81
208	39.38	37.85	40.18	38.54	40.79	37.81	40.32	38.92	40.21	40.98	34.38	31.80	14.55	14.99	0.01	8.82
209	39.35	37.77	40.10	38.46	40.71	37.70	40.32	38.84	40.17	40.98	34.38	31.80	14.55	15.00	0.01	8.82
210	39.33	37.73	40.01	38.33	40.62	37.57	40.32	38.76	40.12	40.94	34.38	31.80	14.55	15.00	0.01	8.82
211	39.31	37.73	39.93	38.29	40.54	37.53	40.32	38.68	40.12	40.98	34.38	31.80	14.51	15.00	0.01	8.83

TABLE A.2. EXPERIMENTAL RESULT OF TEST 6

Parameters Measured: T, P, $\dot{m}$, Tw, and T1;
Ambient=19.4 C, Po=0.101 MPa, Storage Pressure=19.4 MPa, Horizontal Cylinder, Vertical Thermocouples Array Plane
TC- Thermocouple, relative to the numbers in Fig.(4.4).

TIME	TEMPERATURE (C)													P	$\dot{m}$	MASS
(s)	TC.1	TC.2	TC.3	TC.4	TC.5	TC.6	TC.7	TC.8	TC.9	TC.10	TC.11	TC.12	TC.13	MPa	kg/min	kg
1	20.71	21.23	20.81	21.08	20.55	19.88	21.28	20.60	21.12	20.97	19.37	19.46	19.80	0.27	1.71	0.03
2	22.19	22.71	22.28	22.73	21.71	20.82	22.84	21.95	22.42	22.13	19.42	19.51	19.80	8.01	2.77	0.04
3	23.58	24.01	23.67	24.21	22.83	21.89	24.23	23.29	23.50	23.16	19.42	19.51	19.62	8.09	3.74	0.01
4	25.23	25.76	25.33	26.05	24.27	22.88	26.11	24.72	24.84	24.50	19.42	19.51	19.58	8.23	4.77	0.04
5	28.55	29.25	28.65	29.36	27.31	25.48	29.43	27.59	27.80	27.60	19.37	19.55	19.80	8.35	5.75	0.17
6	30.70	31.22	30.80	31.47	29.55	28.03	31.36	29.83	29.68	29.75	19.37	19.55	19.53	8.46	6.72	0.35
7	32.85	33.42	32.95	33.48	31.79	30.40	33.37	31.98	31.79	32.08	19.42	19.55	19.17	8.55	7.74	0.54
8	35.09	35.79	35.19	35.68	34.12	32.69	35.52	34.09	34.21	34.45	19.60	19.55	18.68	8.61	8.78	0.72
9	37.06	37.72	37.16	37.52	36.18	35.11	37.22	36.15	36.36	36.47	19.78	19.55	17.83	8.57	9.43	0.91
10	37.51	37.99	37.61	37.92	36.68	36.00	37.54	36.87	36.98	36.82	19.96	19.60	16.62	8.48	9.56	1.09
11	37.82	38.17	37.92	38.10	36.90	36.32	37.72	37.13	37.25	36.82	20.18	19.64	15.41	8.45	9.51	1.28
12	38.05	38.44	38.14	38.32	37.17	36.50	37.99	37.31	37.61	37.00	20.36	19.69	14.51	8.35	9.55	1.46
13	38.41	38.80	38.50	38.64	37.44	36.77	38.34	37.67	37.97	37.36	20.54	19.73	13.80	8.24	9.49	1.64
14	38.85	39.15	38.95	39.00	37.80	37.12	38.70	38.03	38.42	37.72	20.72	19.78	13.13	8.27	9.56	1.82
15	39.30	39.51	39.40	39.44	38.11	37.39	39.11	38.39	38.86	38.08	20.90	19.82	12.50	8.35	9.63	1.99
16	39.70	39.87	39.80	39.80	38.47	37.84	39.42	38.79	39.40	38.53	21.16	19.87	12.05	8.39	9.64	2.16
17	40.20	40.23	40.29	40.16	38.83	38.24	39.78	39.20	39.85	38.89	21.43	19.96	11.51	8.45	9.71	2.32
18	40.60	40.59	40.70	40.52	39.18	38.56	40.14	39.51	40.34	39.24	21.61	20.04	11.02	8.62	9.72	2.48
19	41.05	41.04	41.15	40.88	39.54	38.83	40.58	39.87	40.84	39.69	21.88	20.18	10.71	8.72	9.79	2.64
20	41.50	41.48	41.59	41.24	39.90	39.23	40.90	40.23	41.28	40.10	22.15	20.31	10.39	8.80	9.89	2.79
21	42.03	41.84	42.13	41.59	40.26	39.59	41.26	40.58	41.64	40.54	22.37	20.45	10.12	8.89	9.97	2.95
22	42.44	42.16	42.53	41.95	40.62	39.95	41.61	40.94	42.00	40.95	22.60	20.54	9.90	9.01	10.08	3.09
23	42.93	42.51	43.03	42.31	41.02	40.30	41.97	41.26	42.36	41.30	22.87	20.72	9.77	9.08	10.09	3.25
24	43.38	42.78	43.48	42.71	41.38	40.66	42.33	41.61	42.72	41.66	23.14	20.85	9.59	9.20	10.09	3.40
25	43.83	43.05	43.92	43.07	41.83	41.11	42.69	41.97	43.08	42.07	23.40	20.94	9.50	9.34	10.17	3.55
26	44.18	43.41	44.28	43.43	42.28	41.38	43.18	42.29	43.43	42.42	23.67	21.08	9.41	9.42	10.12	3.71
27	44.59	43.90	44.68	43.79	42.72	41.74	43.59	42.60	43.75	42.83	23.94	21.21	9.45	9.53	10.07	3.87
28	44.86	44.26	44.95	44.15	43.08	42.23	43.85	43.00	44.11	43.28	24.21	21.30	9.45	9.71	9.99	4.03
29	45.13	44.62	45.22	44.42	43.44	42.54	44.21	43.32	44.38	43.68	24.44	21.43	9.59	9.75	9.86	4.19
30	45.39	44.98	45.49	44.77	43.80	42.95	44.53	43.68	44.64	44.04	24.75	21.61	9.68	9.84	9.79	4.35
31	45.71	45.25	45.80	45.13	44.07	43.40	44.75	44.08	45.00	44.40	25.02	21.79	9.90	10.05	9.69	4.52
32	46.02	45.47	46.12	45.49	44.34	43.80	44.97	44.44	45.32	44.75	25.24	22.02	10.08	10.27	9.63	4.69
33	46.33	45.65	46.43	45.85	44.65	44.02	45.42	44.80	45.58	45.11	25.51	22.20	10.26	10.41	9.56	4.85
34	46.69	46.01	46.79	46.25	44.87	44.38	45.65	45.15	45.94	45.43	25.73	22.42	10.44	10.58	9.44	5.02
35	46.96	46.32	47.06	46.52	45.14	44.70	45.96	45.51	46.21	45.78	25.96	22.60	10.62	10.74	9.36	5.18
36	47.28	46.68	47.37	46.88	45.46	45.01	46.27	45.83	46.48	46.14	26.14	22.73	10.75	10.86	9.24	5.35
37	47.41	46.95	47.51	47.15	45.73	45.32	46.54	46.14	46.75	46.41	26.41	22.87	10.93	11.03	9.12	5.51
38	47.63	47.26	47.73	47.28	45.95	45.73	46.68	46.45	47.02	46.64	26.68	23.00	11.11	11.17	9.04	5.67
39	47.81	47.44	47.91	47.51	46.31	46.04	46.99	46.72	47.20	46.90	26.94	23.09	11.24	11.43	8.88	5.83
40	48.08	47.76	48.18	47.78	46.58	46.22	47.26	46.90	47.47	47.08	27.21	23.23	11.38	11.57	8.74	5.99
41	48.22	47.94	48.31	47.96	46.76	46.40	47.53	47.17	47.69	47.26	27.57	23.40	11.51	11.71	8.59	6.14
42	48.49	48.16	48.58	48.18	47.02	46.58	47.80	47.35	47.96	47.49	27.84	23.58	11.56	11.80	8.43	6.29
43	48.75	48.47	48.85	48.58	47.29	46.71	48.11	47.53	48.14	47.80	28.06	23.76	11.65	12.03	8.26	6.44
44	49.02	48.74	49.12	48.85	47.61	46.98	48.38	47.75	48.41	48.07	28.33	23.94	11.78	12.13	8.07	6.59
45	49.20	48.92	49.30	49.12	47.79	47.07	48.74	48.02	48.68	48.43	28.60	24.17	11.96	12.31	7.93	6.73
46	49.52	49.28	49.61	49.43	48.14	47.38	49.01	48.24	48.94	48.70	28.87	24.35	12.10	12.51	7.80	6.87
47	49.78	49.64	49.88	49.75	48.41	47.61	49.36	48.56	49.17	49.01	29.14	24.52	12.27	12.74	7.62	7.01
48	50.05	49.91	50.15	49.97	48.82	48.01	49.63	48.83	49.48	49.23	29.41	24.70	12.41	12.90	7.50	7.14
49	50.32	50.26	50.42	50.28	49.04	48.28	49.86	49.10	49.75	49.50	29.68	24.88	12.54	13.03	7.33	7.26
50	50.59	50.62	50.69	50.55	49.31	48.64	50.04	49.36	49.93	49.77	29.86	25.06	12.68	13.22	7.19	7.38
51	50.81	50.94	50.91	50.87	49.53	48.86	50.26	49.59	50.15	50.04	30.04	25.24	12.86	13.34	7.03	7.50
52	51.08	51.12	51.18	51.14	49.80	49.13	50.44	49.77	50.38	50.22	30.21	25.38	12.99	13.41	6.87	7.61
53	51.31	51.30	51.40	51.36	50.03	49.26	50.71	49.95	50.60	50.44	30.39	25.60	13.13	13.57	6.74	7.71
54	51.49	51.47	51.58	51.49	50.34	49.53	50.98	50.17	50.74	50.67	30.62	25.78	13.30	13.81	6.63	7.82
55	51.67	51.65	51.76	51.67	50.56	49.80	51.16	50.40	50.96	50.85	30.84	25.96	13.44	13.94	6.45	7.91
56	51.71	51.88	51.81	51.81	50.79	50.03	51.38	50.62	51.10	51.07	31.02	26.14	13.53	14.09	6.31	8.01
57	51.80	52.06	51.90	52.03	50.88	50.30	51.56	50.98	51.27	51.30	31.29	26.36	13.66	14.31	6.15	8.10
58	51.89	52.33	51.99	52.21	50.97	50.61	51.65	51.29	51.45	51.47	31.51	26.54	13.80	14.44	6.02	8.19
59	52.02	52.46	52.12	52.44	51.15	50.83	51.83	51.52	51.77	51.61	31.74	26.72	13.89	14.49	5.82	8.28
60	52.20	52.55	52.30	52.57	51.37	50.97	52.05	51.65	51.99	51.79	32.01	26.85	14.07	14.68	5.65	8.37
61	52.47	52.59	52.57	52.61	51.59	51.15	52.23	51.78	52.13	51.92	32.28	27.03	14.25	14.89	5.47	8.45
62	52.65	52.77	52.75	52.66	51.86	51.19	52.50	51.83	52.30	52.15	32.50	27.26	14.38	14.93	5.29	8.53
63	52.70	52.86	52.79	52.84	52.09	51.19	52.77	51.87	52.44	52.33	32.77	27.44	14.51	14.94	5.05	8.61
64	52.65	53.09	52.75	52.97	52.00	51.15	52.86	52.01	52.48	52.50	32.95	27.66	14.65	15.02	4.88	8.68
65	52.61	53.31	52.70	53.15	52.00	51.19	52.99	52.19	52.53	52.59	33.08	27.88	14.74	15.12	4.69	8.75
66	52.52	53.54	52.51	53.42	51.91	51.19	53.08	52.37	52.71	52.68	33.26	28.06	14.83	15.14	4.45	8.82
67	52.47	53.67	52.57	53.56	51.82	51.19	53.17	52.55	52.89	52.77	33.48	28.24	14.92	15.31	4.24	8.89
68	52.56	53.80	52.66	53.60	51.73	51.15	53.31	52.72	52.93	52.86	33.66	28.42	15.01	15.42	4.07	8.95
69	52.65	53.89	52.75	53.64	51.86	51.37	53.44	52.95	53.07	52.95	33.89	28.56	15.14	15.61	3.94	9.01
70	52.65	53.94	52.75	53.69	52.00	51.46	53.58	53.04	53.20	53.09	34.16	28.74	15.23	15.66	3.76	9.06
71	52.70	53.89	52.84	53.73	52.13	51.59	53.76	53.22	53.25	53.31	34.34	28.92	15.32	15.73	3.56	9.11
72	52.63	54.00	52.90	53.75	52.26	51.46	54.02	53.23	53.26	53.48	34.44	29.08	15.41	15.79	3.38	9.15
73	52.66	54.00	53.08	53.75	52.46	51.56	54.22	53.33	53.33	53.58	34.58	29.26	15.50	15.85	2.89	9.20
74	52.81	54.08	53.23	53.80	52.68	51.81	54.27	53.40	53.38	53.63	34.68	29.41	15.54	15.82	2.51	9.24
75	52.91	54.18	53.33	53.87	52.85	52.03	54.30	53.48	53.48	53.68	34.83	29.56	15.59	15.90	2.25	9.27

TABLE A.2. EXPERIMENTAL RESULT OF TEST 6

TIME	TEMPERATURE (C)													P	$\dot{m}$	MASS
(S)	TC.1	TC.2	TC.3	TC.4	TC.5	TC.6	TC.7	TC.8	TC.9	TC.10	TC.11	TC.12	TC.13	MPa	kg/min	kg
76	52.98	54.25	53.40	53.95	52.93	52.08	54.32	53.48	53.53	53.75	34.96	29.76	15.68	16.03	1.95	9.31
77	53.11	54.28	53.53	53.95	53.00	52.18	54.35	53.53	53.55	53.80	35.06	29.91	15.77	15.99	1.62	9.33
78	53.20	54.30	53.60	53.92	53.08	52.23	54.37	53.53	53.63	53.83	35.18	30.06	15.86	16.12	1.32	9.36
79	53.33	54.30	53.72	53.87	53.15	52.36	54.32	53.53	53.68	53.83	35.36	30.18	15.90	16.23	1.16	9.38
80	53.43	54.20	53.77	53.85	53.23	52.56	54.20	53.53	53.73	53.78	35.48	30.33	16.04	16.26	0.70	9.40
81	53.50	54.10	53.77	53.80	53.18	52.60	54.12	53.55	53.75	53.70	35.63	30.53	16.04	16.21	0.28	9.42
82	53.58	54.00	53.72	53.77	53.13	52.68	54.00	53.55	53.78	53.65	35.78	30.70	16.10	16.27	0.18	9.43
83	53.50	53.80	53.67	53.70	53.05	52.58	54.02	53.55	53.78	53.60	35.93	30.85	16.15	16.29	0.18	9.43
84	53.45	53.58	53.65	53.60	53.03	52.51	54.02	53.50	53.78	53.56	36.03	31.00	16.20	16.33	0.17	9.44
85	53.45	53.36	53.65	53.50	53.03	52.33	54.07	53.38	53.75	53.48	36.13	31.15	16.25	16.28	0.17	9.44
86	53.40	53.13	53.60	53.35	53.03	52.16	54.07	53.20	53.73	53.41	36.25	31.30	16.30	16.30	0.17	9.44
87	53.37	52.88	53.58	53.15	53.03	52.01	54.05	53.03	53.68	53.31	36.33	31.45	16.30	16.31	0.17	9.44
88	53.32	52.66	53.53	53.00	53.00	51.78	54.05	52.83	53.63	53.21	36.38	31.57	16.35	16.34	0.16	9.45
89	53.30	52.39	53.50	52.80	53.03	51.53	54.07	52.58	53.58	53.16	36.45	31.72	16.35	16.31	0.16	9.45
90	53.30	52.16	53.48	52.60	53.05	51.36	54.02	52.33	53.50	53.11	36.55	31.77	16.40	16.31	0.16	9.45
91	53.28	51.96	53.43	52.31	53.05	51.04	54.05	52.03	53.40	53.06	36.60	31.87	16.40	16.31	0.15	9.45
92	53.28	51.79	53.40	52.06	53.05	50.79	53.97	51.71	53.31	53.01	36.70	31.97	16.40	16.31	0.15	9.45
93	53.25	51.59	53.35	51.81	53.03	50.51	53.92	51.41	53.21	52.96	36.78	32.07	16.40	16.31	0.15	9.45
94	53.20	51.39	53.28	51.53	53.03	50.32	53.85	51.14	53.13	52.86	36.87	32.15	16.40	16.31	0.14	9.46
95	53.18	51.24	53.25	51.34	53.03	50.14	53.78	50.89	53.08	52.81	36.95	32.20	16.40	16.31	0.14	9.46
96	53.15	51.14	53.20	51.19	52.98	49.87	53.73	50.61	53.03	52.71	37.05	32.27	16.40	16.31	0.14	9.46
97	53.08	50.97	53.13	51.01	52.95	49.69	53.63	50.37	52.93	52.61	37.15	32.37	16.40	16.31	0.14	9.46
98	53.01	50.89	53.05	50.86	52.88	49.52	53.53	50.17	52.83	52.46	37.22	32.42	16.40	16.31	0.13	9.46
99	52.96	50.79	53.00	50.69	52.83	49.37	53.43	49.97	52.78	52.29	37.27	32.57	16.40	16.31	0.13	9.46
100	52.93	50.64	52.98	50.61	52.78	49.22	53.33	49.77	52.73	52.14	37.37	32.62	16.40	16.31	0.13	9.47
101	52.88	50.49	52.88	50.51	52.73	49.02	53.28	49.57	52.68	51.99	37.42	32.72	16.42	16.31	0.12	9.47
102	52.86	50.37	52.80	50.41	52.65	48.90	53.18	49.42	52.63	51.84	37.50	32.82	16.42	16.31	0.12	9.47
103	52.83	50.22	52.75	50.34	52.56	48.80	53.08	49.32	52.53	51.76	37.55	32.89	16.45	16.31	0.12	9.47
104	52.73	50.07	52.65	50.24	52.46	48.67	53.00	49.22	52.43	51.61	37.60	32.99	16.50	16.29	0.11	9.47
105	52.63	49.92	52.58	50.09	52.41	48.65	52.88	49.12	52.33	51.51	37.67	33.07	16.50	16.29	0.11	9.48
106	52.58	49.85	52.53	49.97	52.36	48.60	52.78	49.02	52.28	51.41	37.72	33.12	16.50	16.29	0.11	9.48
107	52.53	49.70	52.48	49.87	52.31	48.55	52.66	48.90	52.24	51.36	37.77	33.17	16.52	16.29	0.11	9.48
108	52.46	49.50	52.38	49.79	52.26	48.47	52.58	48.80	52.19	51.36	37.82	33.17	16.55	16.34	0.10	9.48
109	52.33	49.35	52.28	49.64	52.21	48.45	52.46	48.70	52.14	51.36	37.85	33.22	16.60	16.34	0.10	9.48
110	52.21	49.22	52.23	49.47	52.16	48.47	52.31	48.62	52.09	51.36	37.90	33.27	16.62	16.37	0.10	9.48
111	52.08	49.05	52.16	49.27	52.11	48.42	52.21	48.52	52.04	51.36	37.92	33.32	16.67	16.33	0.09	9.49
112	51.96	48.88	52.08	49.02	52.11	48.42	52.11	48.42	52.04	51.32	37.97	33.37	16.69	16.33	0.09	9.49
113	51.91	48.70	52.03	48.82	52.06	48.45	51.96	48.35	52.04	51.27	38.02	33.42	16.69	16.33	0.09	9.49
114	51.86	48.50	52.01	48.67	52.01	48.42	51.83	48.25	52.04	51.22	38.09	33.46	16.74	16.33	0.08	9.49
115	51.81	48.30	51.96	48.50	51.93	48.35	51.71	48.13	51.96	51.14	38.14	33.51	16.79	16.34	0.08	9.49
116	51.76	48.15	51.88	48.35	51.83	48.20	51.63	48.00	51.89	51.04	38.22	33.56	16.82	16.37	0.08	9.49
117	51.71	48.05	51.83	48.20	51.73	48.05	51.54	47.85	51.79	50.99	38.24	33.61	16.84	16.37	0.08	9.50
118	51.71	47.93	51.78	48.10	51.63	47.90	51.44	47.70	51.69	50.92	38.32	33.71	16.84	16.37	0.07	9.50
119	51.69	47.78	51.73	47.95	51.53	47.73	51.36	47.55	51.59	50.82	38.37	33.76	16.84	16.33	0.07	9.50
120	51.64	47.68	51.68	47.85	51.46	47.55	51.29	47.38	51.49	50.72	38.44	33.81	16.84	16.37	0.07	9.50
121	51.64	47.63	51.63	47.78	51.36	47.38	51.21	47.23	51.39	50.64	38.49	33.86	16.84	16.33	0.06	9.50
122	51.56	47.56	51.58	47.68	51.31	47.18	51.19	47.06	51.29	50.59	38.54	33.91	16.84	16.34	0.06	9.50
123	51.49	47.51	51.48	47.58	51.26	47.03	51.16	46.93	51.14	50.54	38.57	33.96	16.89	16.37	0.06	9.51
124	51.41	47.46	51.41	47.48	51.24	46.91	51.14	46.81	51.07	50.47	38.59	34.01	16.89	16.41	0.05	9.51
125	51.34	47.41	51.36	47.35	51.19	46.81	51.09	46.71	50.99	50.42	38.64	34.06	16.89	16.43	0.05	9.51
126	51.26	47.33	51.26	47.23	51.14	46.76	51.04	46.66	50.94	50.32	38.72	34.11	16.94	16.43	0.05	9.51
127	51.19	47.28	51.16	47.10	51.09	46.68	51.01	46.61	50.89	50.22	38.74	34.14	16.99	16.44	0.05	9.51
128	51.09	47.23	51.06	47.05	51.04	46.63	50.96	46.56	50.84	50.15	38.79	34.16	17.02	16.47	0.04	9.51
129	51.01	47.16	50.99	46.93	50.94	46.56	50.91	46.53	50.79	50.07	38.84	34.19	17.07	16.48	0.04	9.52
130	50.86	47.08	50.89	46.86	50.84	46.48	50.84	46.48	50.72	49.97	38.89	34.19	17.12	16.46	0.04	9.52
131	50.79	47.03	50.79	46.81	50.74	46.43	50.76	46.46	50.62	49.87	38.92	34.21	17.14	16.46	0.03	9.52
132	50.72	46.93	50.71	46.76	50.64	46.38	50.69	46.43	50.57	49.77	38.92	34.24	17.14	16.49	0.03	9.52
133	50.64	46.84	50.64	46.73	50.51	46.26	50.64	46.38	50.49	49.72	38.97	34.26	17.19	16.45	0.03	9.52
134	50.54	46.71	50.54	46.66	50.44	46.21	50.59	46.36	50.42	49.65	38.97	34.29	17.24	16.45	0.02	9.52
135	50.44	46.61	50.49	46.58	50.34	46.08	50.54	46.28	50.34	49.55	38.97	34.34	17.24	16.45	0.02	9.53
136	50.37	46.49	50.44	46.51	50.24	45.98	50.49	46.23	50.29	49.47	38.97	34.36	17.24	16.42	0.02	9.53
137	50.35	46.39	50.39	46.43	50.14	45.86	50.46	46.18	50.24	49.40	38.97	34.39	17.27	16.42	0.02	9.53
138	50.33	46.31	50.34	46.41	50.09	45.81	50.39	46.11	50.14	49.32	38.97	34.41	17.27	16.40	0.01	9.53
139	50.31	46.21	50.31	46.36	50.04	45.74	50.34	46.03	50.07	49.25	38.97	34.46	17.27	16.45	0.01	9.53
140	50.26	46.06	50.26	46.28	49.99	45.64	50.29	45.94	50.02	49.15	38.99	34.49	17.29	16.42	0.01	9.53
141	50.23	46.01	50.24	46.18	49.94	45.54	50.24	45.84	49.97	49.10	39.02	34.51	17.29	16.41	0.00	9.54
142	50.16	45.91	50.17	46.08	49.87	45.46	50.19	45.79	49.92	49.00	39.02	34.54	17.29	16.41	0.00	9.54
143	50.11	45.84	50.12	46.03	49.82	45.44	50.09	45.71	49.87	48.93	39.02	34.58	17.32	16.41	0.00	9.54
144	50.01	45.76	50.07	45.98	49.79	45.41	49.99	45.61	49.80	48.88	39.06	34.63	17.32	16.41	0.00	9.54
145	49.88	45.72	50.02	45.93	49.74	45.36	49.89	45.51	49.72	48.83	39.11	34.66	17.34	16.44	0.00	9.54
146	49.80	45.64	49.97	45.88	49.69	45.31	49.79	45.41	49.62	48.78	39.16	34.66	17.37	16.42	0.00	9.54
147	49.67	45.57	49.87	45.83	49.64	45.26	49.72	45.34	49.57	48.73	39.21	34.66	17.39	16.43	0.00	9.55
148	49.60	45.47	49.79	45.74	49.59	45.19	49.67	45.26	49.52	48.70	39.29	34.71	17.42	16.37	0.00	9.55
149	49.52	45.42	49.72	45.66	49.54	45.14	49.62	45.21	49.42	48.70	39.34	34.71	17.44	16.40	0.00	9.55
150	49.42	45.32	49.62	45.59	49.49	45.09	49.57	45.16	49.35	48.65	39.39	34.71	17.47	16.42	0.00	9.55
151	49.37	45.27	49.57	45.51	49.49	45.09	49.52	45.11	49.27	48.60	39.46	34.76	17.49	16.43	0.00	9.55
152	49.31	45.22	49.52	45.44	49.44	44.99	49.52	45.06	49.22	48.55	39.51	34.78	17.47	16.41	0.00	9.55
153	49.29	45.17	49.47	45.34	49.37	44.91	49.49	45.04	49.17	48.50	39.56	34.78	17.49	16.37	0.00	9.56
154	49.27	45.12	49.42	45.24	49.32	44.81	49.49	44.99	49.15	48.43	39.61	34.81	17.49	16.36	0.00	9.56
155	49.18	45.09	49.37	45.14	49.32	44.81	49.44	44.94	49.12	48.35	39.64	34.86	17.49	16.41	0.00	9.56
156	49.14	45.07	49.37	45.04	49.27	44.76	49.39	44.89	49.07	48.28	39.64	34.88	17.52	16.39	0.00	9.56
157	49.07	45.02	49.29	44.99	49.22	44.74	49.32	44.84	49.02	48.18	39.61	34.88	17.52	16.43	0.00	9.56

TABLE A.2. EXPERIMENTAL RESULT OF TEST 6

TIME	TEMPERATURE (C)													P	$\dot{m}$	MASS
(S)	TC.1	TC.2	TC.3	TC.4	TC.5	TC.6	TC.7	TC.8	TC.9	TC.10	TC.11	TC.12	TC.13	MPa	kg/min	kg
158	49.02	44.97	49.24	44.94	49.15	44.69	49.25	44.79	49.02	48.08	39.64	34.93	17.52	16.44	0.00	9.56
159	48.97	44.89	49.19	44.91	49.07	44.64	49.17	44.74	49.00	47.98	39.64	34.98	17.54	16.39	0.00	9.56
160	48.92	44.82	49.14	44.89	49.02	44.59	49.10	44.67	49.00	47.93	39.64	34.98	17.54	16.39	0.00	9.57
161	48.86	44.72	49.07	44.81	48.97	44.52	49.02	44.57	48.97	47.83	39.69	34.98	17.57	16.42	0.00	9.57
162	48.80	44.64	49.00	44.76	48.92	44.47	48.95	44.49	48.92	47.73	39.69	34.98	17.59	16.44	0.00	9.57
163	48.75	44.55	48.92	44.71	48.87	44.47	48.85	44.44	48.83	47.66	39.71	34.98	17.62	16.45	0.00	9.57
164	48.69	44.45	48.82	44.66	48.77	44.37	48.80	44.39	48.75	47.58	39.74	34.98	17.64	16.41	0.00	9.57
165	48.63	44.35	48.72	44.62	48.72	44.29	48.77	44.34	48.70	47.51	39.79	35.01	17.64	16.41	0.00	9.57
166	48.57	44.30	48.67	44.57	48.65	44.22	48.72	44.29	48.65	47.46	39.84	35.01	17.67	16.41	0.00	9.58
167	48.53	44.25	48.62	44.52	48.62	44.17	48.70	44.24	48.60	47.41	39.86	35.01	17.74	16.41	0.00	9.58
168	48.48	44.22	48.57	44.44	48.57	44.14	48.62	44.19	48.55	47.36	39.91	35.01	17.79	16.41	0.00	9.58
169	48.43	44.20	48.52	44.34	48.47	44.04	48.60	44.17	48.50	47.31	39.94	35.01	17.84	16.38	0.00	9.58
170	48.40	44.20	48.50	44.29	48.40	43.99	48.57	44.17	48.45	47.31	39.94	35.01	17.86	16.34	0.00	9.58
171	48.35	44.17	48.45	44.24	48.35	43.94	48.52	44.12	48.45	47.31	39.94	35.01	17.89	16.36	0.00	9.58
172	48.33	44.12	48.42	44.19	48.30	43.89	48.47	44.07	48.38	47.26	39.91	35.01	17.94	16.32	0.00	9.58
173	48.33	44.07	48.42	44.14	48.22	43.82	48.42	44.02	48.30	47.26	39.89	35.01	17.96	16.35	0.00	9.59
174	48.28	44.02	48.37	44.09	48.12	43.72	48.37	43.97	48.23	47.26	39.89	35.01	18.01	16.36	0.00	9.59
175	48.34	43.97	48.32	44.04	48.08	43.64	48.35	43.92	48.15	47.23	39.89	35.01	18.06	16.39	0.00	9.59
176	48.29	43.92	48.27	43.99	47.98	43.52	48.30	43.84	48.08	47.18	39.89	35.01	18.06	16.38	0.00	9.59
177	48.23	43.85	48.22	43.97	47.90	43.40	48.30	43.79	48.00	47.13	39.89	35.01	18.06	16.38	0.00	9.59
178	48.17	43.80	48.17	43.97	47.85	43.32	48.25	43.72	47.93	47.11	39.89	35.01	18.09	16.42	0.00	9.59
179	48.11	43.70	48.12	43.97	47.80	43.25	48.20	43.65	47.85	47.06	39.94	35.01	18.14	16.45	0.00	9.60
180	48.07	43.60	48.10	43.97	47.75	43.20	48.15	43.60	47.78	47.01	39.94	35.01	18.16	16.42	0.00	9.60
181	47.99	43.55	48.05	43.92	47.70	43.17	48.10	43.57	47.78	47.01	39.96	35.01	18.16	16.40	0.00	9.60
182	47.92	43.50	47.98	43.87	47.68	43.15	48.05	43.52	47.76	46.96	39.99	35.01	18.19	16.41	0.00	9.60
183	47.87	43.45	47.93	43.82	47.68	43.15	48.00	43.47	47.73	46.91	39.99	35.01	18.19	16.44	0.00	9.60
184	47.71	43.40	47.88	43.77	47.65	43.12	47.95	43.42	47.71	46.84	39.99	35.01	18.19	16.38	0.00	9.60
185	47.66	43.35	47.83	43.72	47.65	43.15	47.90	43.40	47.68	46.79	40.01	35.01	18.19	16.36	0.00	9.60
186	47.61	43.33	47.78	43.64	47.60	43.07	47.85	43.32	47.66	46.74	40.06	35.01	18.19	16.35	0.00	9.61
187	47.57	43.28	47.73	43.57	47.60	43.12	47.78	43.30	47.63	46.66	40.09	35.01	18.19	16.35	0.00	9.61
188	47.54	43.28	47.68	43.50	47.55	43.12	47.68	43.25	47.61	46.61	40.09	35.01	18.19	16.37	0.00	9.61
189	47.51	43.28	47.63	43.40	47.55	43.12	47.63	43.20	47.58	46.54	40.09	35.01	18.19	16.41	0.00	9.61
190	47.49	43.28	47.58	43.37	47.55	43.12	47.58	43.15	47.56	46.46	40.09	35.01	18.19	16.44	0.00	9.61
191	47.46	43.28	47.55	43.35	47.48	43.00	47.58	43.10	47.53	46.39	40.09	35.01	18.19	16.41	0.00	9.61
192	47.46	43.28	47.55	43.30	47.43	42.95	47.53	43.05	47.51	46.29	40.09	35.01	18.19	16.38	0.00	9.62
193	47.46	43.23	47.55	43.25	47.35	42.87	47.48	43.00	47.46	46.26	40.09	35.01	18.19	16.38	0.00	9.62
194	47.41	43.18	47.50	43.20	47.28	42.80	47.43	42.95	47.43	46.24	40.11	35.01	18.21	16.40	0.00	9.62
195	47.36	43.13	47.45	43.15	47.25	42.82	47.35	42.92	47.38	46.19	40.06	35.01	18.21	16.46	0.00	9.62
196	47.31	43.05	47.40	43.12	47.18	42.75	47.30	42.87	47.33	46.14	40.04	35.01	18.24	16.45	0.00	9.62
197	47.23	42.98	47.33	43.10	47.13	42.70	47.28	42.85	47.28	46.11	39.99	35.01	18.26	16.46	0.00	9.62
198	47.18	42.90	47.28	43.10	47.03	42.62	47.25	42.85	47.23	46.11	40.04	35.01	18.29	16.45	0.00	9.62
199	47.11	42.85	47.20	43.07	46.93	42.52	47.23	42.82	47.18	46.09	40.04	35.01	18.31	16.45	0.00	9.63
200	47.03	42.78	47.13	43.05	46.91	42.57	47.15	42.82	47.16	46.06	40.04	35.01	18.34	16.50	0.00	9.63
201	46.93	42.68	47.05	43.05	46.86	42.55	47.10	42.80	47.13	46.06	40.06	35.01	18.36	16.52	0.00	9.63
202	46.83	42.63	46.95	43.00	46.83	42.55	47.06	42.77	47.13	46.04	40.06	35.01	18.39	16.54	0.00	9.63
203	46.78	42.58	46.90	42.95	46.81	42.55	47.01	42.75	47.11	46.01	40.06	35.01	18.39	16.55	0.00	9.63
204	46.73	42.53	46.86	42.92	46.78	42.50	46.98	42.70	47.11	46.01	40.11	35.01	18.41	16.49	0.00	9.63
205	46.68	42.50	46.81	42.92	46.76	42.45	46.96	42.65	47.11	46.01	40.16	35.01	18.44	16.52	0.00	9.63
206	46.64	42.50	46.78	42.87	46.76	42.43	46.93	42.60	47.06	45.99	40.16	35.01	18.46	16.48	0.00	9.64
207	46.59	42.48	46.73	42.82	46.76	42.40	46.91	42.55	47.01	45.94	40.11	35.01	18.49	16.47	0.00	9.64
208	46.57	42.43	46.71	42.77	46.76	42.38	46.88	42.50	46.96	45.91	40.16	35.01	18.51	16.50	0.00	9.64
209	46.53	42.40	46.68	42.72	46.76	42.35	46.86	42.45	46.91	45.86	40.16	35.01	18.54	16.44	0.00	9.64

TBALE A.3. EXPERIMENTAL RESULT OF TEST 8

Paramaters Measured: T, P, $\dot{m}$, Tw, and T1;
Ambient=20.9 C, Po= 0.101 MPa, Storage Pressure=20 MPa, Vertical Cylinder.
TC- Thermocouple, relative to the number in Fig.(4.5)

TIME	Temperature (c)														$\dot{m}$	P	MASS
(s)	TC.1	TC.2	TC.3	TC.4	TC.5	TC.7	TC.8	TC.9	TC.10	TC.11	TC.12	TC.13	TC.14	TC.15	kg/min	MPa	kg
1	19.56	19.56	19.45	19.45	19.45	19.90	19.45	19.56	19.74	18.97	19.35	19.23	19.23	19.26	0.00	0.00	0.00
2	31.20	31.88	30.20	30.88	28.79	31.10	26.62	29.41	29.94	18.92	19.35	21.24	19.23	19.26	5.47	7.67	0.11
3	35.68	36.58	35.36	36.25	34.24	35.58	32.89	34.79	35.98	18.88	19.35	21.92	19.23	19.26	8.32	8.29	0.25
4	35.28	36.00	35.31	36.03	34.46	35.49	33.47	36.36	35.05	18.88	19.26	20.80	19.23	19.26	9.91	8.43	0.41
5	36.62	37.25	36.88	37.51	36.19	36.74	35.45	36.58	36.44	18.87	19.26	20.26	19.23	19.35	10.00	8.62	0.58
6	37.03	37.61	37.46	38.04	36.88	37.24	36.30	36.16	36.53	18.88	19.26	19.54	19.23	19.48	10.24	8.55	0.75
7	37.61	38.06	37.95	38.40	37.39	37.60	36.70	37.23	36.72	18.90	19.30	18.82	19.26	19.48	9.88	8.65	0.91
8	38.01	38.42	38.36	38.76	37.81	38.00	37.10	37.72	37.04	18.98	19.35	18.06	19.26	19.48	10.04	8.66	1.08
9	38.69	38.91	38.85	39.07	38.31	38.40	37.46	38.15	37.41	19.10	19.35	17.35	19.26	19.48	10.07	8.66	1.25
10	39.13	39.31	39.25	39.43	38.76	38.94	37.95	38.55	37.79	19.23	19.35	16.63	19.30	19.52	10.09	8.66	1.42
11	39.76	39.81	39.75	39.79	39.27	39.48	38.36	39.02	38.30	19.38	19.35	15.91	19.49	19.52	10.05	8.64	1.58
12	40.21	40.21	40.15	40.15	39.72	40.02	38.85	39.49	38.67	19.53	19.48	15.24	19.58	19.66	10.06	8.61	1.75
13	40.57	40.57	40.51	40.51	40.07	40.51	39.21	39.96	39.08	19.67	19.62	14.70	19.66	19.79	10.04	8.61	1.92
14	40.93	40.93	40.91	40.91	40.51	41.05	39.70	40.36	39.46	19.82	19.75	14.17	19.75	19.93	10.07	8.64	2.09
15	41.42	41.28	41.40	41.27	41.02	41.54	40.10	40.81	39.92	19.95	19.89	13.81	19.85	19.93	10.06	8.68	2.26
16	41.69	41.51	41.81	41.63	41.42	41.90	40.46	41.23	40.34	20.09	20.06	13.31	19.95	19.93	10.03	8.74	2.42
17	42.09	41.91	42.17	41.99	41.78	42.26	40.82	41.71	40.85	20.24	20.11	12.96	20.04	19.97	10.03	8.85	2.59
18	42.58	42.27	42.66	42.34	42.29	42.43	41.22	42.11	41.22	20.37	20.15	12.64	20.15	20.02	10.03	8.96	2.76
19	42.99	42.63	43.02	42.66	42.66	42.61	41.58	42.50	41.68	20.50	20.20	12.42	20.26	20.06	10.04	9.06	2.92
20	43.30	42.94	43.38	43.02	43.00	42.75	41.90	42.90	42.01	20.63	20.24	12.19	20.37	20.11	10.05	9.17	3.09
21	43.61	43.30	43.69	43.38	43.32	42.79	42.26	43.23	42.38	20.76	20.38	12.02	20.49	20.15	10.06	9.28	3.26
22	43.93	43.61	44.05	43.73	43.66	42.88	42.57	43.55	42.75	20.88	20.56	11.79	20.62	20.15	10.05	9.38	3.43
23	44.15	43.97	44.27	44.09	43.87	43.06	42.88	43.92	43.12	21.03	20.74	11.43	20.76	20.15	10.00	9.49	3.59
24	44.33	44.20	44.58	44.45	44.18	43.38	43.24	44.27	43.40	21.20	20.92	11.12	20.91	20.15	9.99	9.58	3.76
25	44.69	44.55	44.94	44.81	44.55	43.78	43.64	44.64	43.82	21.36	21.10	10.81	21.08	20.15	9.94	9.66	3.93
26	45.09	44.91	45.35	45.17	44.96	44.18	44.00	44.97	44.19	21.54	21.27	10.58	21.25	20.24	9.88	9.75	4.09
27	45.50	45.32	45.70	45.53	45.33	44.58	44.41	45.34	44.56	21.72	21.41	10.40	21.42	20.38	9.81	9.87	4.25
28	46.03	45.67	46.24	45.88	45.88	45.17	44.81	45.71	44.93	21.89	21.59	10.36	21.59	20.51	9.73	10.00	4.42
29	46.70	46.17	46.78	46.24	46.38	45.57	45.03	46.04	45.40	22.06	21.77	10.31	21.76	20.69	9.63	10.14	4.58
30	46.97	46.57	47.00	46.60	46.60	45.79	45.39	46.34	45.77	22.25	21.95	10.31	21.93	20.87	9.50	10.30	4.73
31	47.33	46.93	47.36	46.96	46.96	46.15	45.75	46.71	46.14	22.45	22.08	10.36	22.12	20.96	9.41	10.45	4.89
32	47.56	47.11	47.72	47.27	47.29	46.42	45.97	47.01	46.51	22.65	22.26	10.40	22.31	21.00	9.31	10.60	5.05
33	47.69	47.42	47.90	47.63	47.47	46.60	46.33	47.33	46.88	22.85	22.44	10.45	22.50	21.05	9.18	10.77	5.20
34	47.82	47.65	48.03	47.86	47.65	46.87	46.69	47.63	47.16	23.03	22.62	10.49	22.70	21.18	9.06	10.97	5.35
35	48.09	47.82	48.39	48.12	48.02	47.27	47.00	47.90	47.48	23.17	22.93	10.49	22.89	21.32	8.96	11.15	5.50
36	48.36	48.14	48.57	48.35	48.23	47.54	47.32	48.13	47.81	23.34	23.16	10.58	23.08	21.45	8.82	11.31	5.65
37	48.81	48.50	48.89	48.57	48.59	47.99	47.68	48.35	48.04	23.49	23.34	10.72	23.23	21.59	8.66	11.45	5.79
38	49.03	48.72	49.24	48.93	48.89	48.17	47.86	48.63	48.36	23.64	23.51	10.90	23.38	21.76	8.56	11.60	5.93
39	49.26	49.03	49.51	49.29	49.14	48.39	48.17	48.92	48.69	23.80	23.69	11.07	23.54	21.81	8.44	11.71	6.07
40	49.53	49.39	49.69	49.56	49.30	48.53	48.39	49.15	48.92	23.94	23.74	11.25	23.71	21.85	8.27	11.84	6.21
41	49.84	49.62	49.96	49.74	49.59	48.84	48.62	49.45	49.15	24.05	23.92	11.48	23.88	21.90	8.17	11.97	6.35
42	49.89	49.80	50.18	50.10	49.80	49.02	48.93	49.70	49.52	24.14	24.14	11.70	24.07	21.94	8.03	12.13	6.48
43	50.20	50.15	50.32	50.27	49.99	49.33	49.29	49.92	49.71	24.21	24.32	11.88	24.27	22.08	7.92	12.27	6.61
44	50.24	50.38	50.32	50.45	50.01	49.38	49.51	50.14	49.94	24.28	24.50	12.06	24.50	22.21	7.78	12.41	6.74
45	50.29	50.56	50.50	50.77	50.18	49.56	49.83	50.34	50.13	24.36	24.68	12.42	24.76	22.39	7.67	12.58	6.87
46	50.24	50.74	50.59	51.08	50.29	49.69	50.18	50.62	50.45	24.47	24.86	12.64	25.07	22.57	7.55	12.76	7.00
47	50.47	51.10	50.59	51.22	50.32	49.78	50.41	50.84	50.64	24.58	24.99	12.82	25.37	22.75	7.38	12.90	7.12
48	50.65	51.41	50.63	51.39	50.41	49.96	50.72	51.04	51.06	24.72	25.17	13.14	25.65	22.80	7.22	13.07	7.24
49	51.01	51.77	50.95	51.71	50.72	50.27	51.04	51.34	51.43	24.87	25.35	13.31	25.92	22.97	7.07	13.27	7.36
50	51.27	52.08	51.13	51.93	50.90	50.45	51.26	51.56	51.80	25.03	25.62	13.45	26.17	22.92	6.90	13.46	7.47
51	51.72	52.44	51.44	52.16	51.20	50.72	51.44	51.79	52.03	25.20	25.84	13.58	26.41	23.09	6.77	13.64	7.59
52	51.90	52.62	51.80	52.51	51.54	51.04	51.75	51.99	52.22	25.38	26.07	13.76	26.64	23.26	6.57	13.82	7.70
53	52.26	52.80	52.29	52.83	51.99	51.39	51.93	52.24	52.36	25.55	26.25	13.81	26.85	23.44	6.40	14.00	7.80
54	52.39	52.93	52.51	53.05	52.22	51.62	52.16	52.51	52.54	25.73	26.56	13.99	27.05	23.61	6.22	14.19	7.91
55	52.57	53.16	52.65	53.23	52.39	51.89	52.47	52.73	52.73	25.92	26.78	14.03	27.24	23.79	6.04	14.36	8.01
56	52.57	53.34	52.65	53.41	52.44	52.02	52.78	52.93	52.91	26.09	26.96	14.21	27.43	23.98	5.85	14.53	8.10
57	52.71	53.51	52.65	53.46	52.48	52.16	52.96	53.13	53.10	26.23	27.14	14.34	27.62	24.16	5.68	14.68	8.20
58	52.57	53.56	52.65	53.63	52.48	52.16	53.14	53.31	53.19	26.37	27.32	14.48	27.82	24.32	5.52	14.82	8.29
59	52.80	53.78	52.83	53.81	52.66	52.34	53.32	53.48	53.28	26.48	27.37	14.66	28.04	24.50	5.32	14.94	8.38
60	52.98	53.92	53.05	53.99	52.84	52.42	53.37	53.68	53.42	26.59	27.55	14.84	28.27	24.69	5.11	15.05	8.47
61	53.07	54.10	53.28	54.31	52.98	52.38	53.41	53.88	53.61	26.70	27.73	14.88	28.48	24.88	4.97	15.14	8.55
62	53.07	54.23	53.46	54.62	53.11	52.42	53.59	54.03	53.79	26.85	27.90	15.06	28.69	25.05	4.78	15.23	8.63
63	53.11	54.41	53.50	54.80	53.16	52.47	53.77	54.15	53.93	27.01	28.08	15.11	28.88	25.23	4.56	15.30	8.70
64	52.98	54.41	53.50	54.93	53.16	52.47	53.90	54.25	54.16	27.20	28.40	15.24	29.05	25.39	4.34	15.38	8.78
65	53.07	54.46	53.68	55.07	53.34	52.65	54.04	54.35	54.21	27.38	28.58	15.38	29.22	25.55	4.20	15.48	8.85
66	53.34	54.59	53.86	55.11	53.54	52.92	54.17	54.45	54.35	27.55	28.76	15.51	29.38	25.69	4.02	15.58	8.91
67	53.51	54.63	54.04	55.16	53.72	53.10	54.22	54.48	54.35	27.74	28.94	15.55	29.53	25.84	3.84	15.66	8.98
68	53.78	54.77	54.22	55.20	53.90	53.28	54.26	54.57	54.49	27.93	29.11	15.73	29.67	25.98	3.68	15.76	9.04
69	54.14	54.95	54.40	55.20	54.10	53.50	54.31	54.65	54.49	28.14	29.16	15.78	29.80	26.12	3.53	15.86	9.10
70	54.23	55.13	54.35	55.25	54.10	53.59	54.49	54.72	54.63	28.35	29.29	15.82	29.94	26.25	3.34	15.96	9.15
71	54.28	55.17	54.35	55.25	54.16	53.77	54.66	54.80	54.63	28.57	29.43	15.87	30.07	26.38	3.14	16.05	9.20
72	54.59	55.49	54.35	55.25	54.16	53.77	54.66	54.90	54.77	28.79	29.61	15.87	30.22	26.51	2.99	16.12	9.25
73	54.63	55.53	54.35	55.25	54.16	53.77	54.66	54.97	54.77	29.01	29.79	15.87	30.37	26.64	2.81	16.21	9.30
74	54.72	55.66	54.35	55.29	54.14	53.72	54.66	55.05	54.77	29.22	29.97	15.87	30.52	26.75	2.62	16.27	9.35
75	54.77	55.66	54.40	55.29	54.14	53.63	54.53	55.15	54.77	29.44	30.19	15.87	30.67	26.87	2.42	16.33	9.39

TBALE A.3. EXPERIMENTAL RESULT OF TEST 8

TIME	Temperature (c)														ṁ	P	MASS
(s)	TC.1	TC.2	TC.3	TC.4	TC.5	TC.7	TC.8	TC.9	TC.10	TC.11	TC.12	TC.13	TC.14	TC.15	kg/min	MPa	kg
76	54.90	55.66	54.53	55.29	54.23	53.63	54.40	55.22	54.77	29.64	30.37	15.87	30.82	27.00	2.21	16.39	9.42
77	54.90	55.53	54.66	55.29	54.37	53.77	54.40	55.22	54.81	29.84	30.55	15.87	30.96	27.13	1.99	16.44	9.46
78	54.99	55.49	54.80	55.29	54.50	53.90	54.40	55.22	54.86	30.03	30.73	15.87	31.09	27.27	1.78	16.49	9.49
79	54.90	55.31	54.89	55.29	54.59	53.99	54.40	55.15	54.91	30.20	30.91	15.87	31.22	27.41	1.55	16.54	9.51
80	54.99	55.26	55.02	55.29	54.72	54.13	54.40	55.07	54.95	30.37	30.95	15.87	31.36	27.55	1.42	16.57	9.53
81	54.57	55.00	54.82	55.24	54.59	54.12	54.55	54.97	54.90	30.51	31.10	15.97	31.50	27.70	1.21	16.61	9.55
82	54.38	54.87	54.72	55.22	54.52	54.12	54.62	54.90	54.90	30.64	31.22	16.04	31.64	27.86	1.06	16.63	9.57
83	54.20	54.77	54.55	55.12	54.40	54.12	54.69	54.82	54.90	30.75	31.34	16.12	31.79	28.05	0.90	16.66	9.59
84	54.00	54.65	54.37	55.02	54.26	54.05	54.69	54.72	54.79	30.84	31.44	16.19	31.95	28.23	0.78	16.67	9.60
85	53.83	54.55	54.20	54.92	54.12	53.97	54.69	54.65	54.69	30.94	31.54	16.27	32.11	28.42	0.70	16.68	9.61
86	53.60	54.38	54.05	54.82	54.01	53.92	54.69	54.57	54.59	31.04	31.64	16.34	32.26	28.60	0.62	16.68	9.62
87	53.38	54.20	53.87	54.69	53.87	53.87	54.69	54.48	54.48	31.15	31.82	16.42	32.40	28.78	0.53	16.67	9.63
88	53.26	54.08	53.67	54.50	53.72	53.80	54.62	54.45	54.38	31.27	31.99	16.44	32.52	28.97	0.46	16.66	9.64
89	53.03	53.88	53.48	54.32	53.57	53.77	54.62	54.35	54.30	31.40	32.12	16.49	32.63	29.13	0.39	16.67	9.65
90	53.01	53.70	53.45	54.15	53.58	53.85	54.55	54.25	54.23	31.56	32.22	16.56	32.72	29.29	0.36	16.65	9.65
91	52.98	53.50	53.43	53.95	53.60	53.95	54.47	54.15	54.12	31.73	32.32	16.59	32.80	29.43	0.33	16.62	9.66
92	52.78	53.28	53.33	53.82	53.52	53.90	54.40	54.05	53.94	31.90	32.41	16.59	32.88	29.55	0.32	16.59	9.66
93	52.61	53.08	53.23	53.70	53.45	53.90	54.37	53.95	53.84	32.09	32.51	16.59	32.94	29.67	0.30	16.56	9.67
94	52.43	52.81	53.13	53.50	53.41	53.97	54.35	53.85	53.74	32.28	32.61	16.61	33.01	29.78	0.26	16.51	9.67
95	52.33	52.61	53.03	53.30	53.37	54.05	54.32	53.75	53.63	32.48	32.76	16.61	33.09	29.88	0.21	16.56	9.67
96	52.24	52.41	52.93	53.10	53.30	54.05	54.22	53.65	53.53	32.67	32.86	16.64	33.18	29.99	0.21	16.53	9.68
97	52.06	52.21	52.83	52.98	53.21	53.97	54.12	53.55	53.43	32.85	32.96	16.66	33.29	30.10	0.21	16.59	9.68
98	51.99	52.01	52.75	52.78	53.17	54.00	54.02	53.53	53.40	33.03	33.09	16.66	33.43	30.22	0.21	16.56	9.69
99	51.89	51.81	52.65	52.58	53.10	54.00	53.92	53.48	53.38	33.22	33.19	16.69	33.60	30.37	0.20	16.55	9.69
100	51.79	51.64	52.55	52.40	53.03	53.97	53.82	53.43	53.38	33.40	33.29	16.66	33.78	30.54	0.20	16.55	9.69
101	51.69	51.46	52.45	52.23	52.95	53.95	53.72	53.33	53.43	33.56	33.39	16.69	33.99	30.73	0.20	16.56	9.70
102	51.56	51.26	52.36	52.06	52.88	53.92	53.62	53.23	53.50	33.70	33.48	16.71	34.20	30.94	0.19	16.57	9.70
103	51.44	51.14	52.26	51.96	52.78	53.82	53.52	53.13	53.58	33.83	33.66	16.71	34.42	31.17	0.19	16.50	9.71
104	51.31	51.02	52.16	51.86	52.68	53.72	53.43	53.03	53.66	33.95	33.78	16.74	34.63	31.39	0.19	16.53	9.71
105	51.12	50.82	52.06	51.76	52.60	53.70	53.40	52.96	53.71	34.07	33.88	16.74	34.84	31.59	0.18	16.57	9.72
106	50.94	50.64	51.96	51.66	52.53	53.67	53.38	52.88	53.71	34.17	33.98	16.74	35.03	31.79	0.18	16.51	9.72
107	50.74	50.54	51.83	51.63	52.38	53.48	53.28	52.81	53.63	34.27	34.06	16.74	35.20	31.97	0.18	16.53	9.72
108	50.57	50.44	51.73	51.61	52.26	53.30	53.18	52.76	53.56	34.35	34.13	16.74	35.35	32.12	0.18	16.54	9.73
109	50.44	50.32	51.63	51.51	52.16	53.20	53.08	52.71	53.48	34.42	34.23	16.76	35.47	32.25	0.17	16.56	9.73
110	50.39	50.19	51.61	51.41	52.13	53.18	52.98	52.71	53.43	34.48	34.33	16.76	35.58	32.35	0.17	16.57	9.73
111	50.27	50.07	51.51	51.31	52.04	53.10	52.90	52.71	53.35	34.53	34.43	16.76	35.68	32.42	0.17	16.60	9.73
112	50.09	49.90	51.41	51.21	51.95	53.03	52.83	52.68	53.27	34.59	34.46	16.76	35.77	32.48	0.16	16.61	9.74
113	49.92	49.72	51.31	51.11	51.86	52.95	52.75	52.66	53.20	34.65	34.48	16.76	35.87	32.54	0.16	16.63	9.74
114	49.80	49.62	51.21	51.04	51.76	52.85	52.68	52.63	53.12	34.71	34.51	16.76	35.96	32.60	0.16	16.62	9.74
115	49.67	49.52	51.11	50.96	51.65	52.73	52.58	52.61	53.09	34.77	34.58	16.76	36.06	32.67	0.15	16.62	9.75
116	49.60	49.42	51.04	50.86	51.60	52.73	52.55	52.58	53.07	34.82	34.65	16.76	36.15	32.73	0.15	16.62	9.75
117	49.50	49.32	50.94	50.76	51.53	52.70	52.53	52.56	53.04	34.87	34.75	16.76	36.26	32.80	0.15	16.63	9.75
118	49.30	49.22	50.81	50.74	51.38	52.50	52.43	52.53	52.94	34.92	34.83	16.76	36.36	32.88	0.15	16.64	9.76
119	49.12	49.12	50.69	50.69	51.24	52.33	52.33	52.43	52.83	34.98	34.90	16.76	36.46	32.96	0.12	16.66	9.76
120	49.05	49.05	50.59	50.59	51.14	52.23	52.23	52.33	52.73	35.04	34.98	16.76	36.56	33.05	0.10	16.66	9.76
121	49.02	49.02	50.49	50.49	51.04	52.13	52.13	52.26	52.63	35.10	35.08	16.76	36.66	33.15	0.08	16.67	9.76
122	48.92	48.92	50.39	50.39	50.94	52.03	52.03	52.19	52.53	35.17	35.18	16.76	36.74	33.25	0.08	16.68	9.76
123	48.83	48.83	50.29	50.29	50.84	51.93	51.93	52.11	52.45	35.23	35.28	16.76	36.83	33.35	0.08	16.71	9.76
124	48.73	48.73	50.19	50.19	50.75	51.86	51.86	52.04	52.37	35.30	35.33	16.76	36.91	33.45	0.07	16.74	9.76
125	48.60	48.63	50.09	50.12	50.65	51.76	51.78	51.96	52.27	35.39	35.38	16.76	37.00	33.57	0.07	16.76	9.77
126	48.50	48.53	50.02	50.04	50.57	51.68	51.71	51.89	52.16	35.47	35.40	16.76	37.08	33.69	0.07	16.78	9.77
127	48.48	48.45	49.97	49.94	50.55	51.71	51.68	51.79	52.14	35.57	35.50	16.76	37.16	33.81	0.06	16.80	9.77
128	48.38	48.35	49.89	49.87	50.49	51.68	51.66	51.79	52.14	35.66	35.60	16.76	37.24	33.94	0.06	16.80	9.77
129	48.28	48.25	49.87	49.84	50.46	51.66	51.63	51.76	52.14	35.75	35.70	16.76	37.33	34.06	0.06	16.81	9.77
130	48.15	48.13	49.84	49.82	50.44	51.63	51.61	51.74	52.11	35.84	35.77	16.76	37.43	34.18	0.06	16.81	9.77
131	48.20	48.10	49.82	49.72	50.44	51.68	51.58	51.71	52.09	35.93	35.85	16.84	37.52	34.30	0.05	16.81	9.77
132	48.23	48.05	49.79	49.62	50.44	51.73	51.56	51.69	52.04	36.01	35.92	16.84	37.62	34.41	0.05	16.80	9.77
133	48.18	48.00	49.69	49.52	50.34	51.63	51.46	51.59	52.01	36.09	36.00	16.84	37.71	34.51	0.05	16.79	9.78
134	48.08	47.90	49.59	49.42	50.24	51.53	51.36	51.49	52.01	36.17	36.07	16.84	37.79	34.58	0.04	16.80	9.78
135	47.98	47.80	49.49	49.32	50.14	51.43	51.26	51.39	52.01	36.23	36.17	16.84	37.87	34.64	0.04	16.79	9.78
136	47.85	47.71	49.39	49.24	50.04	51.33	51.19	51.31	51.93	36.29	36.17	16.84	37.93	34.70	0.04	16.77	9.78
137	47.78	47.63	49.32	49.17	49.97	51.26	51.11	51.21	51.83	36.34	36.20	16.84	37.99	34.73	0.03	16.76	9.78
138	47.73	47.56	49.24	49.07	49.90	51.21	51.04	51.14	51.73	36.39	36.22	16.84	38.03	34.73	0.03	16.75	9.78
139	47.71	47.51	49.17	48.97	49.83	51.16	50.96	51.07	51.65	36.44	36.25	16.84	38.06	34.72	0.03	16.75	9.78
140	47.58	47.43	49.09	48.95	49.74	51.04	50.89	50.99	51.57	36.48	36.27	16.76	38.07	34.69	0.03	16.75	9.78
141	47.56	47.38	49.02	48.85	49.68	50.99	50.81	50.92	51.52	36.52	36.30	16.84	38.08	34.64	0.02	16.75	9.79
142	47.51	47.31	49.00	48.80	49.66	50.99	50.79	50.92	51.44	36.56	36.32	16.91	38.10	34.60	0.02	16.75	9.79
143	47.56	47.28	48.97	48.70	49.66	51.04	50.76	50.89	51.37	36.59	36.35	16.99	38.12	34.57	0.02	16.74	9.79
144	47.61	47.26	48.95	48.60	49.63	51.01	50.66	50.87	51.29	36.62	36.35	16.99	38.15	34.54	0.02	16.75	9.79
145	47.58	47.23	48.85	48.50	49.56	50.99	50.64	50.84	51.29	36.64	36.37	17.06	38.20	34.53	0.02	16.76	9.79
146	47.61	47.21	48.80	48.40	49.51	50.94	50.54	50.82	51.29	36.66	36.37	17.06	38.26	34.54	0.02	16.77	9.79
147	47.48	47.11	48.70	48.32	49.40	50.81	50.44	50.79	51.29	36.68	36.37	17.06	38.34	34.57	0.01	16.77	9.79
148	47.36	47.01	48.60	48.25	49.29	50.69	50.34	50.69	51.29	36.70	36.37	17.06	38.44	34.62	0.01	16.76	9.79
149	47.23	46.91	48.50	48.17	49.19	50.56	50.24	50.59	51.29	36.71	36.37	17.14	38.55	34.69	0.01	16.74	9.80
150	47.03	46.81	48.40	48.17	49.05	50.36	50.14	50.49	51.29	36.72	36.42	17.06	38.67	34.77	0.01	16.74	9.80
151	46.93	46.73	48.32	48.12	48.97	50.26	50.07	50.47	51.29	36.75	36.47	17.04	38.79	34.85	0.01	16.74	9.80
152	46.78	46.66	48.25	48.12	48.87	50.12	49.99	50.39	51.29	36.77	36.55	16.96	38.92	34.93	0.01	16.75	9.80
153	46.66	46.59	48.17	48.10	48.80	50.07	49.99	50.32	51.29	36.81	36.62	16.96	39.04	35.00	0.01	16.75	9.80
154	46.61	46.51	48.17	48.07	48.79	50.02	49.92	50.24	51.29	36.85	36.70	16.89	39.16	35.07	0.01	16.75	9.80
155	46.49	46.41	48.12	48.05	48.75	49.99	49.92	50.17	51.29	36.91	36.77	16.89	39.26	35.13	0.01	16.75	9.80
156	46.49	46.39	48.12	48.02	48.75	49.99	49.89	50.09	51.29	36.98	36.84	16.96	39.36	35.17	0.01	16.77	9.80
157	46.49	46.36	48.12	48.00	48.75	49.99	49.87	50.09	51.29	37.05	36.94	17.04	39.45	35.21	0.01	16.80	9.81

TBALE A.3. EXPERIMENTAL RESULT OF TEST 8

TIME	Temperature (c)														ṁ	P	MASS
(s)	TC.1	TC.2	TC.3	TC.4	TC.5	TC.7	TC.8	TC.9	TC.10	TC.11	TC.12	TC.13	TC.14	TC.15	kg/min	MPa	kg
158	46.46	46.34	48.10	47.97	48.72	49.97	49.84	50.09	51.29	37.13	37.02	17.04	39.52	35.23	0.01	16.83	9.81
159	46.44	46.31	48.07	47.95	48.70	49.94	49.82	50.09	51.29	37.22	37.07	17.11	39.59	35.26	0.01	16.83	9.81
160	46.41	46.21	48.05	47.85	48.70	49.99	49.79	50.02	51.29	37.30	37.12	17.06	39.64	35.27	0.01	16.83	9.81
161	46.39	46.11	48.02	47.75	48.70	50.04	49.77	50.00	51.29	37.39	37.14	17.14	39.69	35.28	0.01	16.82	9.81
162	46.34	46.01	48.00	47.68	48.69	50.07	49.74	49.97	51.26	37.46	37.17	17.21	39.72	35.29	0.01	16.82	9.81
163	46.29	45.91	47.97	47.60	48.68	50.09	49.72	49.95	51.24	37.53	37.19	17.29	39.76	35.30	0.01	16.82	9.81
164	46.26	45.84	47.95	47.53	48.65	50.04	49.62	49.90	51.21	37.58	37.22	17.36	39.78	35.31	0.01	16.81	9.81
165	46.24	45.76	47.92	47.45	48.62	50.02	49.54	49.85	51.18	37.62	37.24	17.36	39.81	35.32	0.01	16.79	9.81
166	46.21	45.69	47.90	47.38	48.60	49.99	49.47	49.75	51.16	37.65	37.24	17.36	39.84	35.33	0.01	16.76	9.82
167	46.14	45.61	47.83	47.30	48.52	49.92	49.39	49.65	51.13	37.65	37.27	17.36	39.87	35.35	0.01	16.72	9.82
168	46.06	45.54	47.75	47.23	48.45	49.84	49.32	49.55	51.03	37.65	37.27	17.36	39.90	35.36	0.01	16.71	9.82
169	45.99	45.54	47.68	47.23	48.35	49.69	49.24	49.45	51.00	37.65	37.27	17.44	39.93	35.38	0.01	16.71	9.82
170	45.91	45.54	47.60	47.23	48.25	49.54	49.17	49.37	50.98	37.63	37.27	17.44	39.96	35.41	0.01	16.72	9.82
171	45.84	45.54	47.53	47.23	48.15	49.39	49.09	49.30	50.90	37.63	37.27	17.44	40.00	35.43	0.01	16.71	9.82
172	45.76	45.52	47.45	47.20	48.06	49.27	49.02	49.22	50.82	37.63	37.27	17.44	40.03	35.46	0.01	16.71	9.82
173	45.69	45.49	47.38	47.18	47.98	49.19	49.00	49.17	50.75	37.65	37.27	17.44	40.06	35.49	0.01	16.72	9.82
174	45.61	45.47	47.30	47.15	47.92	49.14	49.00	49.12	50.67	37.68	37.34	17.44	40.09	35.52	0.01	16.75	9.82
175	45.54	45.44	47.23	47.13	47.84	49.07	48.97	49.12	50.59	37.73	37.42	17.44	40.13	35.56	0.01	16.76	9.83
176	45.56	45.42	47.23	47.08	47.85	49.09	48.95	49.12	50.51	37.80	37.49	17.44	40.16	35.59	0.01	16.78	9.83
177	45.64	45.39	47.23	46.98	47.87	49.14	48.90	49.12	50.51	37.89	37.57	17.44	40.19	35.61	0.01	16.78	9.83
178	45.71	45.37	47.23	46.88	47.88	49.19	48.85	49.12	50.44	37.99	37.64	17.44	40.23	35.63	0.01	16.77	9.83
179	45.69	45.27	47.20	46.78	47.88	49.24	48.82	49.12	50.33	38.10	37.72	17.44	40.26	35.64	0.01	16.76	9.83
180	45.74	45.24	47.18	46.68	47.86	49.22	48.72	49.10	50.33	38.20	37.79	17.44	40.30	35.64	0.01	16.75	9.83
181	45.71	45.17	47.15	46.61	47.83	49.17	48.62	49.07	50.33	38.30	37.87	17.44	40.33	35.63	0.01	16.73	9.83
182	45.69	45.09	47.13	46.53	47.80	49.14	48.55	49.05	50.31	38.37	37.94	17.44	40.36	35.61	0.01	16.70	9.83
183	45.66	45.02	47.10	46.46	47.77	49.09	48.45	49.02	50.28	38.43	37.94	17.44	40.39	35.57	0.01	16.67	9.83
184	45.64	44.94	47.08	46.38	47.74	49.07	48.37	49.00	50.26	38.46	37.94	17.44	40.41	35.53	0.01	16.66	9.84
185	45.56	44.87	47.03	46.33	47.68	49.00	48.30	48.97	50.15	38.47	37.94	17.44	40.44	35.48	0.01	16.67	9.84
186	45.44	44.79	46.98	46.33	47.62	48.90	48.25	48.95	50.13	38.47	37.94	17.44	40.45	35.43	0.01	16.67	9.84
187	45.27	44.72	46.88	46.33	47.50	48.75	48.20	48.92	50.02	38.44	37.94	17.44	40.46	35.38	0.01	16.65	9.84
188	45.19	44.72	46.80	46.33	47.40	48.60	48.12	48.90	49.95	38.41	37.94	17.44	40.48	35.35	0.01	16.65	9.84
189	45.04	44.64	46.73	46.33	47.33	48.52	48.12	48.90	49.84	38.36	37.94	17.44	40.49	35.31	0.01	16.64	9.84
190	44.97	44.64	46.66	46.33	47.25	48.45	48.12	48.90	49.79	38.31	37.96	17.44	40.51	35.29	0.01	16.66	9.84
191	44.89	44.64	46.58	46.33	47.18	48.37	48.12	48.83	49.72	38.26	37.96	17.44	40.53	35.27	0.01	16.68	9.84
192	44.82	44.64	46.51	46.33	47.10	48.30	48.12	48.75	49.64	38.22	37.99	17.44	40.55	35.25	0.01	16.70	9.84
193	44.74	44.64	46.43	46.33	47.03	48.22	48.12	48.68	49.56	38.19	38.01	17.46	40.57	35.25	0.01	16.70	9.85
194	44.69	44.64	46.38	46.33	46.97	48.15	48.10	48.60	49.56	38.18	38.04	17.46	40.60	35.24	0.01	16.70	9.85
195	44.64	44.64	46.33	46.33	46.91	48.07	48.07	48.53	49.48	38.17	38.06	17.46	40.62	35.24	0.01	16.71	9.85
196	44.64	44.62	46.33	46.31	46.91	48.07	48.05	48.45	49.48	38.17	38.09	17.46	40.64	35.24	0.01	16.74	9.85
197	44.62	44.59	46.33	46.31	46.90	48.05	48.02	48.38	49.48	38.18	38.11	17.46	40.65	35.24	0.01	16.77	9.85
198	44.62	44.57	46.33	46.28	46.90	48.05	48.00	48.30	49.48	38.19	38.14	17.49	40.66	35.23	0.01	16.81	9.85
199	44.62	44.54	46.33	46.26	46.90	48.05	47.97	48.23	49.43	38.21	38.14	17.49	40.67	35.22	0.01	16.81	9.85
200	44.62	44.52	46.33	46.23	46.90	48.05	47.95	48.23	49.43	38.23	38.16	17.51	40.67	35.21	0.01	16.82	9.85
201	44.54	44.42	46.33	46.21	46.90	48.05	47.92	48.23	49.43	38.25	38.16	17.51	40.67	35.21	0.01	16.82	9.85
202	44.54	44.40	46.33	46.18	46.90	48.05	47.90	48.23	49.41	38.27	38.16	17.51	40.66	35.20	0.01	16.83	9.86
203	44.52	44.37	46.31	46.16	46.89	48.05	47.90	48.20	49.38	38.28	38.16	17.54	40.66	35.20	0.01	16.85	9.86
204	44.44	44.27	46.31	46.13	46.90	48.07	47.90	48.18	49.35	38.29	38.16	17.56	40.65	35.19	0.01	16.84	9.86
205	44.35	44.20	46.28	46.13	46.87	48.05	47.90	48.15	49.33	38.30	38.16	17.59	40.65	35.19	0.01	16.81	9.86
206	44.27	44.12	46.26	46.11	46.83	47.97	47.83	48.13	49.30	38.31	38.16	17.61	40.65	35.19	0.01	16.79	9.86
207	44.17	44.05	46.23	46.11	46.80	47.95	47.83	48.10	49.28	38.32	38.16	17.61	40.66	35.19	0.01	16.76	9.86
208	44.07	43.97	46.21	46.11	46.76	47.85	47.75	48.05	49.25	38.33	38.16	17.64	40.66	35.19	0.01	16.76	9.86
209	44.05	43.90	46.18	46.03	46.73	47.83	47.68	48.03	49.23	38.35	38.16	17.64	40.67	35.19	0.01	16.76	9.86
210	44.02	43.90	46.16	46.03	46.68	47.73	47.60	48.00	49.20	38.38	38.16	17.66	40.66	35.18	0.01	16.76	9.86

APPENDIX B

COMPUTER PROGRAM

A SIMULATION PROGRAM
OF GAS CYLINDER CHARGING PROCESS

```
#include <stdio.h>
#include <math.h>
#define To      17.5    /*      C       */
#define Two1    17      /*      C       */
#define Mo      0.01    /*      kg      */
#define Too     17.5    /*      C       */
#define D       0.3     /*      m       */
#define d       0.282   /*      m       */
#define Cv      716     /*  J/Kg K      */
#define Aoo     0.94    /*    m*m       */
#define Ai      0.87    /*    m*m       */
#define ρ       8000    /*    density kg/(m*m*m)    */
#define C       450     /*   J/(kg.c)   */
#define Vm      0.009   /*    m*m*m     */
#define R       287.1   /*  J/(kg.K)    */
#define Vc      0.054   /*   m*m*m      */
#define g       9.8
#define T1o     17      /*      C       */


double mass(void);
double Tgt(double);
double Tw(void);
double Tf(double);
double Gr(double,double);
double Nu(double);
double hoo(double);
double hi(double,double,double,double,double);
double qqi(double,double,double);
double qqoo(double,double);
double ddU(double,double);
main ()
{
      int kk;
      float cx,dx,ex,hx,ix,jx,lx,qi,qoo,dU,px,qx,bbbb;
      float aax,ccx,ddx,eex,ffx,ggx,hhx,iix,jjx,llx,i, qqq, qqqq;
     double s, T1, T, w1, tt, fx, gx, rx, sx, bx, bbx, lll, llll, ll, wo,
t, tt, w, TT1;
      hx=To+273;
     bx=Two1;
      ix=Tf(bx);
      jx=1/(ix+273);
      cx=Gr(bx,jx);
      dx=Nu(cx);
      ex=hoo(dx);
      printf("\n\nNote:      This  simulation  program  needs  input  values
including:");
      printf("\n\n            Pressure P, Mass M, Mass flow rate w, inlet
temperature T1 and time t.");
      printf("\n\n\nThe initial values of the input variables should be the
measured values \nafter 30 seconds");
      printf("\n\n\nPress any key to continue");
      getchar ();
      printf("\n\ninput wo =");
      scanf("%lf",&wo);
      fx=wo;
      printf("\n\ninput t =");
      scanf("%lf",&t);
      gx=t;
      rx=T1o;
```

```
sx=To;
lx=hi(fx,gx,rx,sx,bx);
printf("hio =");
printf("%f",lx);
qqq=qqi(lx,hx,bx);
printf("\nqio =");
printf("%f",qqq);
qqqq=qqoo(ex,bx);
printf("\nqooo =");
printf("%f",qqqq);
for (i=1;i<1000;++i){
  aax=mass();
  hhx=Tgt(aax);
  qx=hhx-273;
  printf("%f",qx);
  bbx=bx+0.001;
  printf("\n\ninput w =");
  scanf("%lf",&w);
  printf("\n\ninput TT1=");
  scanf("%lf",&TT1);
  sx=hhx;
  printf("\n\ninput tt=");
  scanf("%lf",&tt);
  fx=w;
  gx=tt;
  rx=TT1;
  while(bbx<50){
    bbbb=0;
    iix=Tf(bbx);
    printf("%f",iix);
    jjx=1/(iix+273);
    ccx=Gr(bbx,jjx);
    printf("%f",ccx);
    ddx=Nu(ccx);                    /*    ddx=Gr     */
    printf("%f",ddx);
    eex=hoo(ddx);
    printf("%f",eex);
    llx=hi(fx,gx,rx,sx,bbx);
    printf("hi=");
    printf("%f",llx);
    qi=qqi(llx,hhx,bbx);
    qoo=qqoo(eex,bbx);
      for(kk=1;kk<2;kk++) {
      Tw1=Two1;

      }
     if(bbbb>Tw1){
     Tw1=bbbb;}
    printf("Tw1 =");
    printf("%f",Tw1);
    dU=ddU(bbx,Tw1);
    px=qi-dU-qoo;
    printf("\n\nqi-dU-qoo =");
    printf("%f",px);
          if(-1000>px||px>1000){
          bbx=bbx+0.02;
          printf("\nbbx=");
          printf("%f",bbx);
        }
          else if(px>500||px<-500){
          bbx=bbx+0.01;
         printf("\n\nbbx =");
         printf("%f",bbx);
         }
          else if(px>100||px<-100){
           bbx=bbx+0.01;
           }
```

```
                else if(px>10||px<-10){
                 bbx=bbx+0.0001;}
               else if(px>0.1||px<-0.1){
                 bbx=bbx+0.00001;}
                 else
                 {

printf("\n\n%9s%9s%9s%9s%9s%9s%9s%9s","Mass","Tg","Tw","hi","hoo","qi","qoo
","dU");

printf("\n\n%9.3f%9.3f%9.3f%9.3f%9.3f%9.3f%9.3f%9.3f",aax,qx,bbx,llx,eex,qi
,qoo,dU);
                 bbbb=bbx;
                 bbx=50;
                 printf("\n\ninput any number (<1000) to continue ");
                 printf("or 1000 to exit");
                 scanf("%f",&ttt);
                  if(ttt>999){
                  i=ttt;

            }
          }
          }
      }
          printf("\n\nsimulation finish");

          getch ();
}
double mass ()
{
      float x;
      printf("\n\ninput Mass = ");
      scanf("%f",&x);

      return (x);
}
double Tgt(x)
double x;
{
      float Tgt,P;
      double a,b,c;
      printf("\n\ninput P(Mpa) = ");
      scanf("%f",&P);
      c=P*pow(10,6)*Vc/(x*R);
       if(P<0.69){
        a=0;
        b=0.998;}
       else if(P<1.38){
        a=0.0000717;
        b=0.9749;}
       else if(P<2.07){
        a=0.000116;
        b=0.9609;}
       else if(P<2.76){
        a=0.000188;
        b=0.9378;}
       else if(P<3.45){
        a=0.000215;
        b=0.9281;}
       else if(P<4.14){
        a=0.000287;
        b=0.9059;}
       else if(P<4.83){
        a=0.000341;
        b=0.8890;}
       else if(P<5.52){
        a=0.000404;
```

```
 b=0.8693; }
else if(P<6.2){
 a=0.000467;
 b=0.8505;}
else if(P<6.89){
 a=0.000530;
 b=0.8318; }
else if(P<7.58){
 a=0.000584;
 b=0.8160; }
else if(P<8.27){
 a=0.000646;
 b=0.7977; }
else if(P<8.96){
 a=0.000709;
 b=0.7795; }
else if(P<9.65){
 a=0.000772;
 b=0.7612; }
else if(P<10.34){
 a=0.000844;
 b=0.7396;}
else if(P<11.03){
 a=0.000561;
 b=0.8271;}
else if(P<11.72){
 a=0.000582;
 b=0.8228; }
else if(P<12.41){
 a=0.000576;
 b=0.8262;  }
else if(P<13.10){
 a=0.000619;
 b=0.8147; }
else if(P<13.78){
 a=0.000560;
 b=0.8365; }
else if(P<14.48){
 a=0.000567;
 b=0.8379;  }
else if(P<15.17){
 a=0.000533;
 b=0.8508; }
else if(P<15.86){
 a=0.000636;
 b=0.8209; }
else if(P<16.55){
 a=0.000622;
 b=0.8293; }
else if(P<17.24){
 a=0.000560;
 b=0.8525; }
else if(P<17.92){
 a=0.000670;
 b=0.8211; }
else if(P<18.61){
 a=0.000602;
 b=0.8460; }
else if(P<19.30){
 a=0.000622;
 b=0.8443;}
else if(P<20.00){
 a=0.000650;
 b=0.8379; }
else if(P<20.68){
 a=0.000588;
 b=0.8621;  }
```

```
      Tgt=(-b+pow((b*b+4*a*c),0.5))/(2*a);
      printf("\n\nTgt =  ");
      return (Tgt);
}
double Tw()
{
      float Tw;
      printf("\n\ninput Tw:");
      scanf("%f",&Tw);
      return Tw;
}
double Tf(x)
double x;
{
      double Tf;
      Tf=(x+Too)/2;
      return(Tf);
}
#define v      0.000016
double Gr(x,y)
double x,y;
{
      float Gr;
      Gr=g*y*D*D*D*(x-Too)/(v*v);

      return (Gr);
}
#define     Pr     0.7
double Nu(x)
double x;
{
      double a,b,Nu,ax,bx;
      a=x;
      if(a<0){
      b=(-1)*a;}
      else{
          b=a; }
      ax=b*Pr;
      Nu=0.53*pow(ax,0.25);

      return (Nu);
}
#define      k2     0.027
double hoo(x)
double x;
{
      float hoo;
      hoo=x*k2/D;

      return (hoo);
}
#define cp    1040
#define k     1.4
#define aa    -0.002
#define bb    0.3559
double hi(w,x,y,z,zz)
double w,x,y,z,zz;
{
       float hi,a,b,c,ppp;
       a=w*cp*(y+273)/60;
       if(x<120){
       ppp=2*aa*x+bb;
       b=ppp*Vc*1000000/(k-1);}
       else{
       b=(2*aa*120+bb)*Vc*1000000/(k-1);}
       c=Ai*(z-273-zz);
       hi=(a-b)/c;
```

```
        return (hi);

}

double qqi(x,y,z)
double x,y,z;
{
        float qi;
        qi=x*Ai*(y-273-z);
        return (qi);
}
double qqoo(x,y)
double x,y;
{
        float qoo;
        qoo=x*Aoo*(y-Too);
        return(qoo);
}

double ddU(x,y)         /*      energy change of wall    */
double x,y;
{
        float a,E;
        a= C*Vm*(x-y)/5;
        E=a*8000;
        return(E);
}
```

PROGRAM FOR DATA PROCESSING

```
#include <stdio.h>

#define MAX_CHAN    11
#define MAX_READ    100

int data[MAX_CHAN][MAX_READ];

FILE *come, *back;

main()
{
      int i, j, ch, count;
      come = fopen("inpf.mda","r");
      back = fopen("outf.mda","w");

      while((ch = getc(come)) !=';');
      fscanf(come, "%d", &count);
      i=0;
      j=0;
      do {
        if(fscanf(come, "%d",&data[i++][j])==';') break;
        if(i == MAX_CHAN) {
            i = 0;
            j++;
          }

        } while((MAX_CHAN*j) < count);
      fclose(come);
      for(i = 0; i < MAX_CHAN; i++) {
         printf("\n*******CHANNEL %d*********", i);
         for(j = 0; j < count / MAX_CHAN; j++){
            printf("\n%d",data[i][j]);
            fprintf(back,"\n%d", data[i][j]);
        }
      }
      fclose(back);
}
```

PROGRAM FOR DATA CURVE FITTING

```
#include<stdio.h>
#include<math.h>
main()
{
int N,i,num;
float a1,a2,a3,a4,b2,b3,b4;
float x1,x2,x3,x4,x5,x6,x7,y1,y2,y3,y4,y5,y6,y7;
double X,Y,Z,Zz,Zzz;
N=7;
printf("\ninput num:");
scanf("%d",&num);
printf("\n\ninput x1=");
scanf("%f",&x1);
x1=0;
printf("\ninput y1=");
scanf("%f",&y1);
printf("\ninput x2=");
scanf("%f",&x2);
x2=3.4474;
      printf("\ninput y2=");
      scanf("%f",&y2);
      printf("\ninput x3=");
      scanf("%f",&x3);
      x3=6.8948;
      printf("\ninput y3=");
      scanf("%f",&y3);
      printf("\ninput x4=");
      scanf("%f",&x4);
      x4=10.3422;
      printf("\ninput y4=");
      scanf("%f",&y4);
      x5=13.7896;
      printf("\n\ninput y5=");
      scanf("%f",&y5);
      x6=17.237;
      printf("\n\ninput y6=");
      scanf("%f",&y6);
      x7=20.6844;
      printf("\n\ninput y7=");
      scanf("%f",&y7);
      a1=x1+x2+x3+x4+x5+x6+x7;

a2=pow(x1,2)+pow(x2,2)+pow(x3,2)+pow(x4,2)+pow(x5,2)+pow(x6,2)+pow(x7,2);

a3=pow(x1,3)+pow(x2,3)+pow(x3,3)+pow(x4,3)+pow(x5,3)+pow(x6,3)+pow(x7,3);

a4=pow(x1,4)+pow(x2,4)+pow(x3,4)+pow(x4,4)+pow(x5,4)+pow(x6,4)+pow(x7,4);
      b4=x1*x1*y1+x2*x2*y2+x3*x3*y3+x4*x4*y4+x5*x5*y5+x6*x6*y6+x7*x7*y7;
      b3=x1*y1+x2*y2+x3*y3+x4*y4+x5*y5+x6*y6+x7*y7;
      b2=y1+y2+y3+y4+y5+y6+y7;

Zz=b4*a3*a2*a2-b4*a1*a3*a3+b3*a1*a3*a4-b3*a2*a3*a3+b2*pow(a3,3)-a2*a3*a4*b2
;

Zzz=pow(a2,3)*a3-a1*a2*a3*a3+a1*a1*a3*a4-a1*a2*a3*a3+N*a3*a3*a3-N*a2*a3*a4;
      Z=Zz/Zzz;
      Y=((b4*a3-b3*a4)-(a2*a3-a1*a4)*Z)/(a3*a3-a2*a4);
      X=(b2-N*Z-a1*Y)/a2;
      printf("\n\nEquation No. ");
      printf("%2d",num);
      printf("\n\n%10s%10s%10s","X","Y","Z");
      printf("\n\n%10.71f%10.71f%10.71f",X,Y,Z);
}
```

APPENDIX C

Z functions

Appendix C.1

a and b values of Z functions for air

P (MPa)	a	b	P (MPa)	a	b
0<p<0.69	0	0.998	10.34<p<11.03	0.000561	0.8271
0.69<p<1.38	0.0000717	0.9749	11.03<p<11.72	0.000582	0.8228
1.38<p<2.07	0.000161	0.9609	11.72<p<12.41	0.000576	0.8262
2.07<p<2.76	0.000188	0.9378	12.41<p<13.1	0.000619	0.8147
2.76<p<3.45	0.000215	0.9281	13.1<p<13.78	0.000560	0.8365
3.45<p<4.14	0.000287	0.9059	13.78<p<14.48	0.000567	0.8379
4.24<p<4.83	0.000341	0.8890	14.48<p<15.17	0.000533	0.8508
4.83<p<5.52	0.000404	0.8693	15.17<p<15.86	0.000636	0.8209
5.52<p<6.2	0.000467	0.8505	15.86<p<16.55	0.000622	0.8293
6.2<p<6.89	0.000530	0.8318	16.55<p<17.24	0.000560	0.8525
6.89<p<7.58	0.000584	0.8160	17.24<p<17.92	0.000670	0.8211
7.58<p<8.27	0.000646	0.7977	17.92<p<18.61	0.000602	0.8460
8.27<p<8.96	0.000709	0.7795	18.61<p<19.3	0.000622	0.8443
8.96<p<10.34	0.000844	0.7396	19.3<p<20.0	0.000650	0.8379

Appendix C.2

a, b and c values of Z functions for NGV

Pressure (Mpa)	a $\times 10^{-5}$	b $\times 10^{-3}$	c	Pressure (Mpa)	a $\times 10^{-5}$	b $\times 10^{-3}$	c
0<p<0.69	-0.3	2.11	0.64	10.34<p<11.03	-1.3	11.2	1.69
0.69<p<1.38	-0.6	4.32	0.23	11.03<p<11.72	-0.9	9.1	-1.4
1.38<p<2.07	-0.6	4.56	0.12	11.72<p<12.41	-0.9	8.62	-1.3
2.07<p<2.76	0	0.63	0.71	12.41<p<13.1	-1.3	11.3	-1.7
2.76<p<3.45	-0.3	2.74	0.33	13.1<p<13.78	-0.2	4.18	-0.5
3.45<p<4.14	-0.3	3.20	0.15	13.78<p<14.48	0.4	-0.2	0.19
4.24<p<4.83	-1.3	9.46	-0.9	14.48<p<15.17	0.9	-3.9	0.87
4.83<p<5.52	-0.6	5.67	-0.4	15.17<p<15.86	0.9	-4.1	0.96
5.52<p<6.2	-1.3	9.4	-1.2	15.86<p<16.55	0.5	-1.4	0.56
6.2<p<6.89	-1.3	10.4	-1.3	16.55<p<17.24	0.3	0.48	0.44
6.89<p<7.58	-0.5	5.8	-0.7	17.24<p<17.92	0.4	-1.4	0.64
7.58<p<8	-2.8	20.5	-3.0	17.92<p<18.61	0.1	4.7	0.35
8.27<p<8.96	-0.6	7.02	-0.9	18.61<p<19.3	0.4	-1.3	0.69
8.96<p<10.34	-1.6	13.1	-1.9	19.3<p<20.0	0.3	-0.6	0.61